PREDICTION OF ULTIMATE TORSIONAL STRENGTH OF REINFORCED CONCRETE BEAMS USING ARTIFICIAL NEURAL NETWORKS

A THESIS

SUBMITTED TO THE COLLEGE OF ENGINEERING
UNIVERSITY OF BASRAH
IN A PARTIAL FULFILLMENT OF
THE REQUIREMENTS FOR THE DEGREE
OF MASTER OF SCIENCE IN
CIVIL ENGINEERING

BY

ABDULKHALIQ ABDULYIMAH JAAFER

(B.Sc.CIVIL ENGINEERING)

2008

بسم الله الرحمن الرحيم

قالوا سبحانك لا علم لنا إلا ما علمتنا انك أنت العليم الحكيم

سورة البقرة الآية (32)

صدق الله العلي العظيم

Acknowledgements

Thanks for GOD, TO Him Belongs, Mighty and Majesty

I would like to express my profound gratitude to my supervisors ***Prof. Dr. Nabeel Abdulrazzaq Jasim*** *and* ***Dr. Majid A.Alwan*** *for their much valued advice, contribution and tuition during the various stages of this work.*

I also would like to thank ***Prof. Dr. Saleh E. Najim*** *dean of the college of engineering, and* ***Dr. Ahmad M. Hamad*** *head of civil engineering department, for their help and support.*

Last but not the least; I would like to express my deep thanks to my parents for their encouragement, support in my life, my study and my work.

Abdulkhaliq Abdulyimah

2007

Certification

We certify that this thesis titled "**Prediction of Ultimate Torsional Strength of Reinforced Concrete Beams Using Artificial Neural Networks**" which is being submitted by "***Abdulkhaliq Abdulyimah Jaafer***" was prepared under our supervision at the University of Basrah as a partial fulfillment of the requirements for the degree of Master of Science in Civil Engineering.

Signature:
Name: Prof. Dr. Nabeel Abdulrazzaq
(Supervisor)
Date: / /2007

Signature:
Name: Dr. Majid A. Alwan
(Supervisor)
Date: / /2007

In view of the available recommendation, I forward this thesis for debate by the examining committee.

Signature:
Name: Dr. Ahmad Majeed Hamad
(Head of Civil Engineering Dept.)
Date: / / 2007

Committee Report

We certify that we have read this thesis titled "**Prediction of Ultimate Torsional Strength of Reinforced Concrete Beams Using Artificial Neural Networks**" which is being submitted by "***Abdulkhaliq Abdulyimah Jaafer***" and as Examining Committee, examined the student in its contents. In our opinion, the thesis is adequate for award of degree of Master of Science in Civil Engineering.

Signature:
Name: Prof. Dr. Nabeel A. Jasim
(Supervisor)
Date:

Signature:
Name: Dr. Majid A. Alwan
(Supervisor)
Date:

Signature:
Name: Dr.Ala Nasir Haraib
(Member)
Date:

Signature:
Name: Dr.Mehdi A. Albayyati
(Member)
Date:

Signature:
Name: Prof. Dr. Turki Y. Abdalla
(Chairman)
Date:

Approved of the College of Engineering

Signature:

Name: Prof. Dr. Saleh E. Najim
Dean of Engineering College
Date:

Abstract

This study investigates the feasibility of using artificial neural network (ANN) to predict the ultimate strength of reinforced concrete rectangular beams subjected to pure torsion and to combination of torsion and bending. The fundamental and practical aspects of artificial neural networks are demonstrated and a view of their structures, topology and strengths are presented. The effects of the parameters, such as the number of nodes in the input layer, output layer and hidden layer, the pre-process (normalization) of the training patterns, the weight-factors initialization and the selection of the learning rate and momentum coefficient, on the behaviour of the neural network have been investigated. Due to slower convergence of the gradient descent (GD) backpropagation algorithm, the faster algorithm called "resilient propagation algorithm"(RPROP) has been used to improve the performance of the neural network. After training, the generalization of the neural network was tested by patterns not included in the training patterns.

Two structures of networks are worked out as follows:

1. The configuration 10:25:25:1 is used to predict the ultimate strength of reinforced concrete beams under pure torsion.
2. The configuration 11:8:1 is used to predict the ultimate strength of reinforced concrete beams under combined torsion and bending.

The neural network model was trained based on experimental results of other researches.

It is found that normalizing the input and target values of training patterns reduces the training time. Gaussian weight-factor distribution with range (±1) is found to give a minimum mean square error (MSE). In addition, for gradient descent (GD) algorithm the effective values for learning rate and momentum coefficient are (0.5) and (0.8) respectively. Based on the ANN results, a parametric analysis was carried out to study the influence of parameters affecting the ultimate torsional strength of reinforced concrete beams and these results are compared with equations of ACI-318-89&05 Code.

Contents

Chapter Four: Results and Discussion

Notations

Symbol	Description
A_1	Area of concrete bounded by centerline of transverse hoop bars
A_t	Cross sectional area of transverse hoop bars
A_L	Cross sectional area of longitudinal bars
A_2	The area bounded by the lines connecting the centers of the corner longitudinal bars
A_o	Area bounded by the centerline of the shear flow
a_o	The depth of the equivalent compression stress block
A_{oh}	Gross area bounded by centerline of outermost closed stirrups
b	The shorter side of cross section
$f'c$	Cylinder compressive strength of concrete
f_y	Yield strength of longitudinal steel
fr	Tensile strength of concrete
f_{sy}	Yield strength of transverse steel
h	The longer side of cross section
m	The ratio of volume of longitudinal bars to volume of stirrups
p_1	Perimeter of the centerline of stirrups
q	Shear flow
$S \& S_1$	Spacing of stirrups
t	The thickness of the wall of cross section (for hollow section)
T_e	Elastic torque
T_p	Plastic torque
$T_n \& T_u$	Nominal and ultimate torsional strength respectively
$T_c \& T_{cv}$	The torsional resistance contribution by concrete
U	The perimeter of the area A_1
V_{ca}	The shear stress of concrete due to flexural shear only
V_u	Ultimate shear stress due to flexural shear
x	The shorter side of cross section
x_1	The shorter leg of stirrups
y	The longer side of cross section
y_1	The longer leg of stirrups
α	Coefficient given by Saint Venant's theory
λ_s	Efficiency factor

α	Angle of inclination of the concrete struts
α_t	Coefficient
τ_{ca}	Shear stress of concrete due to torsion only
τ_u	Ultimate shear stress due to torsion
β	Angle of cracking
ψ	The ratio M/T
ρ_t	The ratio of the total volume of reinforcement including longitudinal and transverse steel to the volume of concrete

Chapter One

Introduction

1.1 General:

Reinforced concrete members are commonly subjected to bending moments, to transverse shears associated with those bending moments, and, in the case of columns, to axial forces often combined with bending and shear. In addition, torsional forces may act, tending to twist a member about longitudinal axis. Such torsional forces seldom act alone and are concurrent with bending moment and transverse shear, and some time with axial as well. The action of axial loads and bending, are quite well understood, and the design methods are essentially the same for different nations. In contrast, shear and torsion, are not well understood and the empirical design methods used in codes and specifications are very different around the world [1].

For many years, torsion was regarded as secondary effect and was not considered explicitly in design. Its influence being absorbed in the overall factor of safety of rather conservatively designed structures. Current methods of analysis and design, however, have resulted in less conservatism, leading to somewhat smaller members that, in many cases, must be reinforced to increase torsional strength. In addition, there is an increasing use of structural members for which torsion is a central feature of behavior; examples include curved bridge girders, eccentrically loaded box beams, and helical stair way slabs. In these structures, torsion is considered of primary importance together with flexural and shear, and can not be neglected or overcome by applying certain safety factors to the shear design [2].

1.2: Types of Torsion:

It is useful in considering torsion to distinguish between primary and secondary torsion in reinforced concrete structures.

1. Primary torsion, some times called equilibrium torsion or statically determinate torsion, exists when the external load has no alternative load path but must be supported by torsion. For such cases, the torsion required to maintain static equilibrium can be uniquely determined.
2. Secondary torsion, also called compatibility torsion or statically indeterminate torsion, arises from the requirements of continuity, i.e., compatibility of deformation between adjacent parts of a structure. For this case, the torsional moments can not be found bases on static equilibrium alone. Disregard of continuity in the design will often lead to extensive cracking, but generally will not cause collapse. An internal readjustment of forces is usually possible and an alternative equilibrium of forces found. An example of secondary torsion is found in the spandrel or edge beam supporting a monolithic concrete slab.

1.3: Torsion in Homogeneous Members:

The problem of torsion in an elastic circular member was first studies by coulomb in 1784. He found that the torsional moment is proportional to the twisting angle.

A theoretical equation for torsion of an elastic circular member was derived by Navier in 1826. Three decades later and after the

development of the necessary mathematical tools, Fourier series and theory of elasticity, Saint-Venant used the semi-inverse method to solve the problem of pure torsion of elastic non circular members and predicted a precise expression for the warping of cross-section [3]. In the elastic stage of behaviour, the torque-rotation relationship and the warping displacement expression have been obtained for various cross-sections using Saint-Venant semi-inverse method. However, such a relationship has been only obtained for circular and narrow rectangular cross section for the elastic-plastic stage of behaviour [4]. The fully plastic torque of the cross-sections may be easily calculated using the sand-heap analogy [5].

Prandtl in 1930, as cited in Ref. [6], discovered an interesting analogy between the stress function in the torsion problem and the deflection of membrance under uniform pressure. Prandtl's membrance analogy was extended to the case of plastic material when Nadai [7] applied the sand heap analogy to calculate the fully plastic torque of solid section. Sadowsky [8] extended Nadai's sand-heap analogy to apply to plastic section with holes.

1.4 Torsion of Plain Concrete Members

Three approaches have been developed to predict the torsional strength of plain concrete members. These are based on elastic theory, plastic theory, and skew bending. The elastic theory assumed that the concrete is homogeneous material and stresses distributed according to Saint-Venant's theory. The failure condition is considered to be reached when the maximum shear stress, and therefore the maximum principal

tensile stress, is equal to the tensile strength of concrete. The failure torque for a rectangular member then (T_e) becomes [9].

$$T_e = k.h.b^2.\tau_{\max.} \tag{1.1}$$

where; *(T_e)* is the elastic torsional resistance for plain concrete rectangular beam,*(k)* is a function of *(h/b), (h)* is the longer side of the section, and *(b)* is the shorter side of the section.

Cowan [10] suggested an approximation to the value of *(k),* given by:

$$k = \frac{1}{3 + \frac{2.6}{0.45 + h/b}} \tag{1.2}$$

Concrete in torsion exhibits plasticity. This plasticity leads to a redistribution of the stresses as the load approaches its ultimate value. Turner and Davies, as cited in Ref. [11] draw attention to this fact in 1934 and suggested that this effect might be allowed for in calculating the ultimate torque by multiplying the elastic torque by a factor of $(1.2\frac{4A}{p \cdot b})$ where ; (A) is the cross sectional area, (p) is the periphery of cross section and (b) is the shorter side of the section.

Marshal and Nylander, as cited in Ref. [11] both suggested that by treating concrete as an ideal plastic material, more consistent results are obtained. At failure the shear stress will then be constant over the whole section and equal to the ultimate tensile strength of concrete. For rectangular beam, the torsional strength is given by:

$$T_p = k_p.h.b^2.\tau_{\max.} \tag{1.3}$$

where, $(\tau_{\max.})$ is the maximum torsional stress, and

$$k_p = \frac{1}{2}(1 - \frac{b}{3h}) \tag{1.4}$$

Examining of the two formulas of (k) in equation (1.2) and (k_p) in equation (1.4) reveals that for a wide range of depth to breadth ratios for rectangular sections, the value of (k_p) is 1.66 ± 0.06 times greater than (k). This means that for practical rectangular beams the ultimate torque calculated by plastic theory is 1.66 ± 0.06 times the ultimate torque calculated by elastic theory.

Nadai as cited in Ref. [12] developed the plastic theory by using the sand heap analogy which considers the torsional resistance of cross section to be proportional to the volume of a sand heap over the section. The torsional resistance is then given as twice the volume confined by the surface or:

$$T_p = \frac{1}{2} b^2 (h - \frac{b}{3}) \tau_{\max.} \tag{1.5}$$

Equation (1.5) is basically similar to equation (1.3).

Tests conducted by Hsu [9] revealed that, in the case of a rectangular section, cracks develop on three sides and failure proceeds in the form of skew bending with the neutral axis parallel to the long side of the section and inclined to the axis of twist as shown in figure (1.1).

As shown in figure (1.2) the applied torque can be resolved into two components acting on the failure surface. The first is the bending moment component (T_b) which causes bending about the axis (a-a) and it is really the main cause of cracking, and the second component is the

twisting moment component (T_t) which causes twisting moment about the axis perpendicular to the failure plane. The component (T_b) is given by:

$$T_b = T.\cos\phi \tag{1.6}$$

where, (ϕ) is the cracking angle of the wider face between the tensile crack and the axis of the beam.

The section modulus of the failure plane about the (a-a) axis [2]:

$$z = b^2.h.\csc\phi/6 \tag{1.7}$$

Since the beam will fail in bending, then the maximum tensile bending stress in the concrete can be calculated as [2]:

$$f_r = \frac{T_b}{z} = \frac{T_u.\cos\phi}{(b^2.h.\csc\phi)/6} \tag{1.8}$$

or:
$$T_u = \frac{b^2.h}{6} f_r(\sec\phi.\csc\phi) \tag{1.9}$$

To find the minimum value of torque (T_u) to cause cracking of the section, equation (1.9) is to be differentiated with respect to (ϕ) and equaled to zero.

$$\frac{dT_u}{d\phi} = \frac{b^2.h}{6} f_r \frac{d}{d\phi}(\sec\phi.\csc\phi) = 0 \tag{1.10}$$

This results in $(\phi = 45^\circ)$. Substituting this value of ϕ in equation (1.9) the minimum value of cracking torque becomes:

$$T_u = \frac{b^2.h}{3} f_r \tag{1.11}$$

It should be noted that the value of tensile bending stress (f_r) in the above equation should be reduced, since there are compressive stresses acting in a perpendicular direction to those tensile stresses, as shown in figure (1.2), and those compressive stresses reduce the strength of concrete to withstand the tensile stresses [2].

McHenry and Karni [13] suggested a reduction factor of (0.85) to be applied to the tensile bending stress (f_r) in equation (1.11) to become:

$$T_u = \frac{b^2.h}{3}(0.85 f_r) \qquad (1.12)$$

1.5: Torsional Strength of Reinforced Concrete Beams:

Many theories have been developed for calculating the torsional resistance of members with both longitudinal reinforcement and stirrups. These theories can be roughly divided into two types. The space truss analogy and skew bending theory. The former is the oldest and more commonly used in different codes, the fundamentals of this theory are described below first.

1.5.1: Space-Truss Analogy:

The first theory to predict the ultimate strength of reinforced concrete members subjected to torsion was proposed by Rausch in 1929 in the form of a Ph. D thesis [14]. In this theory a member with an arbitrary, bulk-cross section is assumed to act like a tube so that the applied torsional moment is resisted by the circulatory shear flow in the wall of the tube. Each straight wall-segment of the tube is assumed to

act like a plane truss. In this plane truss the longitudinal bars serve as the chord members with the hoop bars and the concrete struts act as the web members [14].

After cracking the concrete is separated by 45 degrees cracks into a series of helical members. These helical concrete members are assumed to interact with longitudinal steel bars and the hoop steel bars to form a space truss as shown in figure (1.3). Each of the helical members is idealized into a series of 45 degrees short straight struts connected at specified joints. The compression force in the concrete struts will produce an outward radial force at each joint that will be resisted by lateral hoop reinforcement. These lateral hoop bars are also idealized as chains of short straight bars connected to the concrete struts at the joints. The chains of diagonal concrete struts and the chains of hoop bars thus form a mechanism that will lengthen under an infinitesimal external torque. This tendency to the lengthen is resisted by longitudinal reinforcement. Each longitudinal bar is assumed to be a chain of short bars connected at the joints to the diagonal struts and the hoop bars. In this way a space truss is formed that consists of 45 concrete struts in compression and longitudinal and hoop bars in tension, this space truss is able to resist large external torque [15].

A space truss thus formed implies the following assumption:

1- The space truss is made up of 45 diagonal concrete struts.
2- Longitudinal and hoop bars are connected at the joints by hinges.
3- A diagonal concrete member carries only axial compression; i.e.; the shear resistance is neglected.
4- Longitudinal and hoop bare carry only tension; i.e.; dowel

resistance is neglected.

5- For a solid section, the concrete core does not contribute to the ultimate torsional resistance.

6- All the steel bars yield at the time of failure.

For a rectangular member reinforced with four longitudinal corner bars and closed stirrups with spacing, s_1, and by using the equilibrium condition of this 45° space truss model, Rausch derived the following expression below:

$$T = \frac{2A_1 A_t f_{sy}}{S_1} = \frac{2A_1 A_L f_{Ly}}{U} \qquad (1.13)$$

where:

T: torsional strength of a member.

A_1: area bounded by the centerline of transverse hoop bar.

A_t: cross sectional area of transverse hoop bar.

A_L: cross sectional area of the total longitudinal bars.

f_{sy} *and* f_{Ly}:yield strength of the stirrups and longitudinal bars respectively.

S_1 : the spacing of stirrups

U : the perimeter of the area A_1 .

Assuming that both longitudinal bars and stirrups have the same yield stress, the total area of the longitudinal bars can be obtained from equation (1.13) as:

$$A_L = A_t \frac{U}{S_1} = A_t \frac{2(x_1 + y_1)}{S_1} \qquad (1.14)$$

where :

x_1 *and* y_1: smaller and larger center to center dimensions of the stirrup.

Equation (1.14) which is so called equal volume principle, states that the volume of all longitudinal bars within the spacing S_1 should equal to the volume of one closed stirrup.

Although the space truss concept describes the main function of concrete and reinforcement in resisting torsion, Rausch's equation significantly overestimates the actual strength of reinforced concrete members [15]. Therefore, many modifications are introduced in Rausch's equation.

The first modification assumes that the reinforcement is only partially efficient. An efficiency factor, λs which is less than unity was suggested by Andersen in 1934 [16]. This is because Rausch's truss analogy assumed uniform stress along all the reinforcement in a member subjected to torsion.

This assumption of uniform stress contradicts Saint-Venant's stress distribution for all types of cross section expect the circular. In the case of a rectangular section Saint-Venant's stress distribution required the maximum stress to occur at the wider face and decreases to zero at the corner. Andersen suggested that the concrete also contributes to the total strength such as:

$$T_n = T_e + \lambda s \frac{2A_1 \; A_t f_{sy}}{S_1} \tag{1.15}$$

where:

T_e: the torsional resistance of plain concrete computed by Saint Venant's elastic theory.

The second modification to Rausch's equation was to reduce the area A_1, by making an arbitrary definition for the centerline of shear flow. Lampert and Thurliman, in 1969 [17], assumed that the perimeter connecting the centeroids of the corner longitudinal bars represented the centerline of the shear flow.

In this approach, the 45 degrees truss model is generated in order to apply also for members under combined torsion and bending. It was assumed that the angle of inclination of the concrete struts could deviate from 45 degrees and was taken as a variable, the approach which is adopted by the CEB-FIP model code [15]. According to this model the torsional strength of reinforced concrete member is given by:

$$T_n = T_{cv} + 2\frac{A_2 A_t f_{sy}}{S_1}\cot\alpha \qquad (1.16)$$

where:

A_2: the area bounded by the lines connecting the centers of the corner longitudinal bars.

α : angle of inclination of the concrete struts.

T_{cv}: the torsional resistance contributed by concrete.

The third modification which was suggested by Collins and Mitchell [18] in 1980 assumes that the centerline of the shear flow coincides with the centroidal line of the equivalent compression stress block in the concrete struts. In determining the equivalent compression stress block, the concrete cover outside the centerline of a hoop bar is

assumed to be ineffective. Based on this assumption, the following expressions were proposed:

$$T_n = \frac{2A_o A_t f_{sy}}{S_1} \cot\alpha \tag{1.17}$$

$$A_o = A_1 - \frac{a_o}{2} p_1 \tag{1.18}$$

where:

A_o: the area bounded by centerline of the shear flow.

p_1: the perimeter of the centerline of a stirrup.

a_o: the depth of the equivalent compression stress block given by:

$$a_o = \frac{A_1}{p_1}\left[1 - \sqrt{1 - \frac{T_n p_1}{0.85 f'c A_1^2}(\tan\alpha + \frac{1}{\tan\alpha})}\right] \tag{1.19}$$

Although the expression for the equivalent rectangular compression stress block has been found using both equilibrium and compatibility conditions, Collins and Matchell's theory invokes the crude assumption of neglecting the concrete cover. Hsu and Mo [15] have pointed out that the depth (a_o) calculated from equation (1.19) is too small because the standard cylinder compressive strength, f 'c, has been assumed for the strength of concrete struts. The concrete compressive strength can be substantially degraded by the presence of diagonal cracking.

Hsu and Mo in 1985 [15] found that Rausch's theory overestimates the torsional strength. Therefore, Hsu and Mo proposed a new variable-angle truss model using a reduced compressive strength for the

concrete struts. Based on equilibrium and compatibility, a set of eight equations were derived to predict the torsional strength and to determine the angle of twist and the strains in the steel and concrete at any stage of loading. These equations are solved by trail and error procedure. Hsu and Mo then proposed the design recommendations, such as design limitations, design consideration, minimum reinforcement, and design procedure [19].

1.5.2 Skew-Bending Theory:

This theory is much younger than Rauch's theory. It has been widely used to determine the ultimate strength of reinforced concrete member under pure torsion and torsion plus bending and shear. It was first proposed by Lessig in 1958 [14]. The basic characteristic of the skew-bending theory is the assumption of a skew failure surface. The failure surface is initiated by a helical crack on three faces of a rectangular beam, while the ends of this helical crack are connected by a compression zone near the fourth face as shown in figure (1.4). A region close to the line connecting the crack ends is considered to be in compression and the steel in this region is neglected. All bars outside the compression zone are to be in tension and to be stressed to yield [20].

Based on this failure surface, Lessig used two equilibrium equations: equilibrium of moment along the neutral axis x - x, and the equilibrium of forces along an axis perpendicular to the compression zone. By minimizing the moment equilibrium equation, it was found that a theoretical minimum torsional resistance occurs when the neutral

axis x-x is parallel to either a shorter face or a longer face. This results in two modes of failure.

Mode 1 failure, in which the flexural dominates, has the compression zone near the top face of the beam.

Mode 2 failure, in which the torsional moment and shear force dominates, the compression zone is along aside face as in figure (1.4).

Hsu [20] stated that Lessig's theory considers both combined resistance of concrete and reinforcement and the redistribution of stresses, but despite the ability of Lessig's theory to explain the general behavior of reinforced concrete beam loaded in pure torsion it overestimates torsional resistance, and it is dose not satisfactorily explain the following four observed phenomena :-

1- The shorter leg of stirrups usually has only small tensile stresses at ultimate. Occasionally these legs are in compression. Lessig assumed that they yield in tension.

2- Diagonal cracks on the wider face may turn at the corners and extend perpendicularly into short face. Therefore the cracks on the shorter face frequently form an angle much less than (45°).

3- The two surfaces on both sides of a crack at a corner of a rectangular beam are offset, indicating the presence of dowel action in the longitudinal corner bars. This dowel action was confirmed by the bending stresses measured from diametrically opposite sides of a longitudinal corner bar. However, such dowel action was not considered in the Lessig theory.

4- At ultimate torque, the cracks at the center and on the shorter faces are wider than those at the center of the wider faces. This indicates that the free body must rotate about an axis other than the neutral axis assumed by Lessig.

To overcome these discrepancies Hsu in 1968 [20] (figure (1.5)) proposed the failure surface to be a plane perpendicular to the wider face and inclined at (45°) to the axis of the beam. The only difference between this proposed failure surface and that of Lessig in figure (1.4) is that the proposed surface intersects the shorter faces of the cross section by lines at 90^{0} to the axis of the beam, instead of about 45° as assumed by Lessig.

This proposed failure surface does not intersect the shorter legs of the stirrups; thus it omits entirely any torsional resistance contributed by the stirrup forces of the shorter legs. Consequently, this failure surface tends to give a conservative ultimate torque, the theoretical minimum with respect to the angle between intersection lines on the shorter faces and the beam axis [20].

Based on this failure surface Hsu derived this equation to calculate ultimate torque:

$$T_u = T_c + \alpha_t \frac{x_1 y_1 A_t f_{sy}}{S_1} \qquad (1.20)$$

where:-

T_u: the ultimate torque of reinforced concrete rectangular member.

Tc: the torsional resistance contributed by concrete.

α_t: a coefficient given by:

$$\alpha_t = 0.66m\frac{f_{Ly}}{f_{sy}} + 0.33\frac{x_1}{y_1} \le 1.5 \qquad (1.21)$$

m : the ratio of volume of longitudinal bars to volume of stirrups.

An experimental study by Hsu [21] revealed that, for the same overall dimension and reinforcement, the failure torque of solid and hollow rectangular beams are equal.

Therefore, the term T_C can only be attributed to the contribution of shear resistance of the diagonal concrete struts [21].

The coefficient α_t used in Hsu's equation is considerable less than Rausch's coefficient (2.0). Tests by Hsu [21] showed that Rausch's equation is unconservative.

The skew bending mechanism of the torsional failure was investigated by Collins, et al [22]; they had developed a theory based on the analysis of four idealized failure modes of rectangular beams as shown in figure (1.6), to predict the strength of web reinforced beams loaded in combined shear, bending, and torsion. The failure surface is assumed to be bounded on three sides and on the fourth side by a compression zone connecting the ends of spiral crack.

Mode 1: failure surface, where the beam subjected to bending plus torsion, is defined as failure surface where the compression zone is at the tope face.

Mode 2: when the beam is subjected to low shear and high torsion, the failure surface is defined as failure surface where the compression zone forms adjacent to one of the vertical sides of the beam where the

shear and torsional stresses are subtractive, while cracking starts on the other vertical side where the shear and torsional stresses are additive.

Mode 3: in the beams with less top reinforcement than bottom reinforcement, the compression zone could form adjacent to the bottom face in this mode.

Mode 4: failure surface is defined as one where the compression zone forms to adjacent the top corner face, when the beam is subjected to high shear and low torsion.

1.6 Combined Bending and Torsion in Concrete Beams

Beams are rarely subjected to pure torsion, and then it is more practical to study beams under the combined effect of bending and torsion.

Using a similar skew bending failure plane shown in figure (1.7) where the beam is subjected to an additional bending moment (M). The equilibrium of the internal and external moments about the assumed failure plane, using the reduced value for the concrete tensile bending stress thus [2]:

$$M.\cos\beta + T.\sin\beta = \frac{b^2.h}{6}(0.85 f_r / \cos\beta) \qquad (1.21)$$

from which

$$T(\psi.\cos\beta + \sin\beta) = \frac{b^2.h}{6}(0.85 f_r / \cos\beta) \qquad (1.22)$$

where:

$$\psi = \frac{M}{T}$$

Then,

$$T = \frac{0.85}{3} b^2 .h.f_r \left[\frac{1}{2\cos\beta(\psi.\cos\beta + \sin\beta)} \right] \qquad (1.23)$$

To find the minimum cracking torque and angle of inclination (β), equation (1.23) is to be differentiated and equaled to zero [9].

$$\frac{dT}{d\beta} = \frac{0.85}{3} b^2 .h.f_r \frac{d}{d\beta}\left[\frac{1}{2\cos\beta(\psi.\cos\beta + \sin\beta)} \right] = 0$$

or:

$$\frac{d}{d\beta}\left[\frac{1}{2\cos\beta(\psi.\cos\beta + \sin\beta)} \right] = 0 \qquad (1.24)$$

For beams with $\psi = 1$, *then* $\beta = 22.5^\circ$

$\psi = 2$, *then* $\beta = 13.3^\circ$

When comparing equation (1.23) with equation (1.12) it is clearly noticed that the term $\left[\frac{1}{2\cos\beta(\psi.\cos\beta + \sin\beta} \right]$ can be considered as a modifying factor to include the effect of bending moment. It is also noticed that if the value of (β) is (45°), then the corresponding value of (ψ) is zero. In other words, such indication is only expected in the pure torsion condition.

The above expressions define the minimum cracking torque in plain concrete section, while the cracking torque values for reinforced concrete sections are somewhat higher. This difference is overcome by applying certain modifying factors to the above equations. Hsu [23] proposed the factor $(1 + 0.04\rho_t)$ to include the effect of reinforcement, accordingly:

$$T_{cr} = (1 + 0.04\rho_t) T_u \qquad (1.25)$$

where; (ρ_t) is the ratio of the total volume of reinforcement including longitudinal and transverse steel to the volume of concrete, expressed as a percent.

1.7 Design for Torsion in ACI-318-Code

Until the late 1960, the development of recommended design process for reinforced concrete beams subjected to torsion in addition to bending and shear was very slow. The first recommendations by the ACI-Code in 1963 [24] were when it stated that torsional stress should be considered in the design but gave no provisions for allowable stresses in indeterminate structure. The first guide to designers became available in 1969 [25]. The ACI-Committee-438 recommended that torsion should be neglected if the ultimate shear stress due to torsion was less than $\left(0.11\sqrt{fc'}\right)$. This stress corresponding to about 25% of pure torsional strength of a member without web reinforcement. While for section with a shear stress greater than $\left(0.11\sqrt{fc'}\right)$ the contribution of concrete for each of torsional and shear stresses was given by:

$$\tau_{ca} = \frac{\tau_c}{\sqrt{1 + (3v_u/\tau_u)^2}} \quad \text{and} \quad v_{ca} = \frac{v_c}{\sqrt{1 + (\tau_u/3v_u)^2}}$$

where:-

τ_{ca} = the shear stress due to torsion, carried by concrete when the member is subjected to torsion only.

v_{ca} = the shear stress due to flexural shear, carried by concrete, when the member is not subjected to torsion.

τ_u = ultimate shear stress due to torsion.

v_u = ultimate shear stress due to flexural shear.

Any additional shear stresses shall be resisted by stirrups of closed types since diagonal cracks due to torsion should appear on all side of the section. In additional further longitudinal steel reinforcement equal in volume to that of closed stirrup was to be distributed around the beam.

The ACI-Code of 1971 [26] adopted the recommendation made by ACI-Committee-438 and gave the value for the ultimate torsional shearing stress as $\left(\tau_u = \frac{3Tu}{bh^2}\right)$ which can be applied only if the torsional moment (Tu) is known .

The various version of the ACI-318 Code [27] used the skew bending theory for the design of beams under torsion and the ultimate strength of members subjected to torsion may be calculated by equation below:

$$Tu = \phi\left(\frac{\sqrt{f'c}}{15}\sum x^2 y + \alpha_t \frac{A_t X_1 Y_1 f_{sy}}{S}\right) \qquad (1.26)$$

where:

$\phi = 0.85$

$\alpha_t = 0.66 + 0.33\left(\frac{Y_1}{X_1}\right) \le 1.5$

The new ACI-Code-318 [28] criteria adopted the space truss analogy. According to this, beam subjected torsion is idealized as a thin-walled tube with the concrete core in a solid beam neglected as shown in figure (1.8). Once the reinforced concrete beam has cracked in torsion, its torsional resistance is provided primarily by the closed stirrups and longitudinal bars located near the surface of the member. In a thin-walled tube analogy the resistance is assumed to be provided

by the outer skin of the cross-section roughly centered on the closed stirrups. Both hollow and solid sections are idealized as thin-walled tubes both before and after cracking.

In a closed thin-walled tube, the product of the shear stress τ and the wall thickness t at any point in the perimeter is known as the shear flow, $q = t\tau$. The shear flow q due to torsion acts as shown in figure (1.8) and is constant at all points around the perimeter of the tube. The path along which it acts extends around the tube at midthickness of the walls of the tube. At any point along the perimeter of the tube the shear stress due to torsion is:

$$\tau = \frac{T}{2A_0 t} \tag{1.27}$$

where:

A_0: the gross area enclosed by the shear flow bath

t: the thickness of the wall at the point where τ is being calculated.

The shear flow path follows the midthickness of the walls of the tube and A_0 is the area enclosed by the path of the shear flow. For a hollow member with continuous walls, A_0 includes the area of the hole.

It can be noted that the former elliptical interaction diagram between shear and torsion which was used in the former version of the ACI-codes [29] has been eliminated.

The ultimate torsional strength of member according to the ACI (318-05) is given as:

$$Tu = \phi\left(\frac{1.7A_{0h}A_t f_{sy}}{S}\right) \tag{1.28}$$

where:

$\phi = 0.75$

A_{0h}: gross area bounded by centerline of outermost closed stirrups.

1.8 Artificial Neural Networks

In recent years, there has being a growing interest in a class of computing devices that operate in a manner analogous to that of biological nervous system. These devices, known as artificial neural networks (ANN), or connectionist systems. Artificial neural networks are finding applications in almost all branches of science and engineering. Recent development of neural networks offers powerful tool to be used in applications of civil engineering.

1.9 Aim of Study:

The main objective of the present investigation is to use the Artificial Intelligence (AI) known Artificial Neural Network (ANN) as an alternative to mathematical modeling or experimental testing. The study represents an attempt to use ANN for quick prediction of ultimate strength of rectangular reinforced concrete beams subjected to pure torsion and to combined torsion with bending.

After building the proper network, the effect of various parameters on the behaviour of beams is to be investigated and discussed.

1.10 Layout of the Thesis:

This thesis is divided into five chapters. ***Chapter one*** presents a general introduction that deals with the behaviour of reinforced concrete members subjected to torsion and also describes the objectives and scope of the work.

Chapter Two presents a review of the experimental studies on reinforced concrete members subjected to pure torsion, and in combination with torsion and bending. A review of application of artificial neural network in civil and structural engineering is also given.

Chapter Three, deals with the principle of artificial neural network, neuron model and architectures, training of the network, back-propagation and back prorogation algorithm.

Chapter Four, describes the development of two artificial neural networks, first for beams subjected to pure torsion and second for beams subjected to combined torsion and bending. Discussion of the results and observations for each network models is provided.

Finally, ***chapter five*** summarizes the conclusions drawn from this research. Also, suggestions for future works are given.

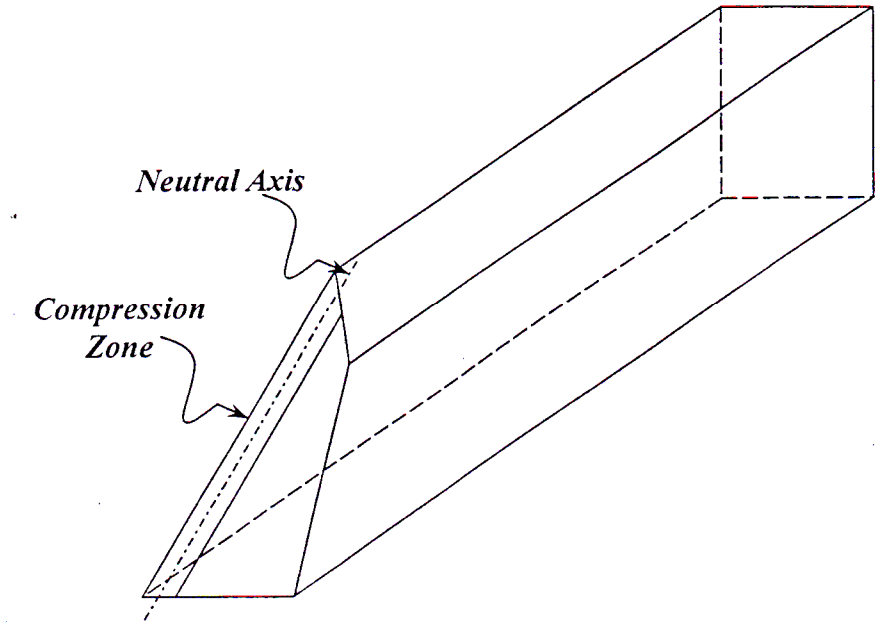

Fig. (1.1) Skewed Bending Failure of Rectangular Beam Subjected to Pure Torsion

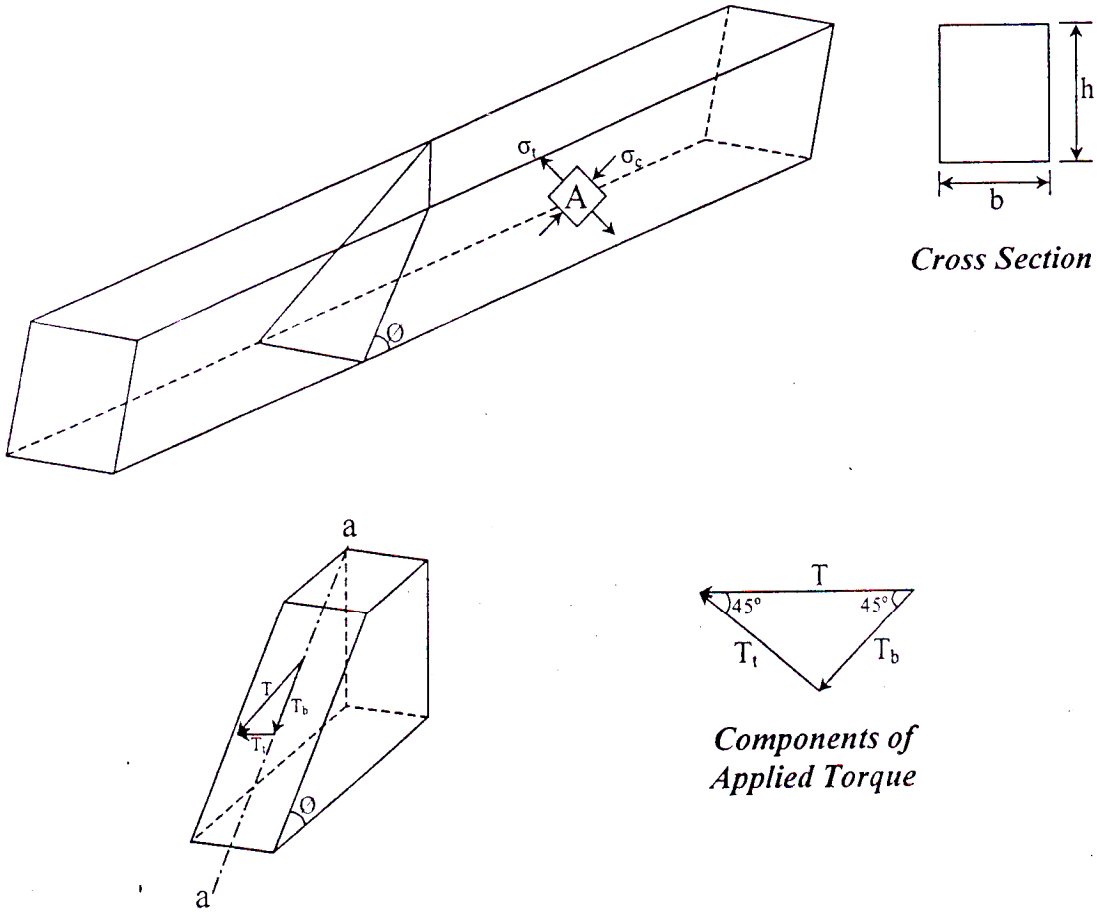

Fig. (1.2) Components of Applied Torque on the Failure Surface

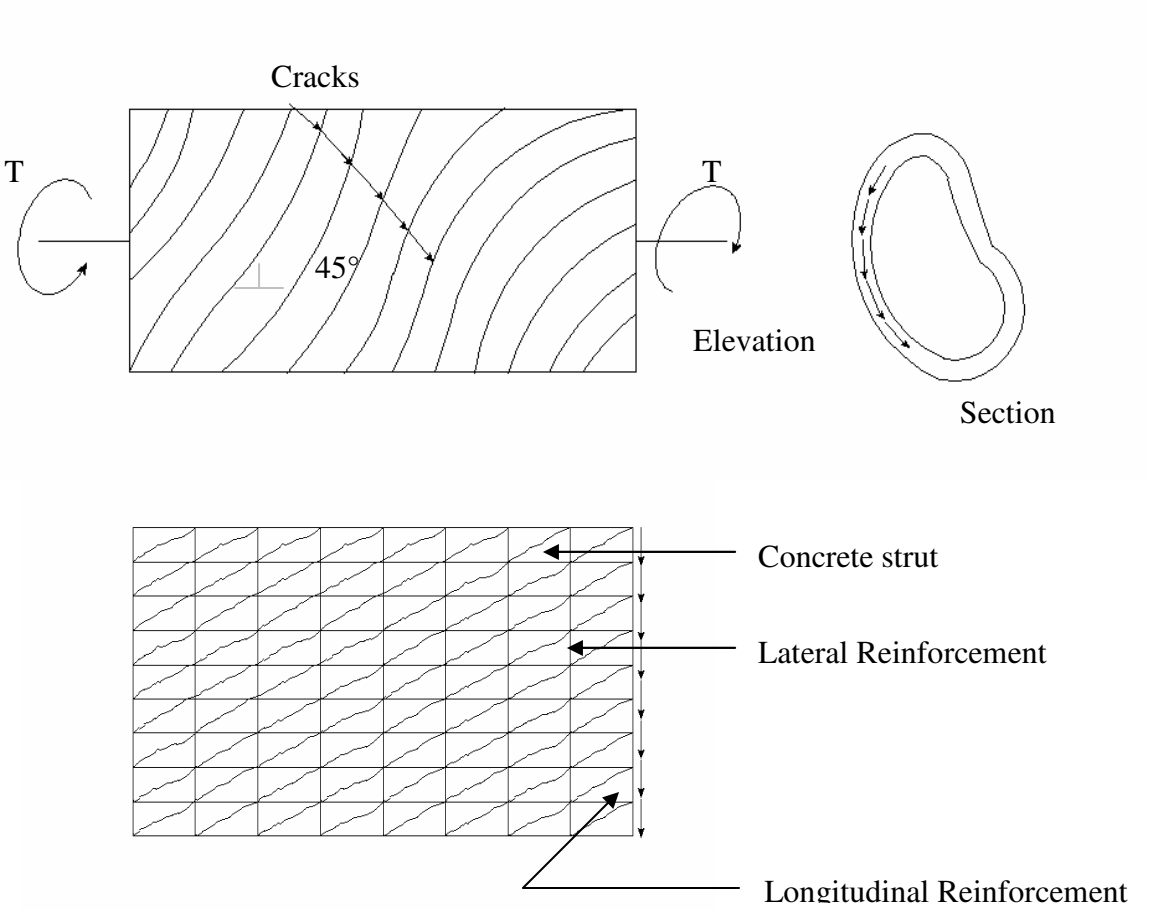

Fig. (1.3) Space Truss Analogy

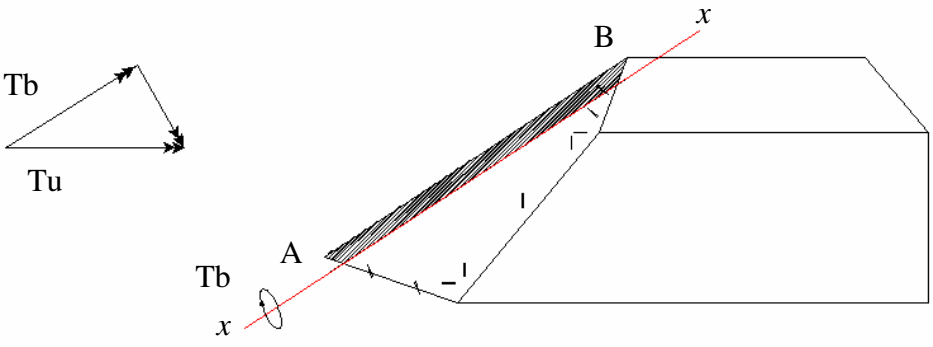

Figure (1.4) Failure Surface of Free Body According to Lessig's Theory

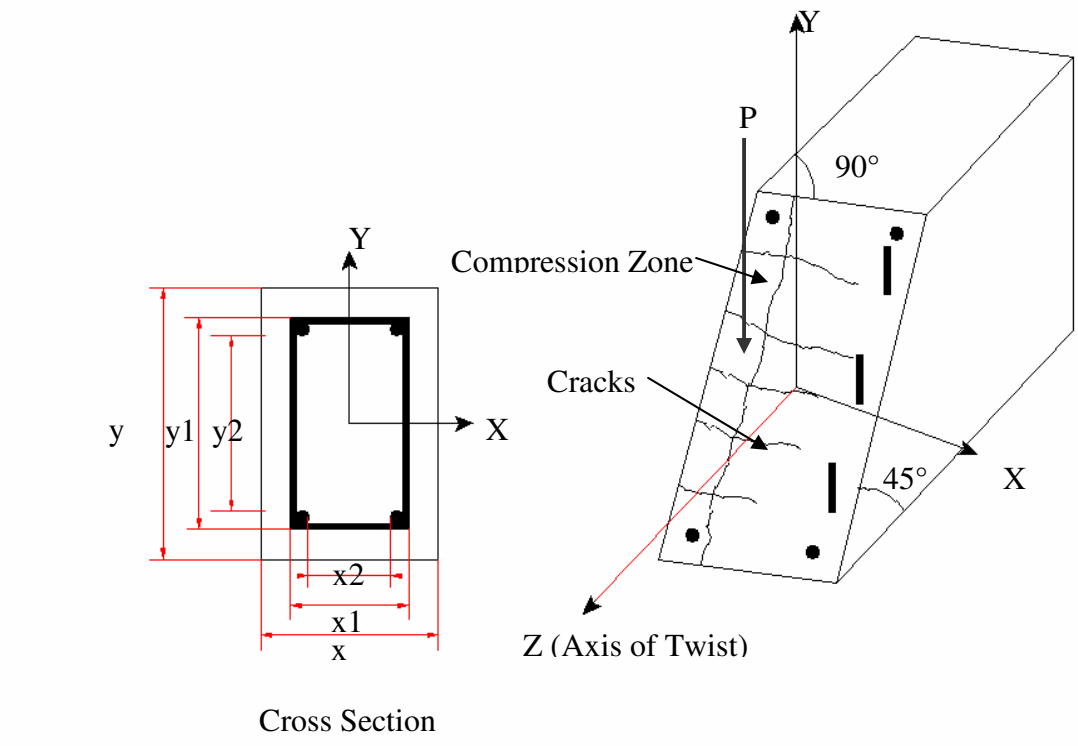

Figure (1.5) Proposed Failure Surface for Skew-Bending Theory

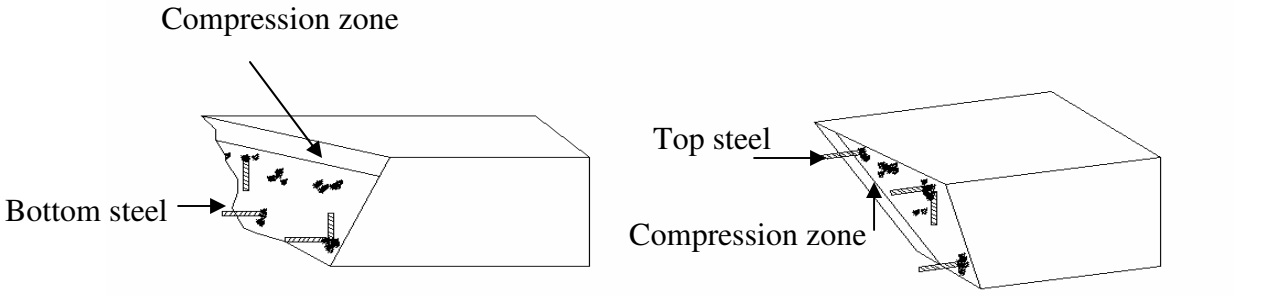

a- Mode 1(bending & torsion) **b- Mode 2(low shear & high torsion)**

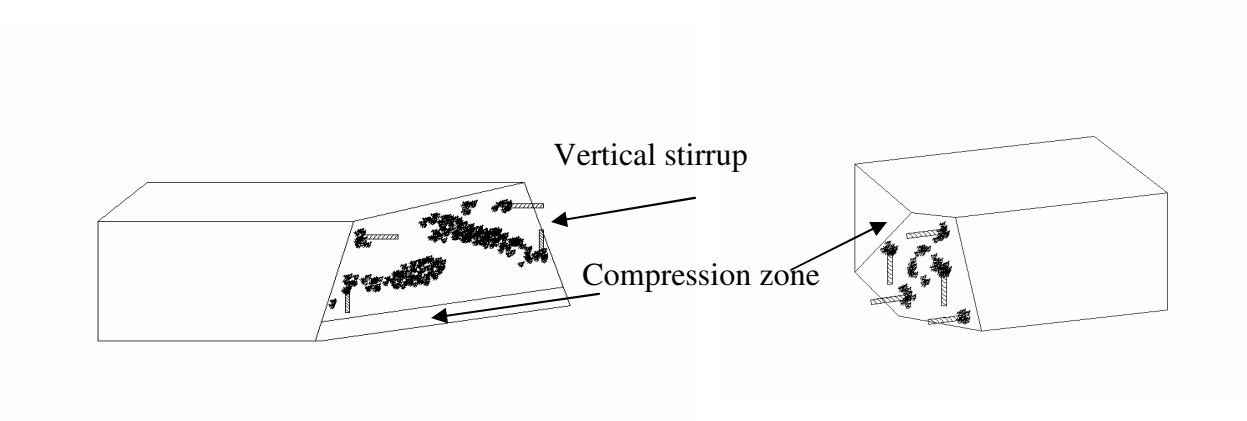

c-Mode 3 (low bending & high torsion weaker top steel)

d-Mode 4 (high shear & low torsion)

Figure (1.6) Idealized Failure Modes for Web Reinforced Concrete Beams

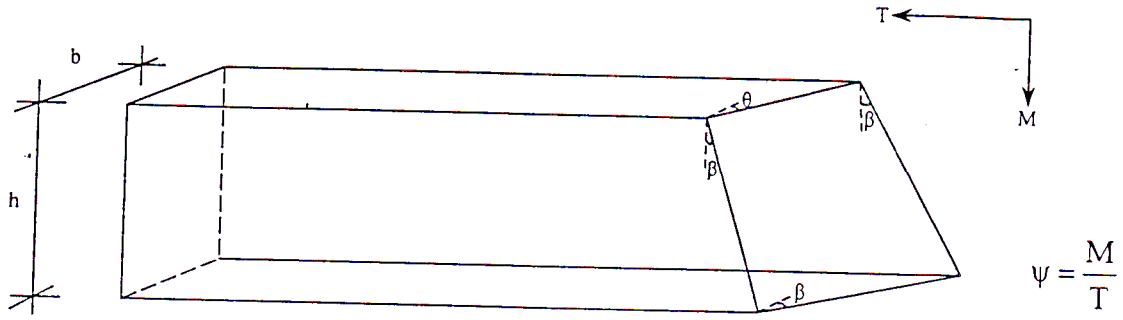

Fig. (1.7) Assumed Failure Surface in Combined Bending and Torsion

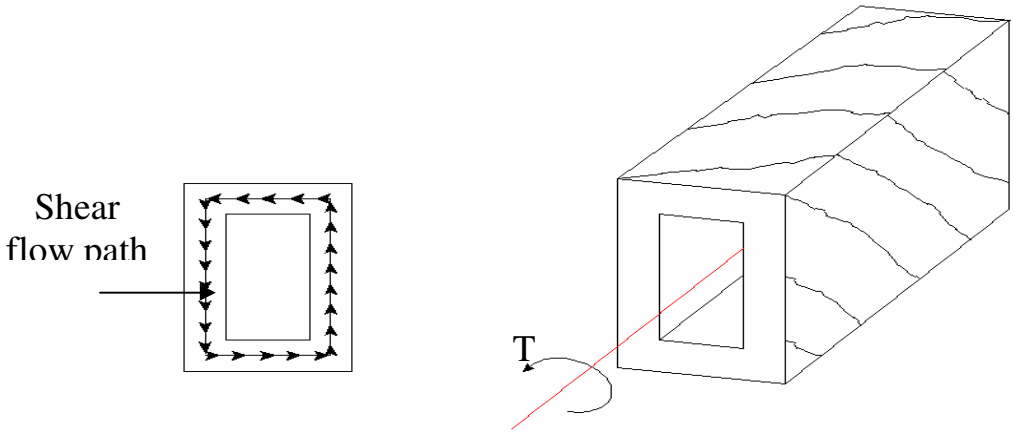

a- Thin Walled Tube

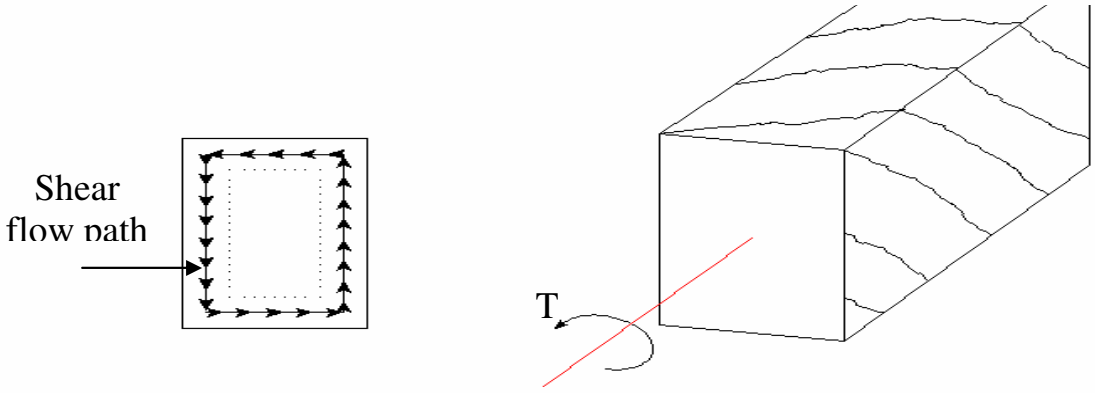

b- Area Enclosed by Shear

Figure (1.8) Thin -Walled Tube Analogy

Chapter Two

Literature Review

2.1 Torsional Behaviour of Reinforced Concrete:

Ernst 1957 [30] tested eighteen reinforced concrete rectangular beams under pure torsion. The principal object of this investigation was to determine the quantity of the transverse steel required to develop the yield point in longitudinal bars placed in the corner of the rectangular beams. The eighteen beams were classified into three groups, each of which consists of six beams. The diameters of longitudinal bars in the four corners of cross section were varied in these groups. The used bars were of (10, 12, and 16 mm) diameter. Transverse ties (6 mm diameter) were spaced at (711, 355.6, and 101.6) mm, and also in pairs at 101.6 mm for each groups. One beam in each group was without transverse reinforcement, and the normal compressed concrete strength of all groups was (27.6 MPa). Results indicated that yield strains can be developed in longitudinal corner bar as well as in transverse ties, resulting in either a diagonal tension type of fracture or hybrid failure in transverse shear and diagonal tension. Initial cracking corresponded to the failure of unreinforced concrete in torsion for all beams was at an average unit shearing stress of (2.15 MPa). Evidence also developed supporting the concept of a transition from elastic to plastic state of stress as the ratio of transverse to longitudinal steel approaches unity.

Gesund and Boston 1964 [31] tested ten rectangular concrete beams under combined bending moment and torsional loads. Eight beams were (200*200 mm) square and two beams were (150*300 mm). The beams contained only longitudinal reinforcement. The concrete strength, amount of reinforcement, and moment-torque ratios were varied. It was found that if there is no transverse reinforcement, the dowel action of the longitudinal reinforcement is of paramount importance in resisting the torsion.

Gesund, Schuette, Buchannan, and Gray 1964 [32] tested to destruction twelve rectangular concrete beams under combined bending and torsional loads. The beams contained both longitudinal and transverse reinforcement. The concrete strength, amount and spacing of reinforcement and moment-to-torque ratios were varied. The main conclusion drawn from this investigation was that transverse reinforcement will transform torque on a reinforced concrete beam into additional bending.

Ramakrishnan and Vijayarangan 1965 [33] tested eighteen reinforced concrete beams subjected to combined bending and torsion. The beams were divided into four series, each series having the size and spacing of reinforcement as variables. The purpose of the experiment was to study the influence of web reinforcement on the ultimate torsional resistance of beams, modes and characteristics of failure in beams, and the torque-twist relationship. Results showed that inclined stirrups increases the strength of the beam considerably more than vertical stirrups.

Hsu 1968 [9] tested ten plain concrete members of rectangular cross-section subjected to pure torsion. Such members were found to fail by bending about an axis parallel to the wider face and inclined at 45 deg. to the longitudinal axis of the member. Based on this failure mechanism, new equations were proposed for the ultimate torque.

Hsu 1968 [21] studied the behaviour of rectangular concrete beams reinforced with both longitudinal and stirrups under pure torsion. Fifty-three beams were tested, involving eight major variables. These variables were amount of reinforcement, solid section versus hollow beams, ratio of volume of longitudinal bars to volume of stirrups, concrete strength, scale effects, depth to width ratio of cross-section, spacing of longitudinal bars, and spacing of stirrups. The behaviour before and after cracking was extensively studied. Provisions of different codes and theories for reinforced concrete design in torsion were evaluated. Design equations for ultimate torque, stiffness before and after cracking, angle of twist at ultimate torque, and at cracking torque and other provisions were given.

Klus 1968 [34] tested ten reinforced concrete rectangular beams with normal percentage of both longitudinal and transverse steel, and interaction of their torsional and flexural shear capacities was developed. The tests were pertaining to only one cross section, one reinforcement arrangement, one concrete strength, and one physical loading condition. The first tests were in pure torsion and in pure flexural shear to provide the ultimate capacities in the two failure modes. The subsequent tests were in combination of torsion and

shear. The tests investigated the complete range of interaction between torsion and flexural shear in the reinforced concrete rectangular beams with stirrups, and the significance of them appears from the fact that the effect of variation of stirrup percentage on the interaction curve has no experimental support. It was found that based on the theory which states that the unreinforced section fails shortly after the first crack, the interaction curve would approach the straight-line concept. Using this as the base, it was suggested that greater percentage of transverse steel would increase the curvature of the interaction, that was assuming that adequate longitudinal steel was available.

McMullen and Warwaruk 1969 [35] tested eighteen rectangular reinforced concrete beams to failure under various combinations of bending and torsion. The principal variables were the ratio of twisting moment to bending moment and the reinforcement configuration. Three different modes of failure were absorbed. Idealized failure surfaces were defined and expressions for the strength of the beams were derived using an equilibrium approach. Test results showed that a beam provided with less top longitudinal reinforcement than bottom and subjected to either pure torsion or torsion in combination with a small bending moment deflects upwards after cracking of the concrete has occurred and exhibits an upward deflection at failure. This type of beams exhibited a greater torsional strength when it is subjected to pure torsion. Results also indicated that the presence of flexure does not increase the torsional strength of a beam that is provided with equal top and bottom reinforcement.

Lampert and Thurlimann 1969 [36] tested seven reinforced concrete beams in combined bending and torsional loads. The beams were (508*508 mm) square in size. All beams except one were of hollow sections and contained longitudinal and transverse reinforcement. The main variable was the ratio of torsion to bending for a given arrangement of reinforcement. Tests confirmed the validity of the space truss failure model in combined torsion and bending. Inclination of the diagonals depends upon the ratio of transverse to longitudinal steel and on the ratio of torsion to bending.

McMullen and Rangan 1978 [37] tested ten beams in pure torsion. The five beams of series A were (254 * 254 mm) square and the other five beams of series B were (178 * 356 mm). The principal variables being aspect ratio and amount of reinforcement. Results of tests showed that, other things beings constant, the strength decreases with an increase in aspect ratio. Equations were derived for ultimate torque and minimum reinforcement. Correlation between predicted and experimental strength was good, not only for the ten beams tested but for sixty four others available in the literature.

Ewida and McMullen 1982[38] tested twelve reinforced concrete rectangular beams in different combination of shear and torsion. The beams were divided into three categories according to the reinforcement provided. They were under-reinforcement, partially over-reinforcement, and completely over-reinforcement. Both longitudinal reinforcement and stirrups were provided in all beams, and the beams were instrumented to enable measurement of angle of twist, reinforcement strain and concrete strain. Vertical and torsional

loads were applied simultaneously and monotonically in predetermined increments, and the size of each increment was reduced in the latter stages of the test. The ratio between the vertical and the torsional loads was kept constant during test. The results obtained using the analysis presented in this study was compared to the test results and to the results of beam that were tested by other investigators. The analysis developed was found to satisfactorily predict the deformation at all levels of load and the length of beams under combined torsion and shear.

Abas 1985 [39] tested twelve reinforced concrete rectangular beams subjected to torsion, bending, and shear. All beams have a same nominal cross section and quantity of longitudinal of reinforcement. The effect of the amount of stirrups, torque-moment ratio in combined bending and torsion, and torque-to-shear in combined bending, shear, and torsion were examined. Using optimization approach, simple non-dimensional interaction equation representing, non-dimensional interaction surface and curves were developed. These equations were presented as a suggested approach for designing reinforced concrete beams subjected to combined loading. These theoretical approaches gave a reasonable prediction for test results, obtained from the available literature, of ultimate strength of reinforced concrete beams under combined loading.

Rasmussen and Baker 1995 [40] tested series of reinforced normal concrete (NSC) and high-strength concrete (HSC) beams subjected to pure torsion. The test series consisted of twelve totally over-reinforced beams, with the concrete strength as the only variable.

Therefore, the cross sectional dimensions, and strength and quantity of the reinforcement, were constant for all beams. The concrete strength was varied between (36 to 110 MPa). The test series has shown the advantage of using (HSC). In addition to higher cracking load and higher ultimate torsional capacity, using of (HSC) for a given torque resulted in higher torsional stiffness, lower crack width, and lower reinforcement stresses compared to (NSC).

Rahal and Collins 1995 [41] investigated the effect of increasing thickness of the concrete cover on behavior of reinforced concrete section subjected to combined shear and torsion. Seven large reinforced concrete beams with two different thicknesses of concrete cover were tested at different shear-to-torque ratios, and relatively low bending. The testing program, experimental results, and interaction diagrams were presented. It was shown that increasing thickness of the concrete cover can substantially increase the strength of sections subjected to pure shear, or combined shear and torsion, but that it resulted in an undesirable increase in crack spacing. It was also shown that the sections subjected to combined shear and torsion experience lateral curvature.

Panchacharam and Belarbi 2002 [42] investigated the behaviour and performance of reinforced concrete members strengthened with externally bonded Glass Fiber Reinforced Polymer (GFRP) sheets subjected to pure torsion. The variables considered in the experimental study included the fiber orientation, the number of beam faces strengthened (three or four), the effect of number of FRP plies used, and the influence of anchors in U-wrapped test beams.

Experimental results revealed that externally bonded GFRP sheets can significantly increase both the cracking and ultimate torsional capacity of reinforced concrete members.

Chaisomphob, Kritsanawonghong, and Hansapinyo 2003 [43] investigated the capacity of rectangular reinforced concrete beams with stirrups subjected to combined bi-axial shear and torsion by using simple test method. The two main parameters in this study were eccentricity of the load which represents the magnitude of torsional moment, and tilted angle of specimens which represents the ratio of bi-axial shear. From the experimental results, it was found that the increase in the magnitude of torsion about 69 percent drastically decreases bi-axial shear capacity as much as 12 to 39 percent according to the ratio of bi-axial shears. The experimental results were compared with the capacities calculated by the available current design codes, ACI and JSCE, and it indicated that the current design codes give quite conservative values of ultimate capacity.

Abdalkarim 2004 [44] investigated the influence of section aspect ratio of fifty-four rectangular beam on the efficiency of ACI design codes. 54 beams of rectangular cross section that failed under pure torsion were considered in this work. These have been taken from literature. The rise of aspect ratio was found to have no influence on the factor of safety in the ACI-1999 method. In contrast, the aspect ratio has a significant effect in the ACI-1989 in such a way that the factor of safety decreases as the aspect ratio rises. However, the two methods become close in prediction as the aspect ratio approach 2. In addition, thirty –one further beams were investigated theoretically by

the two design methods: ACI-89 code (relying on the skew bending theory) and ACI-99 code (relying on the space truss analogy). It was found, in 31 theoretically tested beams, that at an aspect ratio of 1.67 the two methods gave similar predictions for torsional strength. At values of aspect ratio less than 1.67 the ACI-99 method is less conservative in requiring less reinforcement than the ACI-89 method. The opposite occurs with aspect ratio values greater than 1.67.

Chiu, Fang, Young, and Shiaw 2007 [45] investigated the behaviour of thirteen high-strength concrete (HSC) and normal-strength concrete (NSC) full-size beams with relatively low amount of torsional reinforcement. The crack patterns, the maximum crack widths at service load level, torsional strength, torsional ductility, and post-cracking reserve strength results of the experiments were discussed. The main parameters included the volumetric ratio of torsional reinforcement, the compressive strength of the concrete, and the aspect ratio of the cross section. It was found that the adequacy of the post-cracking reserve strength of the specimens with relatively low amounts of torsional reinforcement was primarily related to the ratio of the transverse to the longitudinal reinforcement factors in addition to the total amounts of torsional reinforcement. The minimum requirements of torsional reinforcement for NSC beams proposed by other researchers were also discussed on the base of test results of both HSC and NSC beams.

Ameli, Ranagh, and Dux 2007 [46] investigated behaviour of reinforced concrete beams strengthened with fiber reinforced plastics subjected to pure torsion. Twelve rectangular reinforced concrete

beams with cross-section (150*350 mm) were cast in two batches of six beams each. Beams of first batch were strengthened by carbon fiber (CFRP) whereas beams of second batch were strengthened by glass fiber (GFRP). The experimental results shown that CFRP materials increases the ultimate torsional strength more than GFRP. It was also found that the pattern of concrete cracks in the strengthened beams have a wider spread along the length compared to individual cracks formed in beams without strengthening.

2.2 General Application of Neural Networks in Structural Engineering

Most civil engineering systems are complex and are subjected to a wide variety of internal and external forces. Analyzing such systems is a difficult task and traditional tools that accurately predict and model the behaviour of such systems are limited in scope. As a result civil engineers have, in recent years, found increasing interest in neural network as an aid for both design and analysis. The first prototype application of neural networks as a tool for structural design was proposed by Vanluchene and Sun in 1990 [47]. The study demonstrated, through the use of three examples (a pattern recognition problem, a simple concrete beam design and analysis of a rectangular steel plate).

Hajela and Berke 1991 [48] used Backpropagation Neural Network (BPNN) to represent the force-displacement relationship in static structural analysis. Such models provided computational efficient capabilities for reanalysis and appeared to be well suited for

application in numerical optimum design.

Hajela and Berke 1992 [49] provides a broad overview of neural network computing applications in problems of structural analysis and design. Neural networks which require a supervised training approach were discussed, with special emphasis on their application in modeling functional relationships between some input and output quantities.

Szewezyk and Hajele 1994 [50] investigated the detection of damage in structural systems. It was formulated as an inverse problem and solved by neural network. Damage was modeled through reduction in the stiffness of structural elements, and manifests itself in the form of variations in observable static displacements under prescribed loads. A modified counter propagation neural network was used to develop the inverse mapping between a vector of the stiffness of individual structural elements and the vector of the global static displacements under testing loads. It was shown that the network functions as an associative memory device capable of static factory diagnostics even in the presence of noisy or incomplete measurements. Numerical examples involving frame and structures showed that the network approximations are fully acceptable from a practical standpoint.

Gagarin, Flood and Albrecht 1994 [51] described the application of neural networks to the problem of determining truck attributes (such as velocity, axle spacing and axle loads) purely from strain-response reading taken from the structure over which the truck is

traveling. The approach was designed to remove both the need for tape switches on the deck of the bridge to obtain such data and associated problems so as to provide a convenient and viable means of collecting bridge loading statistics. The application and performance of a radial-Gaussian-based networking system with its own training algorithm to the truck attribute determination problem was detailed. The chosen approach was a two layered modular network structure. This solution provided a fast, accurate, and convenient means of determining truck attributes.

Zeng 1995 [52] mapped a structural analysis problem onto continuous Hopfield neural network by means of the connection weights represented by the coefficient of the stiffness matrix and the nodal loads of bar, beam and triangular elements as the inputs to the network. The case study was carried out for 4-bar truss, a 7-bar truss, a 15-bar truss, a beam structure and a planar continuous structure. The analysis results converged to a stable state.

Mukherjee and Anmala 1996 [53] mapped the relationship between the slenderness ration, the modulus of elasticity and the buckling load for columns. As the input was taken directly from the experimental results, factors affecting the buckling load of columns are automatically incorporated in the model to a great extent.

Tully 1997 [54]developed four neural network to predict the following aspects of the overall behavior of a concrete slab load deflection behaviour, crack pattern at failure, concrete strain distribution, and reinforcing steel strain distribution. Results from experimental tests on thirty-four full scale slabs were utilized to

develop these four models, incorporating all of the parameters that govern their behaviour. The rationale behind and the details involved were explained for the setup, computer implementation and selection of each optimum neural network model. Results showed that the neural network technique can be used as a satisfactory alternative to experimental testing or detailed calculations to provide speedy predictions of all four aspects of the structural behavior of concrete slabs. A comprehensive spreadsheet tool was next created to incorporate all four the optimum neural networks.

Hajela 1998 [55] applied the binary Adaptive Resonance Theory (ART) neural network in the conceptual design of a structural system. Two distinct processes were considered. The first encompasses a class of structures where the structural layout was generally known and the load and support conditions were allowed to vary. The second class of problems was one where the loads and support points were assumed given, and the object of the design was to generate a near-optimal structural topology. The problem may be best understood as the use of ART networks to provide a memory capacity or knowledge base for design, from which information can be recovered upon presentation of relevant features.

Lu 2000 [56] used a two-layered backpropagation neural network to predict the local and distortional buckling behavior of cold-formed steel compression members. The topology of the neural network for the C-section without considering the effect of thickness was presented. Thus, the effects of the parameters, such as the number of nodes in the input layer, output layer and hidden layer, the pre-process

of the training patterns and the selection of the learning rate and momentum rate, on the behavior of neural network have been investigated. Further, the effect of thickness has been included in predicting the elastic local and distortional buckling behavior of cold-formed steel C-sections. Due to the slower convergence of the back-propagation algorithm, the faster algorithm called "resilient propagation algorithm" has been used to improve the performance of the neural network and the training. The generalization of the neural network was tested by the patterns not included in the training patterns. With this model, the elastic local and distortional behavior can be predicted by taking the whole section into account instead of separating the section into different parts. Once the neural network has been trained, the local and distortional buckling stress is obtained very easily and efficiently.

Bohigas 2002 [57] developed two artificial neural networks to predict the shear strength of reinforced concrete members based on database available from experimental tests. First network model was for members without stirrups reinforcement and second was for members contain both longitudinal reinforcement and stirrups. Based on the artificial neural network results, a parametric analysis was carried out to study the influence of each parameter affecting the failure shear strength.

Yildiz 2003 [58] used ANN to obtain a solution to assess the total lateral thrust and its point of application on non-yielding wall due to a strip load. Data used to trained neural network was obtained from the finite element analysis. A two layered back propagation type neural

network was used. An artificial neural network solution was obtained, as a function of six parameters including the shear strength parameters of soil (cohesion and angle of friction). The effects of each parameter on lateral thrust and point of application were summarized and the results were compared with the conventional linear elastic solution.

Hadi 2003 [59] discussed the application of neural network in concrete structures. Two applications of neural network were used and backpropagation network was chosen for the proposed network. Beam structures were selected in this study. The first application was reinforced concrete beam design and cost optimization. The beam design aimed at the estimation of the best dimensions, depth and width of its cross-section, and the cross-sectional area of reinforcement. The second application was the optimum design of fiber reinforced concrete beams. It was found that neural networks reduced the overall time required for implementations by a significant amount when compared with conventional methods.

Lima, Vellasco, Andrade, and Silva 2005[60] proposed the use of ANN to predict the flexural resistance and initial stiffness of beam-to-column steel joints using the back propagation supervised learning algorithm. Three types of steel beam-to-column joint were investigated: welded, endplate and polted with top, seat and double web angles, respectively. The neural networks results were proved to be consistent with experimental and design code reference values.

Hola and Schabowics 2005 [61] investigated the neural network identification of compressive strength of concrete on non-

destructively determined parameters. Basic information on artificial neural networks and the types of ANN most suitable for the analysis of experimental results were given. A set of experimental data for the training and testing of neural network was described. The data set covers a concrete compressive strength ranged from 24 to 105 MPa. The results showed that the artificial neural networks are highly suitable for assessing the compressive strength of concrete.

2.3 Summary

This chapter has reviewed the previous work related to neural networks in structural engineering. While it is apparent that a large amount and variety of applications of neural networks exists in this field, there is no application concerning the use of this technique to determine the ultimate strength of reinforced concrete members subjected to torsion. However, all of the previous works described provide significant insight into the development and modeling of a neural network for current investigation.

Chapter Three

Neural Networks Computation

3.1 –Introduction

Artificial neural networks (ANN) are computational networks that attempt to simulate the networks of nerve cells of the human or animal central nervous system [62]. They are collections of simple, highly connected processing elements that respond (or learn) according to sets of inputs. As such they are capable of realizing a greater variety of non-linear relationships of considerable complexity between input and output data sets [62].

Artificial neural networks can be trained to perform a particular function by adjusting the interconnections (weights) between neurons. Neural networks are trained to perform complex functions in different fields of application such as pattern recognition, classification, identification, speech, prediction, and control systems [58].

Engineers have used various tools to perform casual modeling (mapping from cause to effect for estimation and prediction) and inverse mapping (mapping from effect to cause) which include statistics, regression, probability, optimization, and others. The nature of neural network is to map from the input patterns to output patterns. Therefore an artificial neural network is another tool for engineers to perform both causal modeling and inverse mapping [58].

3.2-The Human Neural Network vs. Artificial Neural Networks

Although artificial neural network try to simulate some characteristics of human nervous system, their real behaviour is quite different.

The human brain consists of a large number of highly connected element called "neurons". These neurons have three principal components: the dendrites, cell-body, and axon as can be seen in figure (3.1-a) [63]. The dendrites are tree-like respective networks of nerve fibers that carry electrical signals into cell-body. The cell- body effectively sums and thresholds these incoming signals. The axon is a single long fiber that carries the signal from cell-body out to other neurons. The point of contact between an axon of one cell and a dendrite of another cell is called synapse. It is the arrangement of neurons and the strengths of the individual synapses, determined by a complex chemical process that establishes the function of the neural network [63].

An impulse, in the form of an electric signal, travels within the dendrites and thought the cell-body towards the pre-synaptic membrane of the synapse. Upon arrival at the membrane, a neurotransmitter (chemical) is released from the vesicles in quantities proportional to the strength of the incoming signal.

The neurotransmitter diffuses within the synaptic gap towards the post-synaptic membrane, and eventually into the dendrites of neighboring neurons, thus forcing them (depending on the threshold of the receiving neuron) to generate a new electrical signal as shown in figure (3.1-b) [64].

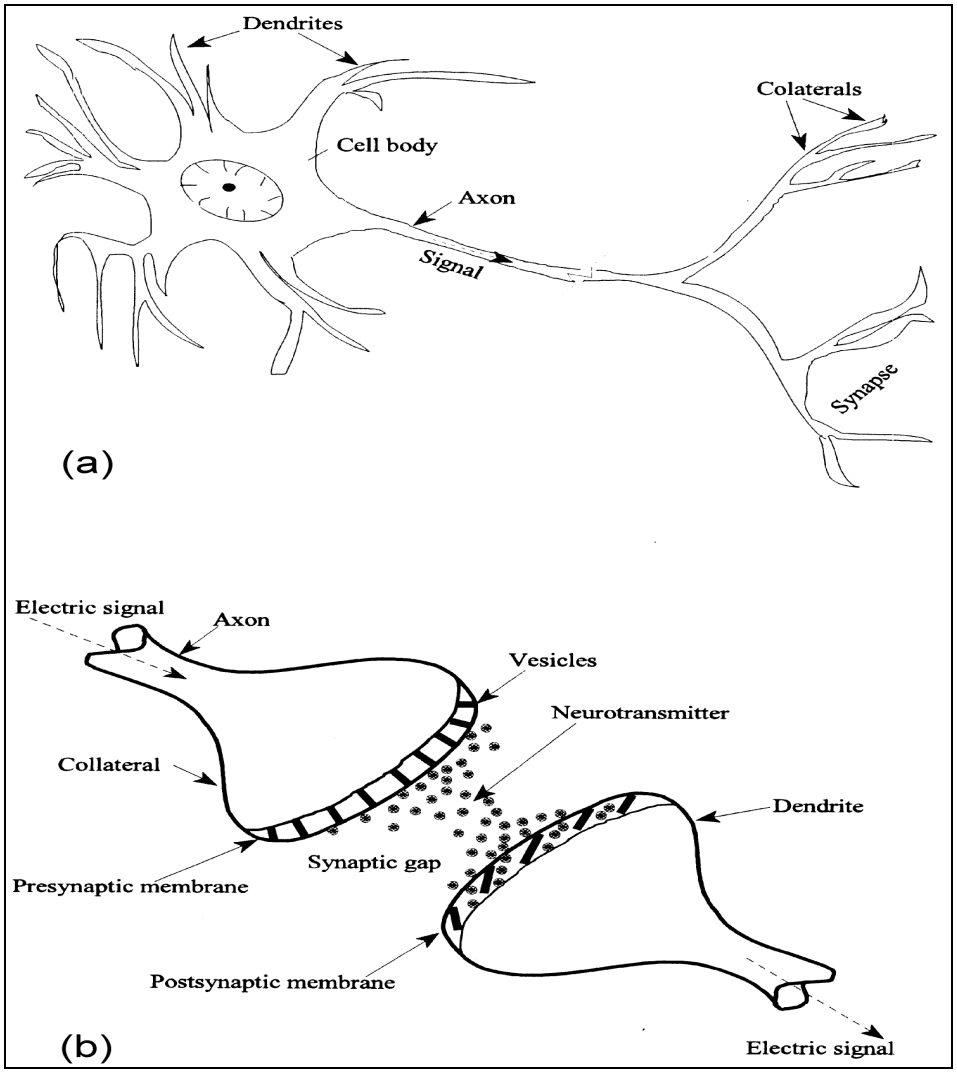

Figure (3.1) a-Schematic biological neuron. b- Mechanism of signal transfer between two biological neurons.

The generated signal passes through the second neuron(s) in a manner identical to that just described. The resulting inputs can be either excitatory or inhibitory. If the impulse is strengthened the synapse is excitory; else it is inhibitory [65].

The ability of the nervous system to adjust signals is a mechanism of learning, and the rate of firing an output (response) is altered by the activity in the nervous system.

Simply, a single neuron processes information by receiving signals from its dendrites, and produces an output signal which is then transmitted to other neurons.

The brain learns online, based on experience, and normally without supervision. During this process, the strength of connections between neurons changes, and some connections added or deleted. Learning in artificial neural networks are based on adjusting the weights of previously established internal connections to satisfactorily reproduce a training pattern of data. The learning process is generally controlled by the computer user [57]. ANN does not approach the complexity of the brain. There are two key similarities between biological and artificial neural network. First, the building blocks of both networks are simple computational devices that are highly interconnected. Second, the connections between neurons determine the function of the network [63].

3.3-Architecture of Neural Network

The commonest type of artificial neural network consists of three groups or layers, of units: input layer units connected to a layer of hidden units which is connected to a layer of output units as shown in figure (3.2). The function of input layer is to receive input or information from the outside world, and to pass this information to the network for processing. These may be either sensory input or signals from other systems outside the one being modeled.

The function of hidden layer is to extract and remember useful feature and sub-feature from the input patterns to predict the outcome

of the network (values of output layer). This layer link input layer to the output layer.

The function of the output layer is to receive the processed information from the neural network and sends the response to an external receptor.

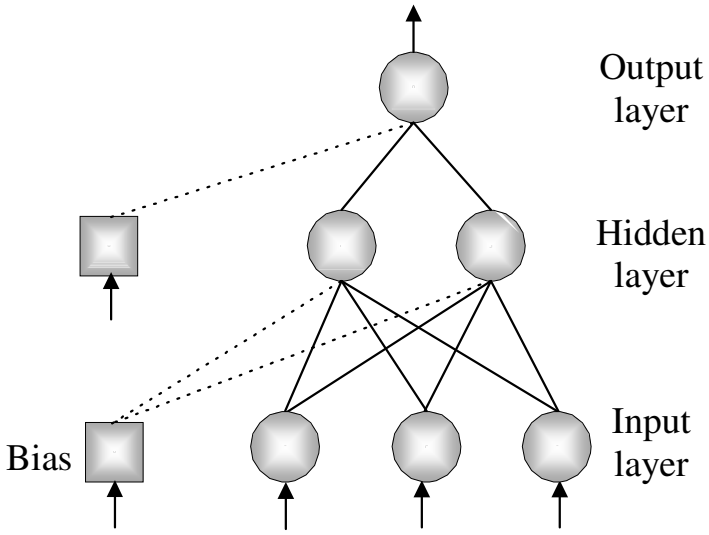

Fig. (3.2) Structure of a typical multilayer neural network

In figure (3.2) the bias acts on a neuron like an offset. The function of the bias is to provide a threshold for the activation of neurons. The bias input is connected to each of the hidden and output neurons in a network [66].

In engineering problems the numbers of input and output parameters are generally determined by design requirements. The number of input parameters determines the spatial dimensions of network and the number of output parameters determines the number of solution surfaces generated by network [67, 68]. The number of

hidden layers and neurons in the hidden layer(s) depends on the application of the network [69].

The units in a network are connected by a set of connections, or weights (w_{ij}), shown in figure (3.3). Each weight has a real value, typically ranged from ($-\infty$ to $+\infty$), although some times the range is limited. The value or "strength" of weight describes how much influence a unit has on its neighbor, a positive weight causes one unit to excite another, while a negative weight causes one unit to inhibit it.

3.4- Elements of Neural Networks

The basic component of a neural network is the neuron, also called “node”, or the “processing element, PE”. Nodes contain the mathematical processing elements which govern the operation of a neural network. Figure (3.3) illustrates a single node of a neural network, in which it can be distinguished:

(a) Inputs and Outputs

Inputs are represented by a_1, a_2, …, and a_n, and the output by b_j. Just as there are many inputs to a neuron, there should be many input signals to the processing element (PE). The PE manipulates these inputs to give a single output signal.

(b) Weighting Factors

The values w_{1j}, w_{2j}, …, and w_{nj} are weight factors associated with each input to the node. This is something like the varying synaptic strengths of biological neurons. Weights are adaptive coefficients within the network that determine the intensity of the input signal.

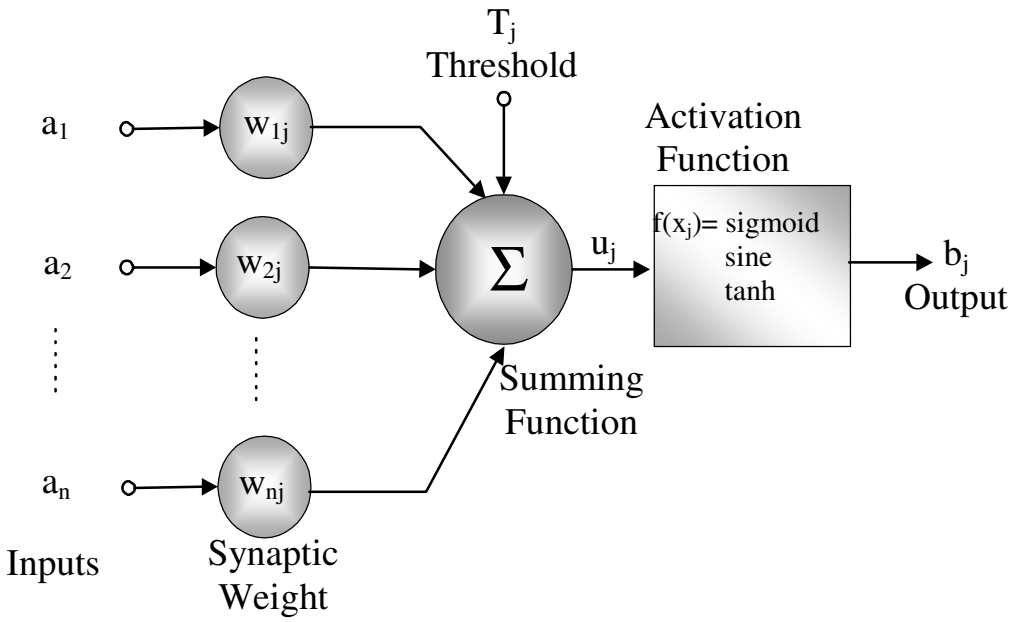

Fig. (3.3) Single node anatomy

Every input (a_1, a_2, …, a_n) is multiplied by its corresponding weight factor (w_{1j}, w_{2j}, …, w_{nj}), and the node uses this weighted input (w_{1j} a_1, w_{2j} a_2, …, w_{nj} a_n) to perform further calculations. If the weight factor is positive, then (wij ai) tends to excites the node. If the weight factor is negative, then (w_{ij} a_i) inhibits the node.

In the initial setup of a neural network, weight factors may be chosen according to a specified statistical distribution. Then these weight factors are adjusted in the development of the network or "learning" process.

(c) Internal Threshold

The other input to the node is the node's internal threshold, T_j. This is a randomly chosen value that governs the "activation" or total input of the node through the following equation [66].

$$\text{Total Activation} = u_j = \sum_{i=1}^{n} (w_{ij} a_i) - T_j \qquad (3.1)$$

The total activation depends on the magnitude of the internal threshold T_j. If T_j is large or positive, the node has a high internal threshold, thus inhibiting node-firing. If T_j is zero or negative, the node has a low internal threshold, which excites node-firing [66]. If no internal threshold is specified, a zero value is assumed.

(d) Transfer Functions

The node's output is determined by using a mathematical operation on the total activation of the node. This operation is called a transfer function. The transfer function can transform the node's activation in a linear or nonlinear manner [66]. Figure (3.4) shows several types of commonly used transfer functions.

The pure linear activation function is shown in figure (3.4-a).In the pure linear case, the function is simply f(x) =x .This function is not used very often because it is not very powerful: multiple layers of linear units can be collapsed into a single layer with the same functionality [70].

Sigmoid functions on the other hand have the advantages of non-linearity, continuity, and differentiability, enabling a multi layered network to compute any arbitrary real-valued function. Multilayer networks often used sigmoid transfer function that generates outputs between 0 and 1 as the neurons net input goes from a negative to positive infinity (figure (3.4-b)). This can be described in the following equation:

$$f(x) = \frac{1}{1 + e^{-x}} \qquad 0 \le f(x) \le 1 \qquad (3.2)$$

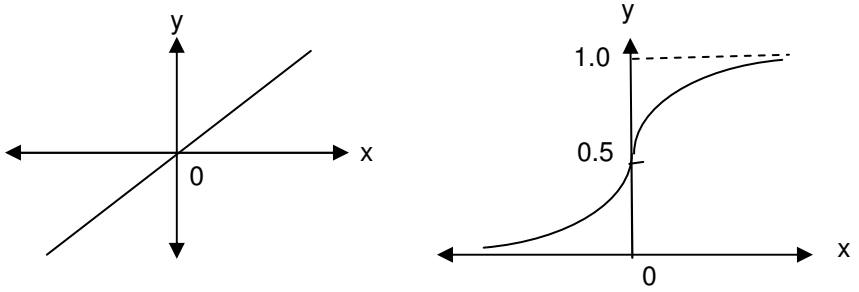

a) A pure linear transfer function

b) A sigmoid transfer function

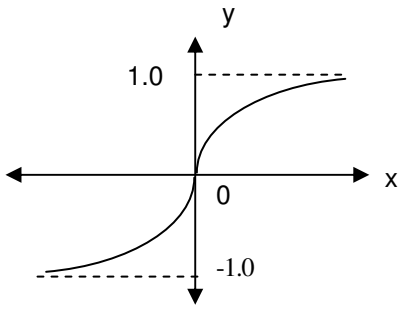

c) A hyperbolic tangent transfer function

Figure (3.4) commonly used transfer function

Alternatively, multilayer network may use the hyperbolic tangent transfer function shown in figure (3.4-c)that generates outputs between -1 and +1 as the neurons net input goes from negative to positive infinity as is described in the following equation

$$f(x) = \tanh(x) = \frac{e^{x} - e^{-x}}{e^{x} + e^{-x}} \qquad -1 \le f(x) \le 1 \qquad (3.3)$$

The hyperbolic tangent function is preferred over the sigmoid function for the following reasons [66]:

1. The output varies from -1 to +1 for the hyperbolic tangent and only 0 to 1 for the sigmoid function. This means that the hyperbolic tangent function has a negative response for a negative input value and a positive response for a positive input value, while the sigmoid function always has a positive response.

2. The slope of the hyperbolic tangent is much greater than the slope of the sigmoid function. This means that the hyperbolic tangent function is more sensitive to small changes in input

The output, bj, is found by performing one of these functions on the total of activation, xi.

3.5 Topology of a Neural Network

There are several general external arrangements for neural networks: single-input and single-output (SISO), multiple-input and single-output (MISO), and multiple-input and multiple-output (MIMO). The fourth arrangement, single-input and multiple-output (SIMO), is not generally used, because data for a single input are not sufficient to predict the behavior of several output variables. Any of these arrangements may have one or multiple hidden layers [71].

The most complex network arrangement is the MIMO network. In this type of network, input data for multiple variables are used to predict the values of multiple output variables. The MIMO network is particularly convenient for on-line applications (such as CNC machine and robot), as it can predict the values of several variables that may be of interest in the process with only a single pass of input data through the network. Figure (3.5) illustrates a MIMO network [71].

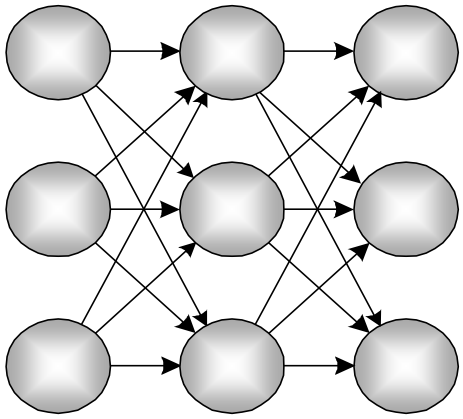

Fig. (3.5) Example of a MIMO feedforward network with three inputs, three outputs, and one hidden layer with three nodes

Most neural networks contain one to three hidden layers [72]. The function of the hidden layer is to intervene between the external input and the network output. The feedforward network of figure (3.5) is formed by cascading a group of single layers; the output of one layer provides the input to the subsequent layer. Large and more complex networks generally offer greater computational capabilities. These multilayer networks have greater representational power than single-layer networks if nonlinearity is introduced.

3.6-Data Selection of Neural Network

In order to ensure that the network has properly mapped input training data to the target output, it is essential that the set of patterns presented to the network is appropriately selected to cover a good sample of the training domain. A well trained network is one which is able to respond to any unseen pattern within an appropriate domain. At present neural networks are not good at extrapolating information outside the training domain [67].

The selection of an adequate number of training patterns is therefore, an extremely important issue. There are no acceptable generalized rules to determine the size of the training data for suitable training. Patterns chosen for training must cover upper and lower boundaries and a sufficient number of samples representing particular features over the entire training domain. Usually, data selection for neural network may be divided into two types: training set and testing set or validating set. The validating set of data should be contains approximately 15% of the total database [57]. The training phase needs to produce a neural network that is both stable and convergent. Therefore, selection what data to use for training a network is one of the most important steps in building a neural network model.

3.6.1 Training the Network

Training can be defined as the modification of the connection strength (weight) of the network by a specified learning rule to reach the desired solution. Training of the network required a set of data consists of input and output. The best "learning" possible, needs a large and robust set of historical input/output data.

3.6.2-Learning Modes

There are a number of approaches to training neural network. Most fall into one of two modes.

***(a) Supervised learning*:** in this mode the learning rule is provided with a set of examples (the training set) of proper network behavior: $(x_1,t_1),(x_2,t_2)...(x_n,t_n)$, where x_n is an input to the network, and t_n is the corresponding correct output (target). As the inputs are

applied to the network, the network outputs are compared to these targets. The learning rule is then used to adjust the weights and biases of the network in order to move the network outputs closer to the targets in the next epoch .This paradigm can be applied to many types of networks, such as feedforward and current networks.

(6) Unsupervised learning: In this mode the weights and biases are modified in response to network input only. There are no target output variables. Most of these algorithms perform clustering operations. They categorize the input patterns into a finite number of classes [73]. Such self-organizing networks can be used for compressing, clustering, quantized, classification, or mapping input data.

In *a feedforward network*, the direction of the signals flow is from the input layer through to the output layer via unidirectional connections. The interconnection between layers is from one layer to the next; no connection is there within the same layer.

In this work, a multi –layer perceptron (MLP) network (which is an example of feedforward neural network) is used.

3.7 Multi-layer Perceptron

The most used neural network is the multilayered perceptron (MLP). That is a feedforward model based on layers of neurons. It has been shown that almost any function can be represented by three layer neural networks [74].

The input to the network is referred as the input layer and units in the input layer are used as points in which input are applied to the network. Signals are prorogated forward from input layer through one

or more hidden layer(s) of units, to the output layer of nodes (figure (3.6)).

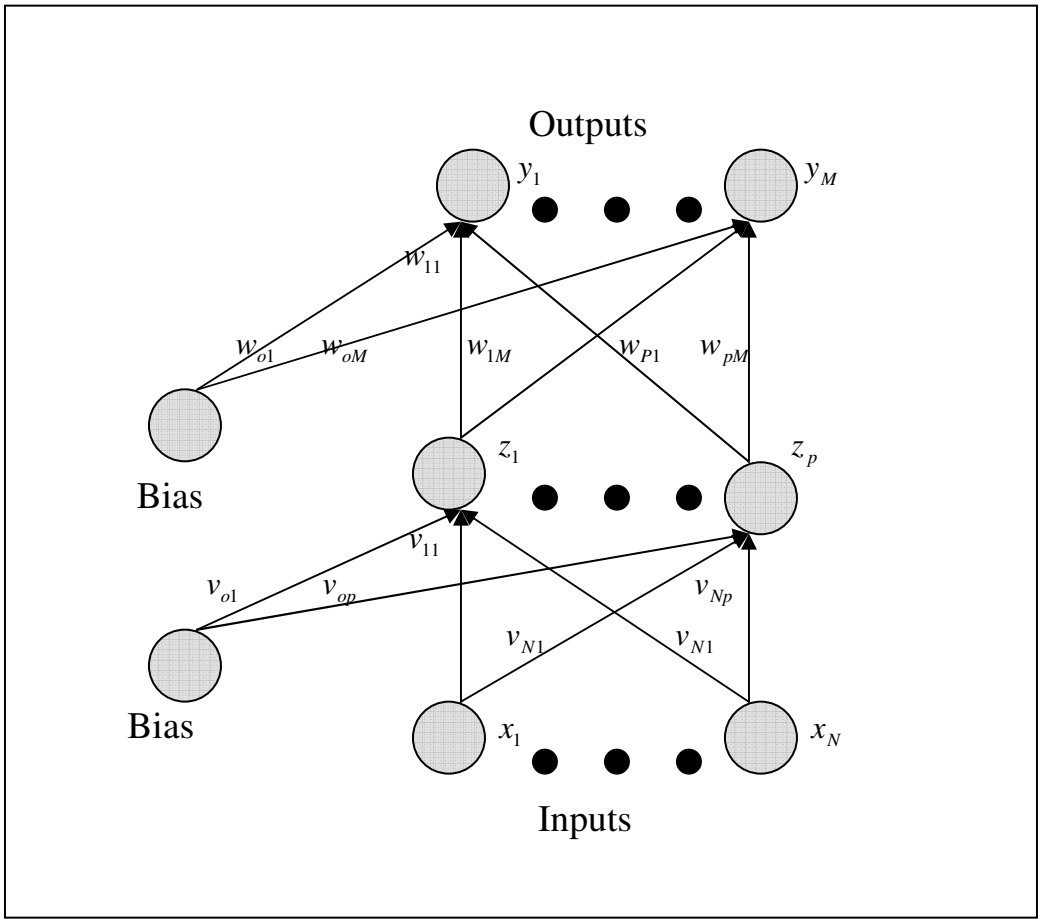

Figure (3.6) MLP General Architecture

3.8 Training Multi-layer Perceptron (Backpropagation)

As it has been mentioned before, multi-layer perceptrons are trained with supervised learning rules. Hopefully, a network that produces the right output for a particular input will be obtained. The most widely used supervised learning algorithm for neural networks is the backpropogation, also known as Error Backpropagation or Generalized Delta Rule. Training is implemented by adjusting the weights according to the error (the distance between the target and the

actual output vector) in the output layer that is measured by the following performance function usually called the mean-square error [70]:

$$E=\frac{1}{2}\sum_{p=1}^{p}\sum_{m=1}^{m}\left(t_m^p-y_m^p\right)^2 \qquad (3.4)$$

where p is the number of pairs of the input activation vectors x^p and the target activation vectors t^p, the corresponding output vector is y^p and m is the number of units in the output layer.

Errors in the output layer are "backpropagated" to the hidden layer, and weights are adjusted in the direction in which the performance function decreases most rapidly (the negative of the gradient). A small constant called the learning rate (α) is used to control the magnitude of weight modifications. Finding a good value for the learning rate is very important, if the value is too small, learning takes forever; but if the value is too large, learning disrupts all the previous knowledge. Unfortunately, there is no analytical method for finding the optimal learning rate; it is usually optimized empirically, through simple trying different values. The training algorithm can be realized via the following steps [74].

Step 0: all weights are initialized to small random values.

Step 1: while stopping condition is false step (2) to (9) should be done.

Step 2: for each training pair (input x and target t) step (3) to (8) should be done.

Step 3: each input unit $(x_i, i=1,2,...,N)$ receives an input signal and broadcasts this signal to all the units, in the hidden layer.

Step 4: each hidden unit $(z_j, j = 1,2,...,P)$ sums its weighted input signals

$$z_{inj} = v_{oj} + \sum_{i=1}^{N} x_i v_{ij} \tag{3.5}$$

where v_{oj} is the weight of the link from the bias unit to the unit z_j and v_{ij} is the weight of the link of the unit x_i to the unit z_j. Then each hidden unit computes its output using some hyperbolic activation functions:

$$f(z_{inj}) = \tanh(z_{inj}) = \frac{e^{z_{inj}} - e^{-z_{inj}}}{e^{z_{inj}} + e^{-z_{inj}}} \qquad -1 \le f(z_{inj}) \le 1 \tag{3.6}$$

$$z_j = f(z_{inj}) \tag{3.7}$$

and send this signal to all units in the layer above (the output layer).

Step 5: each output unit ($y_k, k = 1,2,..., M$) sums its weighted input

$$y_{ink} = w_{ok} + \sum_{i=1}^{p} z_j w_{jk} \tag{3.8}$$

where w_{ok} is the weight of the link from the bias unit to the unit y_k.

w_{ok} is the weight of the link from unit z_j to the unit y_k .

Then each output unit computes its output

$$y_k = f(y_{ink}) \tag{3.9}$$

Step 6: each output unit ($y_k, k = 1,2,..., M$) receives target pattern $(t_k, k = 1,2,..., M)$ corresponding to the input training pattern and computes its error information term:

$$\delta_k = (t_k - y_k) f'(y_{ink}) \tag{3.10}$$

where f ' is the derivative of activation function, then it calculates its weight correction Δw_{jk}, which is used to update the weight w_{jk},

$$\Delta w_{jk} = \alpha \delta_k z_j \tag{3.11}$$

where α is a learning rate which is in the range (0-1) and bias correction term Δw_{ok}

$$\Delta w_{ok} = \alpha \delta_k \tag{3.12}$$

and sends δ_k to units in the layer below (hidden layer).

Step 7: Each hidden unit ($z_j, j = 1,2,..., P$) sums its delta input (from units in the layer above).

$$\delta_{inj} = \sum_{k=1}^{M} \delta_k w_{jk} \tag{3.13}$$

and computes its error information term:

$$\delta_j = \delta_{inj} f'(z_{inj}) \tag{3.14}$$

Then it calculates its weight correction term:

$$\Delta v_{ij} = \alpha \delta_j x_i \tag{3.15}$$

and bias correction term (used to update v_{oj})

$$\Delta v_{oj} = \alpha \delta_j \tag{3.16}$$

Step 8: each output ($y_k, k = 1,2,..., M$) updates its bias and weights *(j=0, 1, 2… P)* as shown below

$$w_{jk}(new) = w_{jk}(old) + \Delta w_{jk} \tag{3.17}$$

each hidden unit $(z_j, j = 0,1,2,..., P)$ updates its bias and weights (*i=0, 1, 2… N)* as shown below

$$v_{ij}(new) = v_{ij}(old) + \Delta v_{ij} \tag{3.18}$$

Step 9: if the stopping conditions are satisfied either by reducing the error to an acceptable value or reaching to the predefined number of cycles, the training process is terminated; else the steps from (2) to (8) would be repeated.

There are, generally speaking, two different modes of training an artificial neural network using the backpropagation algorithm: batch learning (offline) and online learning. In the batch mode, a single error is computed when the entire set of training data is presented to the network and the weights in the network are updated according to that error.

In the alternative online or "pattern" mode, the weights are updated immediately after reading each data point.

There is no general rule for choosing any of these two training modes. The batch mode requires less weight updates and hence may be faster to train, but it is also more likely to become trapped in local optima. Rafiq et al. [67] suggested training the network using batch mode to start with and testing and analysing the network output. If the level of error after testing the network with unseen data was not satisfactory then a pattern mode should be used.

3.9 Neurocomputing and Optimization

There are several different backpropagation training algorithms. They have a variety of different computation and storage requirements

and no one algorithm is best suited to all locations [63]. The resilient backpropagaton algorithm is used in this work.

Multilayer networks typically use sigmoid transfer functions in the hidden layers. These functions are often called "squashing" functions, since they compress an infinite input range into a finite output range. Sigmoid functions are characterized by the fact that their slope must approach zero, as the input gets large. This causes a problem when using steepest descent to train a multilayer network with sigmoid functions, since the gradient can have a very small magnitude; and therefore, cause small changes in the weights and biases, even though the weights and biases are far from their optimal values [63].

The aim of the resilient backpropagation (RPROP) training algorithm is to eliminate these harmful effects of the magnitudes of the partial derivatives. Only the sign of the derivative is used to determine the direction of the weight update: the magnitude of derivative has no effect on the weight update [63].

RPROP is generally much faster than the standard steepest descent algorithm. It also has the nice property that it requires only a modest increase in memory requirements, as it needs to store the update values for each weight and bias, which is equivalent to storage of the gradient.

RPROP performs a direct adaptation of the weight step based on local gradient information. For each weight w_{jk}, its individual update value Δ_{jk}, which solely determines the size of the weight update, is introduced. This adaptive update value evolves during the learning

process based on its local sight on the error function *E*, according to the following learning rule:

$$\Delta_{jk} = \begin{cases} \eta^{+} * \Delta_{jk}(t-1), & if \ \frac{\partial E}{\partial w_{jk}}(t-1) * \frac{\partial E}{\partial w_{jk}}(t) > 0 \\ \eta^{-} * \Delta_{jk}(t-1), & if \ \frac{\partial E}{\partial w_{jk}}(t-1) * \frac{\partial E}{\partial w_{jk}}(t) < 0 \\ \Delta_{jk}(t-1), & else \end{cases} \tag{3.19}$$

where $0 < \eta^{-} < 1 < \eta^{+}$

Every time the partial derivative of the corresponding weight (w_{jk}) changes its sign, which indicates that the last update was too big and that the algorithm has jumped over a local minimum, the update value Δ_{jk} is decreased by the factor η^{-}. If the derivative retains its sign, the update value is slightly increasing in order to accelerate the convergence in shallow regions.

The update value for each weight update itself follows a very simple rule. If the derivative is positive (increasing error), the weight is decreased by its update value. If the derivative is negative, the update value is added:

$$\Delta w_{jk}(t) = \begin{cases} -\Delta_{jk}(t), & if \ \frac{\partial E}{\Delta w_{jk}}(t) > 0 \\ +\Delta_{jk}(t), & if \ \frac{\partial E}{\partial w_{jk}}(t) < 0 \\ 0 & else \end{cases} \tag{3.20}$$

$$w_{jk}(t+1) = w_{jk}(t) + \Delta w_{jk}(t) \tag{3.21}$$

However, there is one exception: if the partial derivative changes sign, i.e., the previous step was too large, and the minimum was missed, the previous weight update is reverted:

$$\Delta w_{jk}(t) = -\Delta w_{jk}(t-1), \qquad if \frac{\partial E}{\partial w_{jk}}(t-1) * \frac{\partial E}{\partial w_{jk}}(t) < 0 \tag{3.22}$$

The update values and weights are changed every time the whole pattern set has presented once to the network (batch training) [75].

3.10 Validation of the Network

After the training is completed, usually, the network error is minimized and the network output shows reasonable similarities with the target output, and before a neural network can be used with any degree of confidence, there is a need to establish the validity of the results it generates. Network could provide almost perfect answers to the set of problems with which it was trained, but fail to produce meaningful answers to other examples. Usually, validation involves evaluating network performance on a set of test problem that were not used for training. Generalization testing is so named because it measures how well the network can generalize what it has learned and form rules with which to make decisions about data it has not previously seen. The error between the actual and predicted outputs of generalization testing and training testing converges upon the same point corresponding to the best set of weight factors for the network. If the network is learning an accurate generalized solution to the

problem, the average error curve for the test patterns decreases at a rate approaching that of the training patterns.

3.11 Practical Aspects of Neural Computing

There are many neural network parameters that control the network's performance and prediction capability [69]. Figure (3.7) illustrates these parameters that control the network's performance.

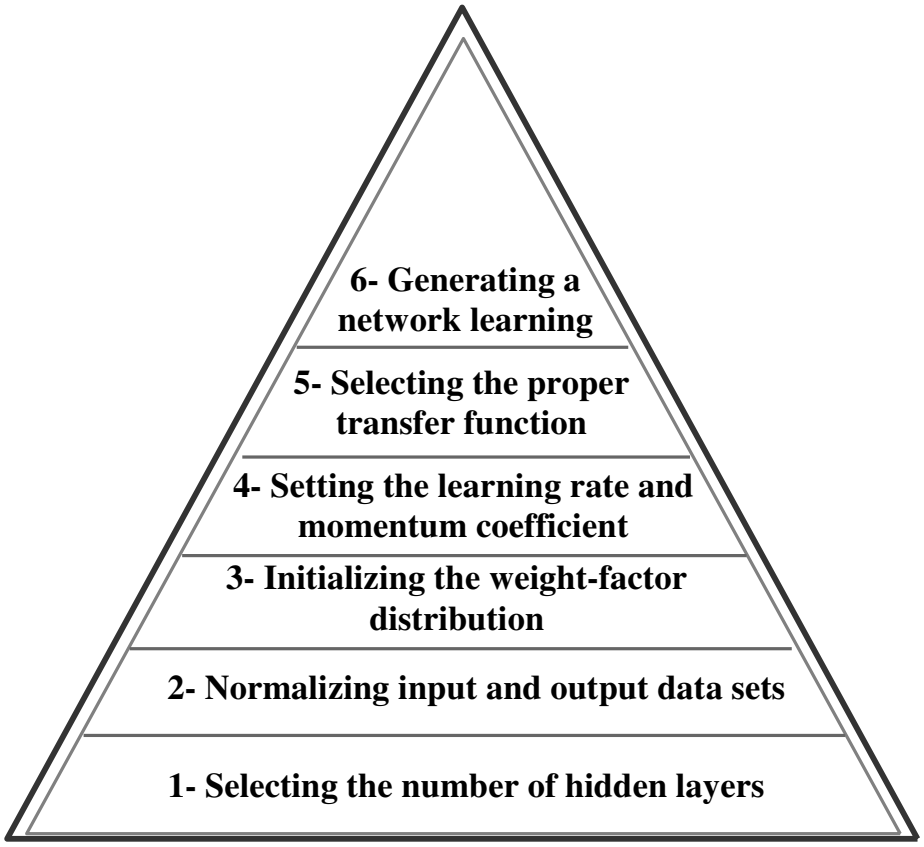

Fig. (3.7) Neural network parameters that control the network's performance and prediction capability (Ref.69)

3.11.1 Selection of Number of Hidden Layer

The function of hidden layer is to extract and remember useful features and sub-features from the input patterns to predict the outcome of the network [67].

The number of hidden layers are not straightforward. No rules are available to determine the number exactly [56]. The choice of the number of hidden layers and the nodes in the hidden layer(s) depends on the network application [69]. Flood [68] suggests that two hidden layers provide the greater flexibility necessary to model complex-shaped solution surface, and are thus recommended as a starting point when developing a layered feedward network of sigmoid neurons. Rafiq [67] suggests that for continuous functions a single hidden layer with a sufficient number of neurons will be suitable while a second layer will be needed for discontinuous problems.

The number of neurons in the hidden layer will be defined by a process of trial and error. A large number of hidden neurons well lead to over fitting at intermediate points. In addition a large number of hidden neurons can slow down the operation of neural network, both during training and in use. On the other hand, if too few processing units are considered then the artificial network will not be able to learn satisfactorily and the response of the network to unseen data will be poor [67]. Eberhart et al [76] recommended the number of hidden-layer nodes be at least greater than the square root of the sum of the number of components in the input and output vectors. Carpenter and Barthelemy [77] suggested that the number of nodes in the hidden layer be between the sum and the average of the number of nodes in the input and output layers. Moreover, Hajela [48] suggested the number of hidden-layer neurons in one hidden layer network to be between the average of the input and output layer neurons and the sum of these two-layer neurons.

Although using a single hidden layer is sufficient for solving many functional approximation problems, some problems may be easier to solve with a two-hidden-layer configuration.

3.11.2 Pre-process and post-process of the training patterns

The training patterns should be normalized before they are applied to the neural network so as to limit the input and output values within a specified range. This is due to the large difference in the values of the data provided to the neural network. Besides, the activation function used in the backpropagation neural network is a sigmoid function. The lower and upper limits of the function are 0 and 1, respectively. But hyperbolic tangent function generates limits between (-1 and +1). The following formula is used to pre-process the input data sets whose values are between −1 and 1.

$$x_{i,norm.} = 2.\frac{x_i - x_{i,\min.}}{x_{i,\max.} - x_{i,\min.}} - 1 \tag{3.23}$$

where:

$x_{i,norm.}$ is the normalized variable.

$x_{i,\min.}$ the minimum value of variable xi (input)

$x_{i,\max.}$ the maximum value of variable xi (input)

Since the output value of the sigmoid function is between 0 and 1, the following function might be used.

$$O_{i,norm} = \frac{t_i - t_{i,\min}}{t_{i,\max} - t_{i,\min}} \tag{3.24}$$

where:

$t_{i,\min}$:the minimum value of variable t_i (output)

$t_{i,\max}$: the maximum value of variable t_i (output)

However, using this formula, the normalized value of the output usually approaches 0 and 1. This makes the training process more difficult. Even the generalization of the neural network will be affected. Therefore, the following formula suggested by Rafiq et al [67] is used:

$$O_{i,norm} = \sqrt{\frac{t_i}{10^n}} + C \qquad (3.25)$$

where C is a constant between –0.25 and 0.25 to ensure that the output values are in the range of 0.2 to 0.8, and n is a constant that reduces y to a number between 0 and 1. In this analysis, $n=4$ and c =0.2 are used.

3.11.3 Initializing the Weight-Factor Distribution

Initialization of network involves assigning initial values for weights and thresholds (biases) of all connections links. Weights initialization can have an effect on network convergence. The weights initialization has a significant effect on both convergence and final network architecture by reducing the error in the output. Typically, weights and thresholds are initialized uniformly in a relatively small range with zero-mean random numbers. The choice of small numbers is essentially to reduce the likelihood of premature neurons saturation.

However, when using a very large data set or complex network architecture, the weight- factor distribution must be set to coincide with the normalized input and output variables.

3.11.4 Setting the Learning Rate and Momentum Coefficient

There are two very important parameters that are used in more complex backpropagation algorithms: the learning rate and the momentum coefficient. The use of more complex algorithm leads to significantly faster training times and also better results.

Selection of value of the learning rate parameter (α) has a significant effect on the network performance. The learning rate is a positive parameter that regulates the relative magnitude of weight changes during learning. This is accomplished by multiplying the learning rate by the change in weight factor from the previous iteration in order to determine the new weight factors (Eq.3.11).

The momentum coefficient is a parameter of what has been termed "gradient-descent learning". In gradient-descent learning, the momentum coefficient is used to allow the network to avoid settling in local minima of the error (mean-squares error, MSE). Local minima in the MSE error do not represent the best set of weight factors and the global minimum does. Figure (3.8) illustrates the problems associated with network training.

The momentum coefficient is used to promote stability of weight adaptation in a learning rule, and it tends to accelerate descent in a steady downhill direction. Momentum coefficient can be added to backpropagation learning by making weight changes equal to the sum of a fraction of the last weight change and the new change suggested by backpropogation rule. Momentum allows the network to ignore small features in the error surface. Without momentum a network may get "stuck" in a shallow local minimum.

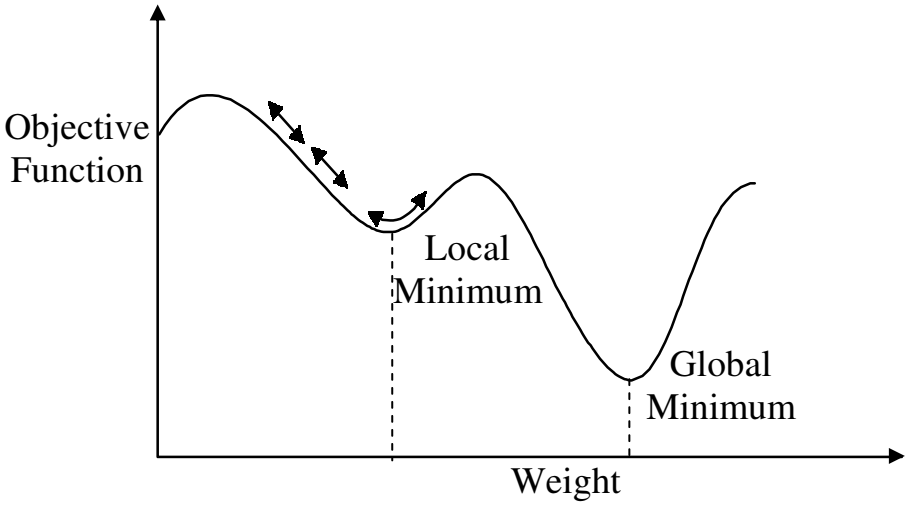

Fig. (3.8) Problems associated with network training (local and global minimum)

3.11.5 Selecting the Proper Transfer Function

The transfer (activation) function is necessary to transform the weighted sum of all signals impinging onto a neuron so as to determine its firing intensity [64]. A transfer function is chosen based on the function of the network being used. The hyperbolic tangent and sigmoid functions are appropriate for most types of networks, especially prediction problems [66].

3.11.6 Generating a Network Learning Curve

To visualize how well a network performs recall and generalization steps, a learning curve is generated, which represents the average error for both the recall of training data sets and the generalization of the testing sets. The error between the actual and

predicted outputs of generalization testing and training testing should converge upon the same point corresponding to the best set of weight factors for the network. If the network is learning an accurate generalized solution to the problem, the average error curve for the test patterns decrease at a rate approaching that of the training patterns as shown in figure (3.9) .

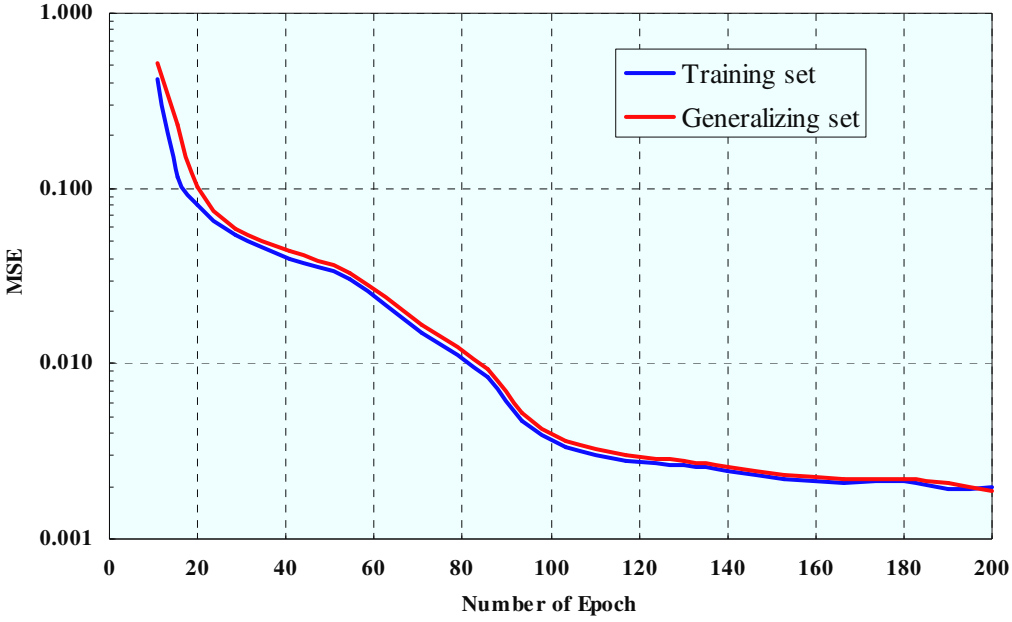

Fig.(4.1) Learning curve for the training and generalization sets patterns

Chapter Four
Results and Discussion

4.1 Introduction

The computer program "MATLAB version 7.0 Neural Network Toolbox" is employed for the neural network models in this study. The advantage of using this program is that many types of networks are included in the program and many training algorithms with different properties can be used for a specific network model.

This technique is used to investigate the ultimate resistance of reinforced concrete beams subjected to torsion. The results of these investigations are presented and discussed through selected case studies to show the performance of the neural network model in dealing with this problem. It is proposed to find the relationship between input parameters and output parameters using a feedforward back propagation type neural network. The configuration and training of neural networks is a trial-and-error process due to such undetermined parameters as the number of nodes in the hidden layer, the learning parameter, and the number of training patterns.

Two case studies are considered in this work:

(1) The prediction of ultimate resistance of reinforced concrete rectangular beams subjected to pure torsion.

(2) The prediction of ultimate resistance of reinforced concrete rectangular beams subjected to combined torsion and bending moment.

4.2 Case Study (1): Artificial Neural Network for Members Subjected to Pure Torsion:

An artificial neural network was developed to predict the ultimate strength of rectangular reinforced concrete beams under pure torsion. This section describes the data selection for training and testing patterns, the topology of the constructed network, the training process and the verification of the neural network results. Finally, a parametric study is carried out which is based on the artificial neural network predictions.

4.2.1 Selection of the Training and Testing Patterns

The experimental data that are used to train the neural network as training data are obtained from literature **[**21, 30, 37, 40, and 78**]** as shown in (appendix A). The data used to build the neural network model should be divided into two subsets: training set and validating or testing set. The validating set contains approximately 15% from total database. The training phase is needed to produce a neural network that is both stable and convergent. Therefore, selection of what data to use for training a network is one of most important steps in building a neural network model. The total number of (100) test beams were utilized. The training set contained (85) beams and the testing set comprised of (15) beams.

Neural networks interpolate data very well. Therefore, patterns chosen for training set must cover upper and lower boundaries and a sufficient number of samples representing particular features over the entire training domain [67].

An important aspect of developing neural networks is determining how well the network performs once training is complete. The performance of a trained network is checked by involving two main criteria:

(1) How well the neural network recalls the predicted response from data sets used to train the network (called the recall step). A well trained network should be able to produce an output that deviates very little from desired value.

(2) How well the network predicts responses from data sets that were not used in the training (called the generalization step). Generalization is affected by three factors: the size and the efficiency of the training data set, the architecture of the network, and the physical complexity of the problem. A well generalized network should be able to sensible the new input patterns.

To effectively visualize how well a network performs recall and generalization steps, the learning curve is generated which represents the mean square error (MSE) for both the recall of training data sets and generalization of testing set with the number of iteration or epoch. The error between the training data sets and the generalization of testing sets should converge upon the same point corresponding to the best set of weight factors for the network.

In figure (4.1), the network provides an accurate generalized solution to the problem, the average error curve for the test patterns decreases at a rate approaching that of the training patterns.

4.2.2 Model Development and Optimization

In developing a neural network model for application in this study, the performance of the model developed was tried to maximize speed of convergence and accuracy of prediction by investigating the network characteristics before experimenting with any future tests.

4.2.2.1 Input and Output Layer

The nodes in the input layer and output layer are usually determined by the nature of the problem. In this study the parameters which may be introduced as the components of the input vector consist of the total depth of beam cross section (h), the width of beam cross section (b), the concrete compressive strength (f'c), the ratio of longitudinal reinforcement (pl), yield stress of longitudinal steel (fy), the ratio of transverse steel (pw), yield stress of transverse steel (fsy), longer and shorter leg of stirrups (y1,x1) respectively, and spacing of stirrups (s). The output vector is the ultimate torsional strength of beams (Tu). Table (4.1) summarizes the ranges of each different variable.

4.2.2.2 Weight Initialization

The first step in the neural network computations, prior to training a neural network, is to initialize the weight factors between the nodes of the different layers (input to hidden layer, hidden to output layer)[69]. Since no prior information about the system being modeled is available, so in this study it is first tried to use random numbers to initialize the weight factors of the neural network.

Table (4.1) range of parameters in the database

Parameters	Ranges
Width of beam (b)	150-254 mm
Total depth of beam (h)	250-508 mm
Compressive strength of concrete (f'c)	14.6-105 MPa
Longitudinal reinforcement (pl)	0.4-3.86 %
Yield strength of longitudinal steel (fy)	283-460 MPa
Transverse reinforcement (pw)	0-3.2 %
Yield strength of Transverse steel (fsy)	275-672 MPa
Longer leg of stirrups(y1)	no stirrups & 216-470 mm
Shorter leg of stirrups (x1)	no stirrups &110 -222 mm
Spacing of stirrups (s)	no stirrups & 42 -711 mm
Torsional strength of beam (Tu)	1.3-75 kN.m

This selection is found to generate a different MSE error at any time the neural program is executed. Therefore, the Gaussian distribution at specific range is used to overcome this phenomenon. In this study Gaussian weight-factor distribution at range between (-1 to +1) is used.

4.2.2.3 Normalizing Input and Output Data Sets

Normalization (scaling down) of input and output data sets within a uniform range before they are applied to the neural network are essential to prevent larger numbers from overriding smaller ones, and to prevent premature saturation of hidden nodes, which impedes the learning process.

The limitation of input and output values within a specified range are due to the large difference in the values of the data

provided to the neural network. Besides, the activation function used in the backpropagation neural network is a hyperbolic tangent function, the lower and upper limits of this function are -1 and +1 respectively.

In this study equation (3.23) of the previous chapter is used to normalize the input and output parameters. That equation gives the required results with a certain mean square error.

4.2.2.4 Number of Hidden Layers and Nodes in Each hidden Layer:

The number of hidden layers and the number of nodes in one hidden layer are not straightforward to ascertain. No rules are available to determine the exact number. However, the choice of the number of hidden layer and number of nodes in the hidden layer depends on the network application [69]. Although using a single hidden layer is sufficient in solving many functional approximation problems, some problems may be easier to solve with a two hidden layer configurations [69]**.**

The number of nodes in the hidden layer will be selected according to the following rules [56]:

(1) The maximum error of the output network parameters should be as small as possible for both training patterns and testing patterns.
(2) The training epochs (number of iteration) should be as few as possible.

The network is tested with one and two hidden layer configurations with an increasing number of nodes in each hidden layer(s). Figure (4.2) illustrates the network response as the number of nodes in one-and two-hidden layer networks increases. The results show that the two-hidden layer network performs significantly better than the one-hidden layer network. The optimal configurations of two-hidden layer networks with minimum mean square error (MSE) are 25:25 (25 nodes in the first hidden layer and 25 nodes in the second hidden layer). This configuration will be used in this case study.

Figure (4.3) shows the effect of the node number in the hidden layers on the required number of epochs for which the neural network converges. In this figure, a node number of 50 (25:25) corresponds to the smallest number of epochs (number of iterations).

The optimal configuration of the neural network is depicted in Figure (4.4). The hyperbolic tangent transfer function will be used in this case study.

4.2.2.5 Selection of the Learning Rate and Momentum Coefficient:

The learning rate and momentum coefficient are two important parameters that control the effectiveness of the training algorithm. Using the steepest descent algorithm (Gradient Descent, GD) with momentum, the network performance can be improved by finding optimal values for learning rate (α) and the momentum coefficient (μ).The neural network is trained with different learning rates

values and momentum coefficients. The effective values for both the learning rate and momentum coefficient are 0.5 and 0.8 respectively. These values give the least mean square error.

The performance for training and generalization (test) sets are simulated using gradient descent algorithm, as shown in Fig. (4.5). The network was trained for 4000 epoch to check if the performance (MSE) for either training or testing sets might diverge.

The results of MSE appear reasonable in terms of generalizing the neural network for new test sets. In order to confirm these results, the actual values are compared with those produced by the neural network for the training and generalizing patterns, as shown in Figures. (4.6) and (4.7).

Figures (4.6) and (4.7) show the regression analysis between the output of the neural network and the corresponding targets.

This has been performed using the routine 'postreg' in MATLAB ver. (7.0). The format of this routine is [m, b, r] =postreg (a, t), where m and b correspond to the slope and the intercept of the best linear regression that relates the targets to the network outputs. If the fit is perfect (outputs exactly equal to targets), the slope would be 1, and the intercept with the y-axis would be 0. The third variable, r, is the correlation coefficient between the outputs and targets. It is a measure of how well the variation in the output is explained by the targets. If this number is equal to 1, then there is perfect correlation between targets and outputs.

Figure (4.6) and (4.7) shows that the gradient descent (GD) with momentum backpropagation algorithm gives accepted but low correlation coefficient. Therefore, another algorithm called the resilient backpropagation (RPROP) algorithm is explored to train the neural network.

Similarly, the training and testing sets are treated with the resilient backpropagation algorithm as in the gradient descent backpropagation. Compared to the gradient descent backpropagation, the resilient backpropagation algorithm produced a smaller MSE for the two phases of training and testing. Figure (4.8) shows that, the resulting MSE error for the resilient backpropagation training algorithm is less than that for the gradient descent algorithm. From figures (4.8) and (4.5), it is found that the resilient backpropagation with line search backpropagation is an order of magnitude faster (low number of epochs) than the gradient descent backpropagation. The resilient backpropagation with line search required exactly 262 epochs for MSE (for training set) to drop to a value of (0.0015), compared to (4000) epochs required to reach a value of (0.010) MSE for gradient descent backpropagation method. The comparison between the results of both algorithms relating to the performance of neural network is shown in Fig (4.9).

The network performance with resilient backpropagation training algorithm have been tested for training and generalizing patterns, as shown in figures (4.10) and (4.11). An excellent agreement has been noted in the predicting values compared with the actual (targets) values.

Based on the above analysis, the optimal network architecture (25:25 hidden layers) is recommended for this case study. The neural network is based on a backpropagation algorithm using the resilient backpropagation training algorithm and the hyperbolic transfer function.

4.2.3 Parametric Analyses based on Artificial Neural Network

Once the artificial neural network has been trained, a parametric analysis was used to study the influence of the various parameters on the ultimate torsional strength of members.

4.2.3.1 Influence of Concrete Compressive Strength

Figures (4.12), (4.13) and (4.14) show the effect of concrete compressive strength on ultimate torsional strength of reinforced concrete beams. It can be seen from the three diagrams that as the concrete compressive strength increases, the ultimate torsional strength increases.

ACI-89 code (equation 1.26), gives a reasonable agreement with the values predicted by using neural network, but ACI-05 code (equation 1.28), does not take into account the compressive strength of concrete influence.

4.2.3.2 Influence of Ratio of Web Reinforcement

The amount of web reinforcement has a very important influence on the torsional strength of beams. The ACI-89 Code limits the torsional reinforcement in a member by requiring T_S not to exceed $4T_C$. This requirement is equivalent to limiting T_n to $5T_C$. This

is because, as long as T_S does not exceed $4T_C$, torsional failures are ductile, i.e., the stirrups and the longitudinal steel yield before the concrete crushes [79].

The artificial neural network predicts a non-linear response of beams with the amount of web reinforcement. However, the ACI-89 and ACI-05 codes give a linear response as it can be seen in figures (4.15), (4.16), and (4.17). The results obtained from the neural network show that the effectiveness of stirrups becomes less as the ratio of this type of steel increases.

4.2.3.3 Influence of Ratio of Longitudinal Reinforcement

The chief functions of longitudinal steel reinforcement are [79]:

1. It anchors the stirrups, particularly at the corners, which enables them to develop their full yield strength.
2. It provides at least some resisting torque because of dowel forces which develop where the bars cross torsional cracks.
3. After cracking, member subject to torsion tend to lengthen as the spiral cracks widen and become more pronounced. Longitudinal reinforcement counteracts this tendency and control crack width.

The influence of the amount of longitudinal reinforcement as predicted by artificial neural network results is analysed here and compared with the ACI-89 and ACI-05 code equations.

Figures (4.18), (4.19), and (4.20) show that the increase of amount of longitudinal reinforcement leads to increase in the

ultimate torsional strength. However, the ACI-code equations do not reveal this effect for the longitudinal reinforcement.

4.2.3.4 Size effect, Influence of the Beam Depth

In figure (4.21), the ultimate torsional strength of reinforced concrete beams is plotted versus the total depth of beam (h mm). It can be seen from the figure that the increase in depth of beam leads the ultimate torsional strength to increase. A reasonable agreement between the results of ACI-equations and those of the neural network is achieved.

4.2.3.5 Influence of Stirrups Spacing

The effect of the spacing of stirrups is depicted in figure (4.22). In this figure, it can be seen that the increase of spacing of stirrups, while keeping the volume percentage of stirrups for these beams identical, results in a decrease in the torsional strength. ACI-code equations do not take into account the influence of stirrups spacing but they limit the maximum stirrups spacing to ($\frac{x_1 + y_1}{4}$ or 300 mm whichever is smaller) to assure that every 45-deg.crack on the wider face of the beam should be crossed by at least two stirrups. In figure (4.22), (s =175 mm) corresponds to the maximum spacing of ACI-code.

4.2.3.6 Influence of Yield Point of Stirrups

In figure (4.23) the ultimate torsional strength of beams is plotted versus the yield stress (fsy MPa) of stirrups. In this figure, it can be seen that as fsy increases, the ultimate torsional strength is increased. A reasonable agreement between the results of ACI-code equations and artificial neural network is obtained.

4.3 Case Study (2): Artificial Neural Network for Members Subject to Combined Torsion and Bending

The complete database for members subjected to combined torsion and bending moment which is described in appendix B was used to develop the neural network model. These data represent the experimental results obtained by Refs. [21, 31, 32, 39, 80 and 81]. Therefore, a total number of 54 test beams was utilized. These data were divided into two sets: a training set containing 45 beams and a validating set comprised of 9 beams.

The input parameters used were the total depth of beam cross section (h), the width of beam cross section (b), the concrete compressive strength (f'c), the amount of longitudinal reinforcement (pl), yield stress of longitudinal steel (fy), the amount of transverse steel (pw), yield stress of transverse steel (fsy), longer and shorter leg of stirrups (y1, x1) respectively, spacing of stirrups (s), and bending moment to torsion ratio (m/t). The output vector is the ultimate torsional strength of beams (Tu). Table (4.2) summarizes the range of each different variable.

The optimum solution was obtained after (262) epochs with a neural network topology as (11:8:1) units, as shown in figure (4.24).

The resilient backpropagation training algorithm and sigmoid activation function for the hidden layer and purelinear for output layer are used in the network for the training and testing sets and the results are shown in figure (4.25).

Table (4.2) range of parameters in the database

Parameters	Ranges
Width of beam (b)	100-254 mm
Total depth of beam (h)	203-381 mm
Compressive strength of concrete (f'c)	16.3-42 MPa
Longitudinal reinforcement (pl)	0.44-3.2 %
Yield strength of longitudinal steel (fy)	316-540 MPa
Transverse reinforcement (pw)	0-3.2 %
Yield strength of Transverse steel (fsy)	275-358 MPa
Longer leg of stirrups(y1)	no stirrups & 127-343 mm
Shorter leg of stirrups (x1)	no stirrups & 63.5-216 mm
Spacing of stirrups (s)	no stirrups & 40.6 -216 mm
Ratio of bending moment to torsion (m/t)	0-4.33
Torsional strength of beam (Tu)	4.2-62.9 kN.m

The suitability of neural network model is checked by plotting the predicted values of ultimate torsional strength (the output of neural network) versus the experimental results (the target or actual values) for the training and testing sets as shown in figures (4.26), and (4.27). As can be seen the correlation factor, r, for both sets is quite high, which proves the high accuracy of training neural network model.

The ultimate strength of the reinforced concrete members under combined torsion and bending are greatly influenced by the member cross section, the amount and distribution of steel, and the torque-to-bending moment ratio [82].

Figure (4.28) shows the interaction diagram for beams subjected to combined torsion and bending moment. This figure contains

different types of interaction curves. Curve (1) represents a quarter circular curve which is suggested by McMullen and WarWaruk [39], curve (2) represents a tri-linear interaction curve which has been suggested by Zia and Cardenas [82], curve (3) suggested by Abas [39] represents a parabola interaction curve, curve (4) represents a linear interaction curve which suggested by Mirza [82], and curve (5) shows the predicted interaction diagram between torsion and bending moment by using neural network model adopted in the present study.

In curve (5) it can be seen that a small amount of bending moment will reduce the torque capacity by a small amount. On the other hand when the $\frac{T}{T_0} \leq 0.5$ there is a little effect on bending capacity and the torsion effect may be neglected, where

T_o:the ultimate torque capacity in pure torsion(kN.m), and can be calculated by eq.(1.28).

T :the ultimate applied torque(kN.m)

M_o:the ultimate bending capacity in pure bending (kN.m), and can be calculated according to the ACI-Code equation as below.

$$M_0 = \phi\left[As.fy(d - \frac{a}{2}) \right],$$

$As =$ area of tension reinforcement(sq.mm).

$d =$ distance from extreme compression fiber to centeroid of tension reinforcement (mm).

$a = \frac{As \cdot fy}{0.85 f'c \cdot b}$, where b = the width of compression face.

M :the ultimate applied bending (kN.m)

4.4 Computer Program for Backpropagation Neural Network

The computer program that is coded in MATLAB (7.0) languages realizes the training and generalization processes of the backpropagation neural network. The structure of the computer program is shown in Fig. (4.29). The main variables are stored using the cell arrays. The cell arrays in MATLAB are multidimensional arrays whose elements are copies of other arrays.

4.4.1 Pseudo-Codes of the Program for BPNN

The pseudo-code of the program for training and testing the neural network is listed below:

(i) Training program

input the parameters of the network
initialize the weight matrix
input the training pattern
pre-process the training pattern set key=0, epoch=0
set initial value of Δw = 0
while (key ≠1) & epoch < given epoch number, epochNum)
i = 1
while (i ≤ number of training pattern, pNum)
calculate the error for one training pattern
calculate the error which back-propagate to each layer

calculate the weight changing

calculate the changed weight

i = i + 1

end

if the error sum is less than the required error

set key=-1 and finish training

otherwise epoch=epoch+1;

end

(ii) Testing program

load the weight values for the trained neural network

provide the input for the neural network

pre-process the input data

calculate the output of the neural network

post-process the calculating results

4.4.2 Pseudo-Code of the Program for RPROP

The neural network is trained in off-line mode. In the program, the calculation of the value of $\frac{\partial E}{\partial w_{ij}}$ *(t)* is performed with the same code as in the program for the BPNN algorithm. The update of the weight is performed by the procedure shown below.

input the training patterns and pre-process these data
input initial values of these parameters such as $\Delta_0, \Delta_{\min}, \Delta_{\max}, \eta^+$ *and* η^-
calculating the value of $\frac{\partial E}{\partial w_{ij}}(t)$
according to the sign of $\frac{\partial E}{\partial w_{ij}}$ *(t)* $\frac{\partial E}{\partial w_{ij}}$ *(t –1) and* $\frac{\partial E}{\partial w_{ij}}$ *(t), changing the weight value*

save the weight value for the trained network

if ($\frac{\partial E}{\partial w_{ij}}(t)\ \frac{\partial E}{\partial w_{ij}}(t-1) > 0$) *then {*

$\Delta_{ij}(t) = min\ (\Delta_{ij}(t\text{-}1).\ \eta^{+}, \Delta_{max})$

$\Delta w_{ij}(t) = -\ sign\ (\frac{\partial E}{\partial w_{ij}}(t)).\ \Delta_{ij}(t)$

$w_{ij}(t+1) = w_{ij}(t) + w_{ij}(t\text{-}1)$

}

else if ($\frac{\partial E}{\partial w_{ij}}(t)\ \frac{\partial E}{\partial w_{ij}}(t-1) > 0$) *then {*

$\Delta_{ij}(t) = min\ (\Delta_{ij}(t\text{-}1).\ \eta^{-}, \Delta_{min})$

$w_{ij}(t+1) = w_{ij}(t) - w_{ij}(t\text{-}1)$

$\frac{\partial E}{\partial w_{ij}}(t) = 0$

}

else {

$\Delta w_{ij}(t) = -\ sign\ (\frac{\partial E}{\partial w_{ij}}(t)).\ \Delta_{ij}(t)$

$w_{ij}(t+1) = w_{ij}(t) + w_{ij}(t\text{-}1)$

}

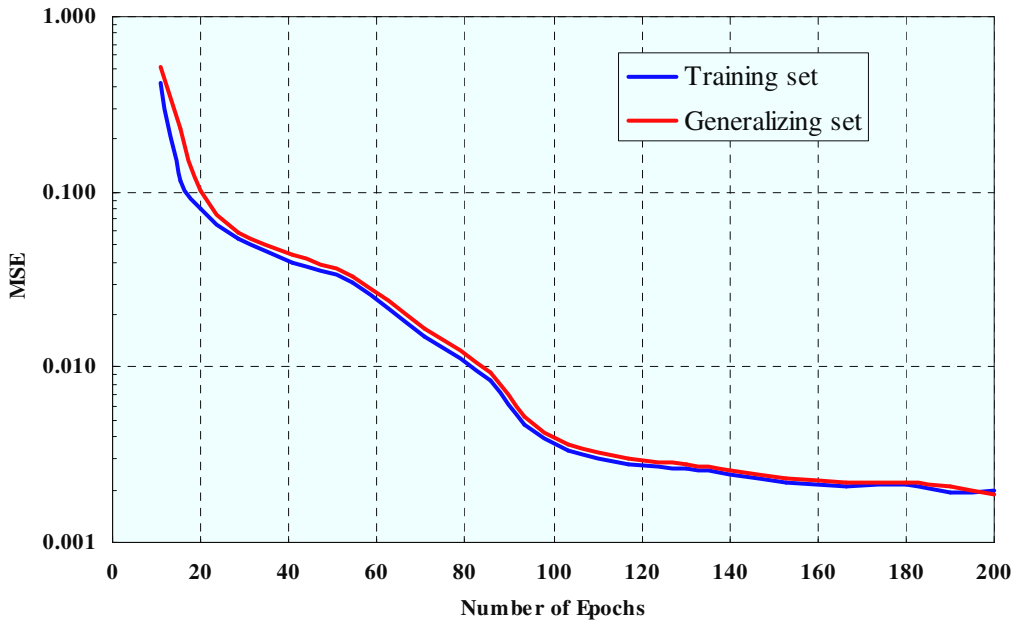

Fig.(4.1) Learning curve for the training and generalization sets patterns

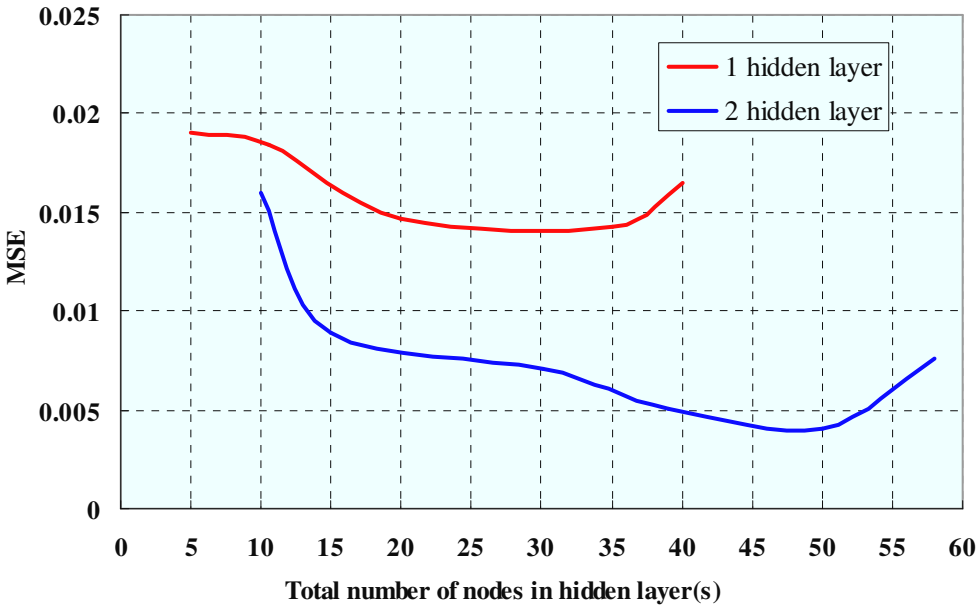

Fig.(4.2) A comparison of MSE errors for the prediction NN trained with various 1 and 2 hidden layer configurations

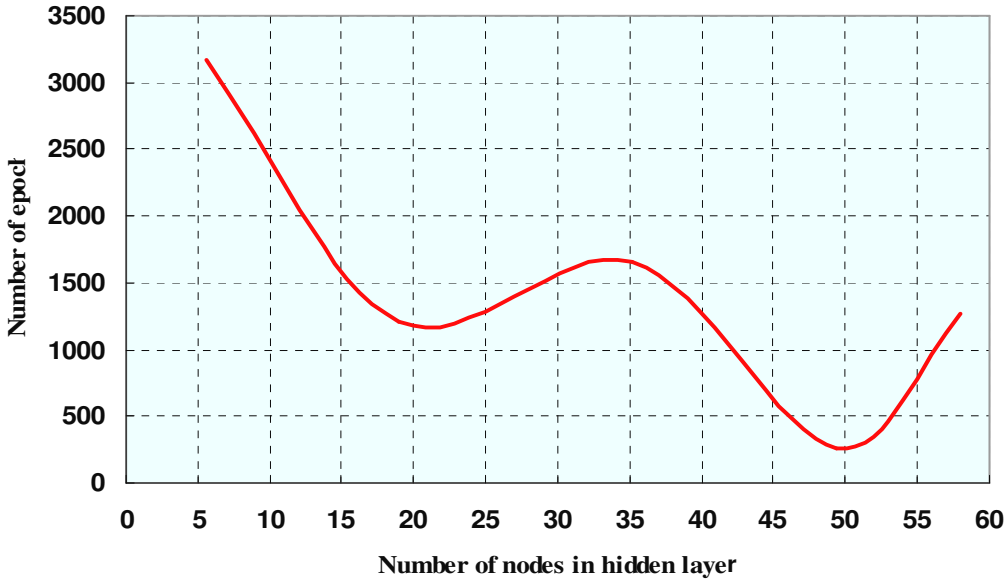

Fig.(4.8) Effect of the node number in two hidden layers on number of epoch

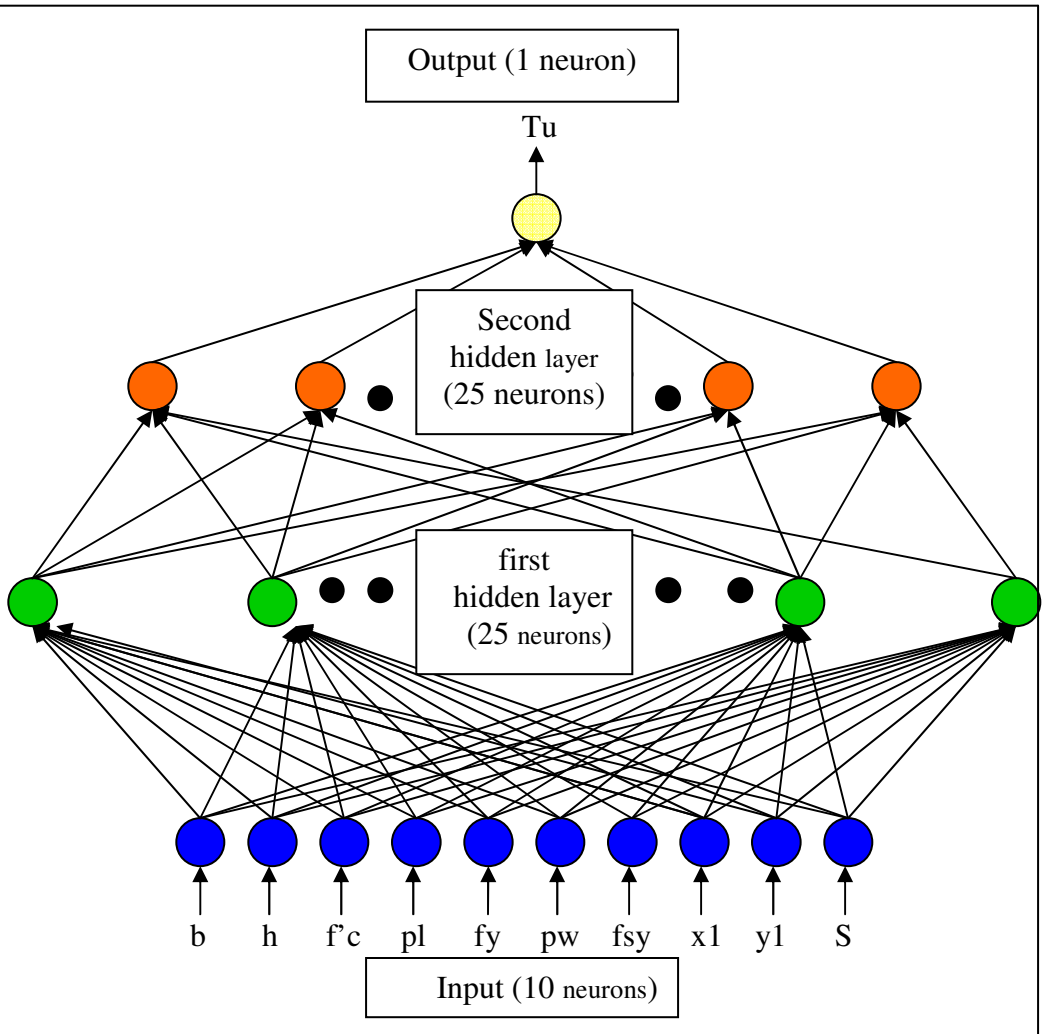

Fig.(4. 4) The structure of the proposed NN model

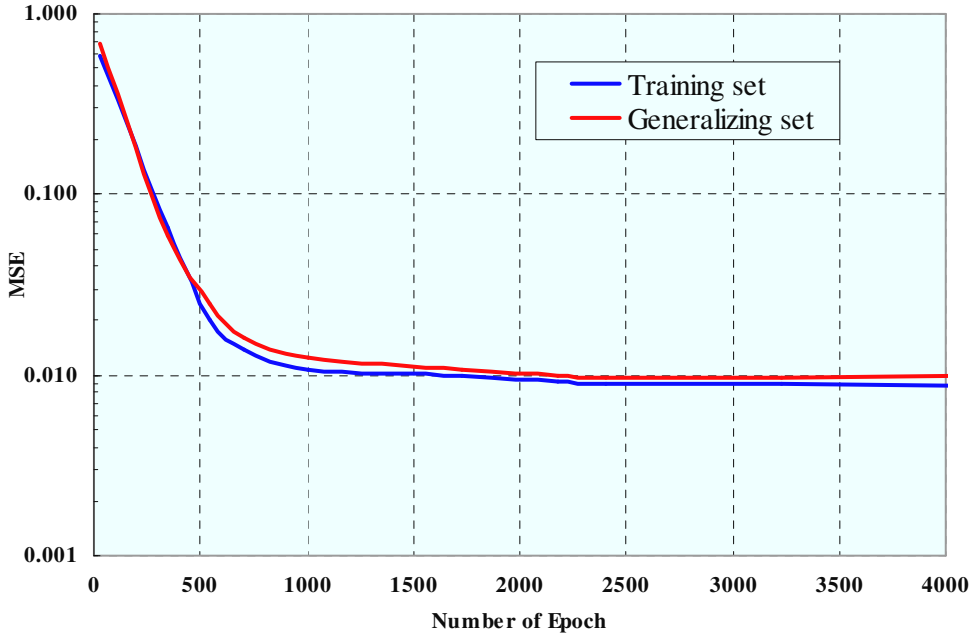

Fig.(4.5) Convergence of NN for training and testing sets based on the GD with momentum algorithm

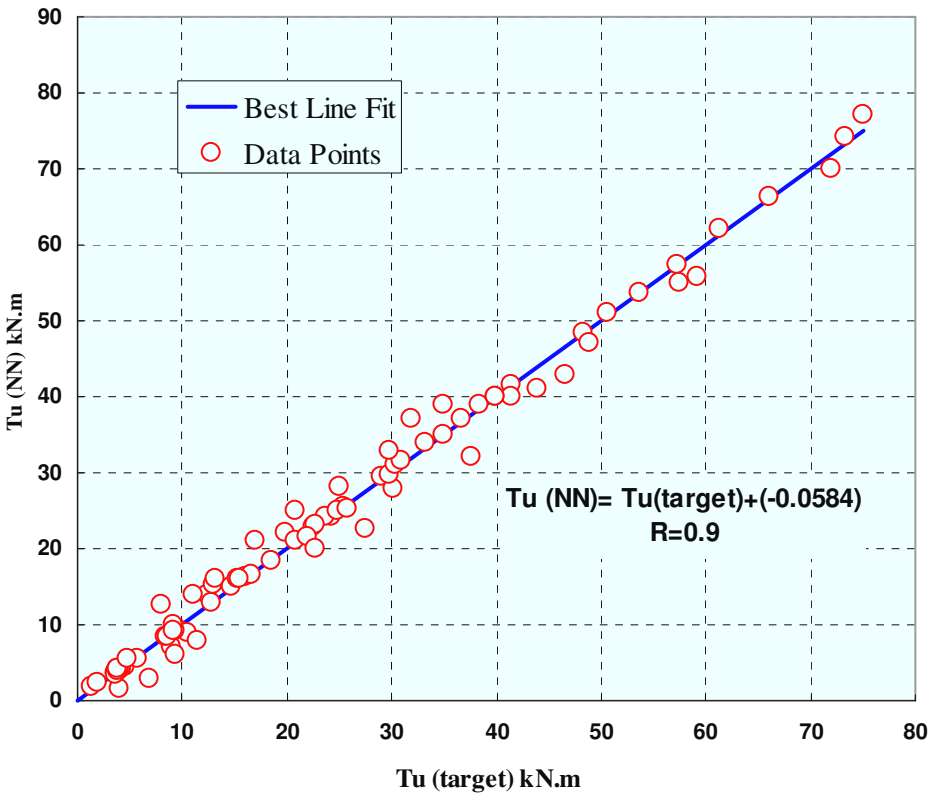

Figure (4.6)Comparison between NN results and target results for training patterns based on GD with momentum algorithm

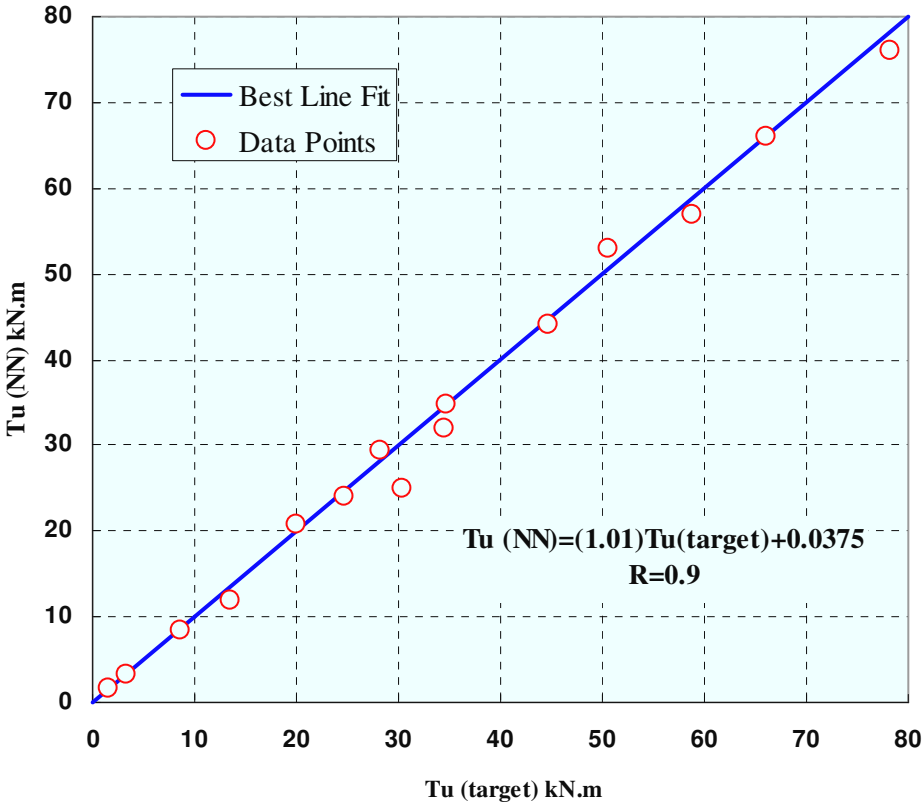

Fig (4.7) Comparison between NN results and target results for testing patterns based on RPROP algorthim

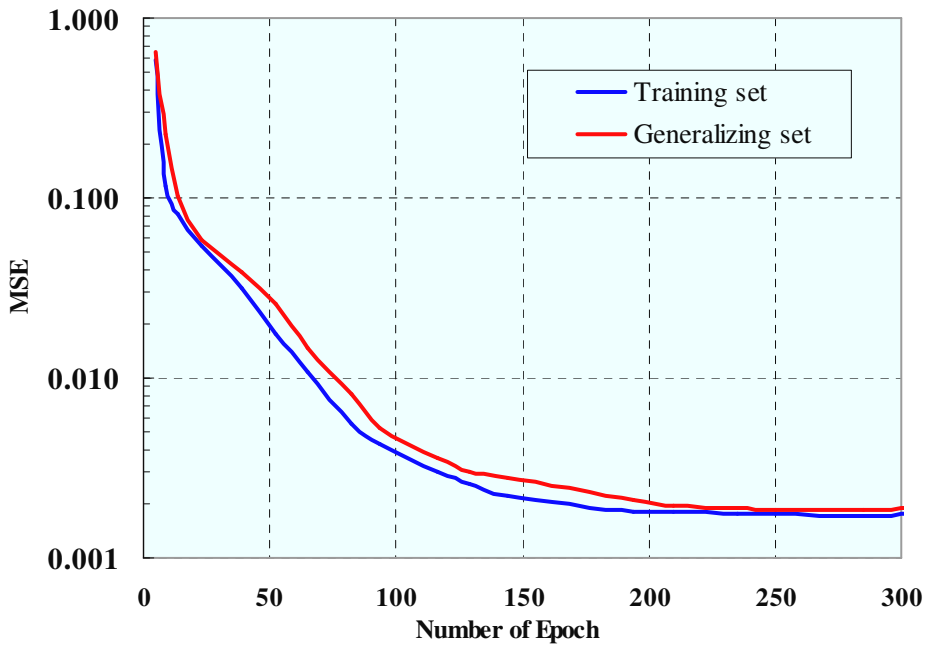

Fig.(4.8) Convergence of the NN for training and testing sets based on the RPROP algorithm

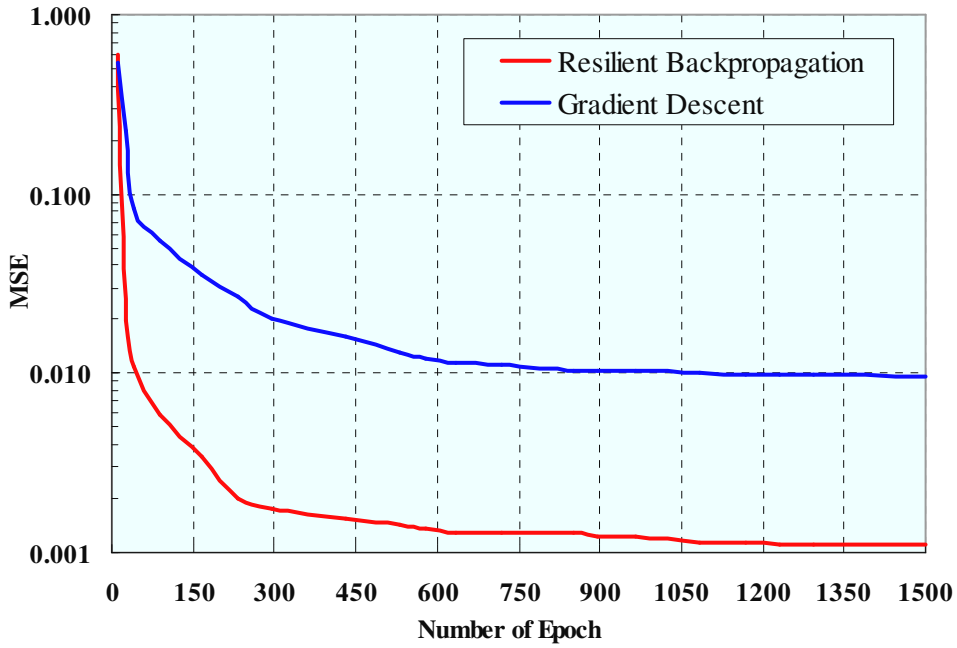

Fig. (4.9) The convergence of the NN results for testing sets based on the GD with momentum and RPROP algorithms

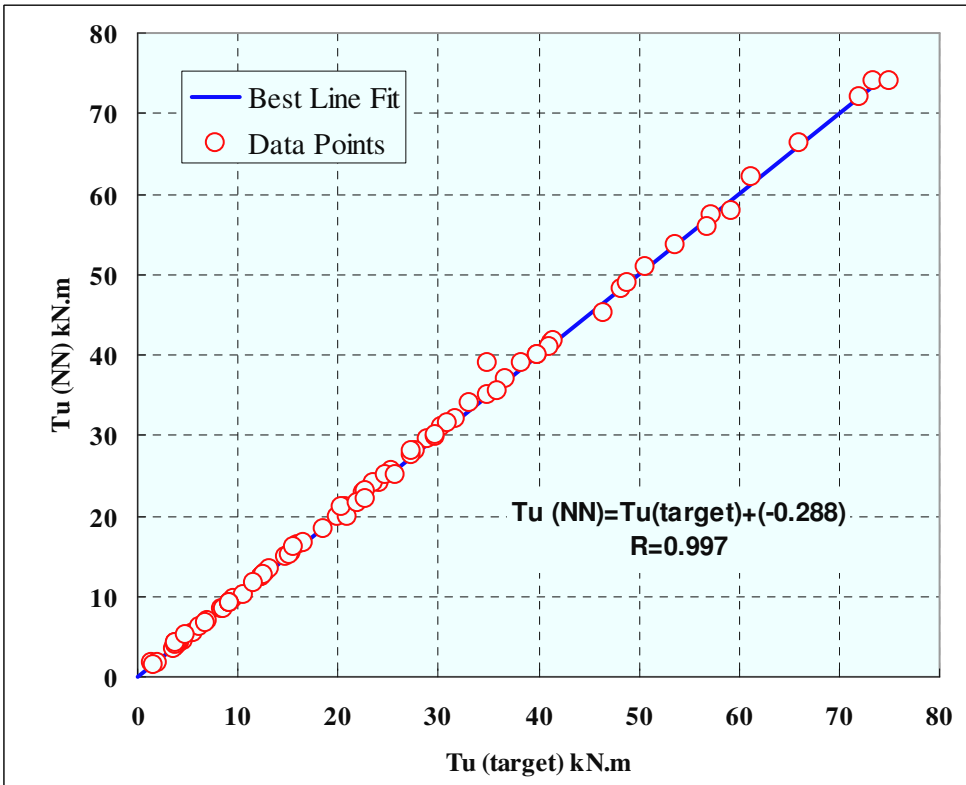

Fig(4.10) Comparison between NN results and target results for training patterns based on RPROP algorithm

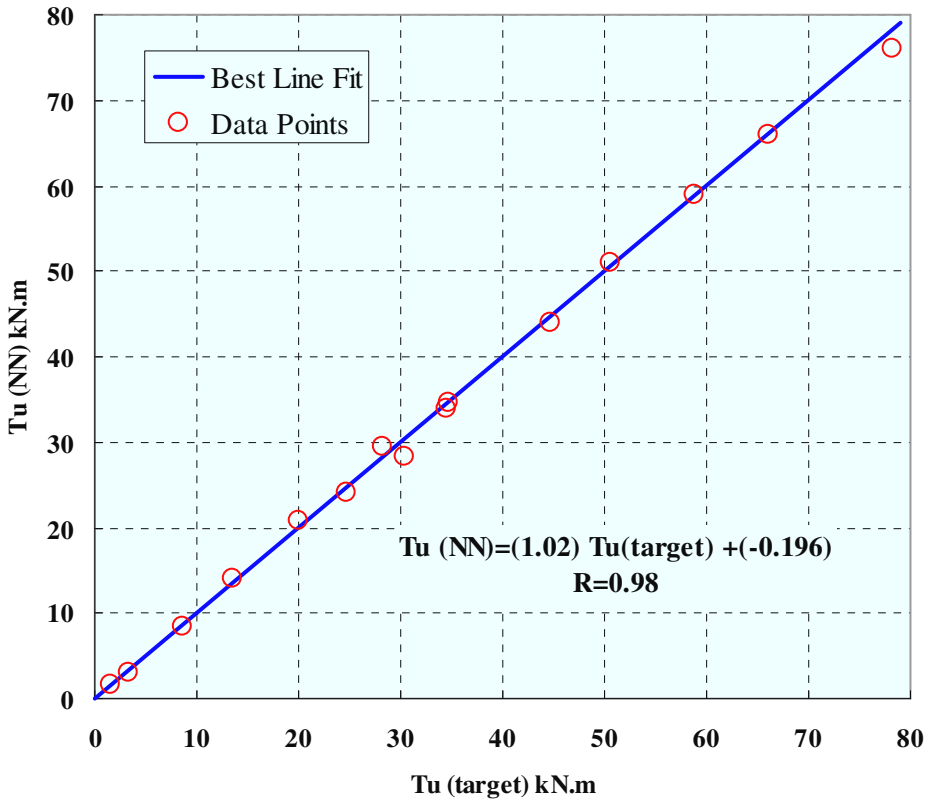

Fig.(4.11) Comparison between NN results and target results for testing patterns based on RPROP algorithm

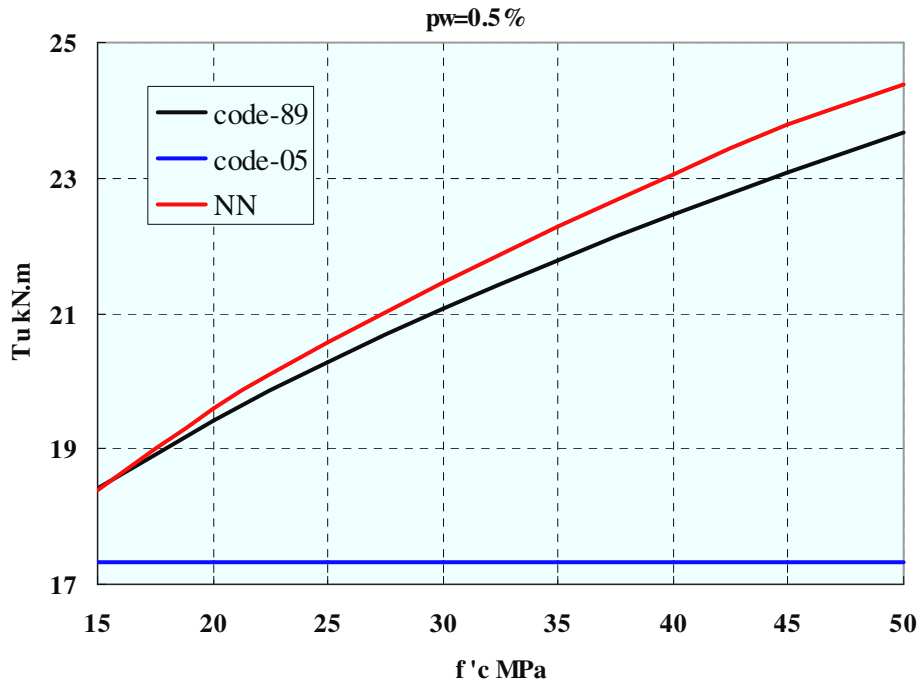

Fig.(4.12) Influence of the concrete compressive strength as related to amount of transverse reinforcement (pw=0.5%)

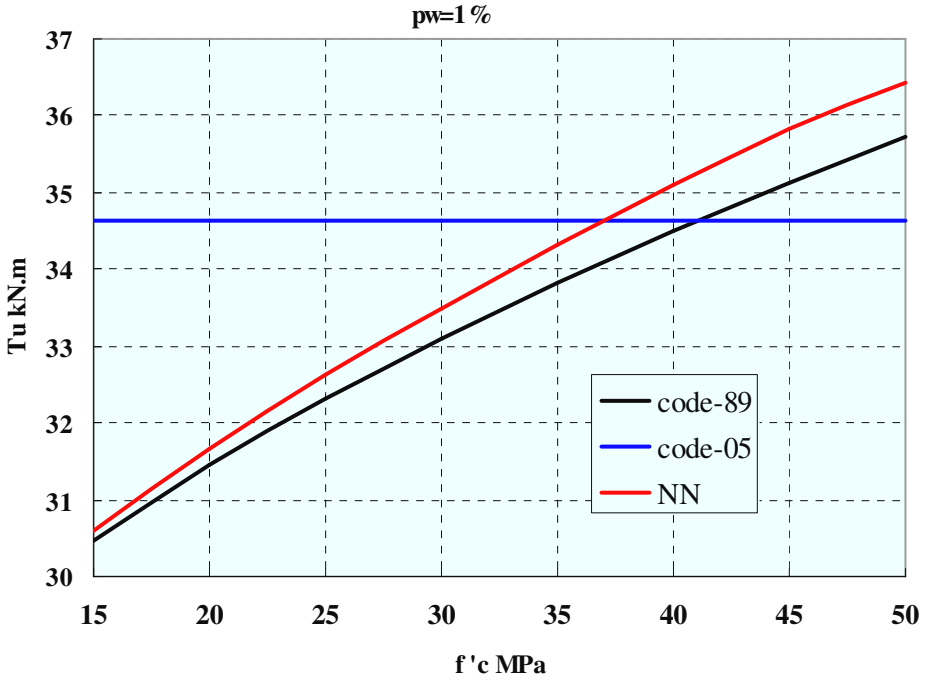

Fig.(4.13) Influence of the concrete compressive strength as related to amount of transverse reinforcement (pw=1%)

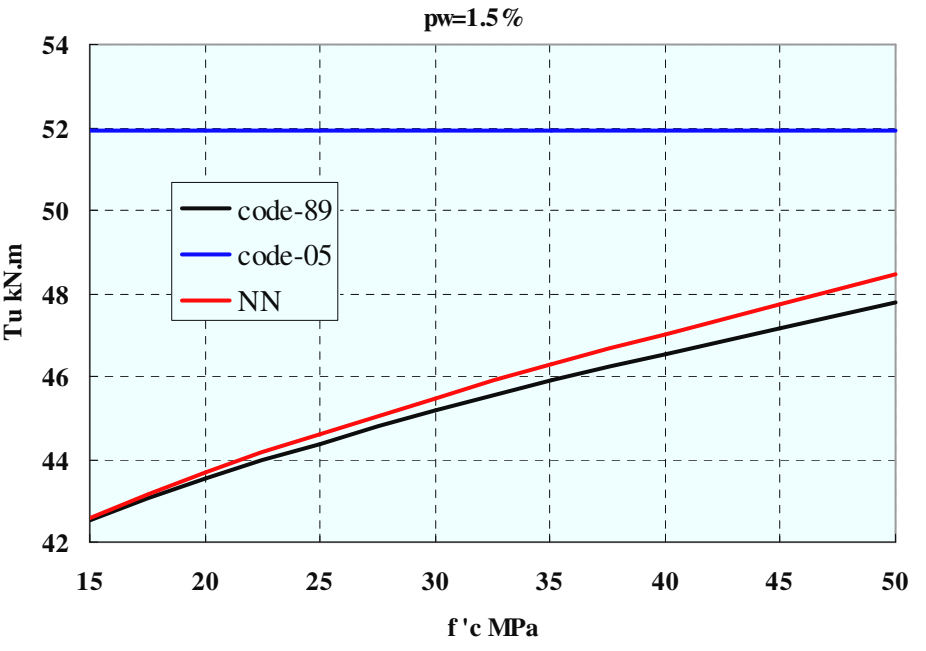

Fig.(4.14) Influence of the concrete compressive strength as related to amount of transverse reinforcement (pw=1.5 %)

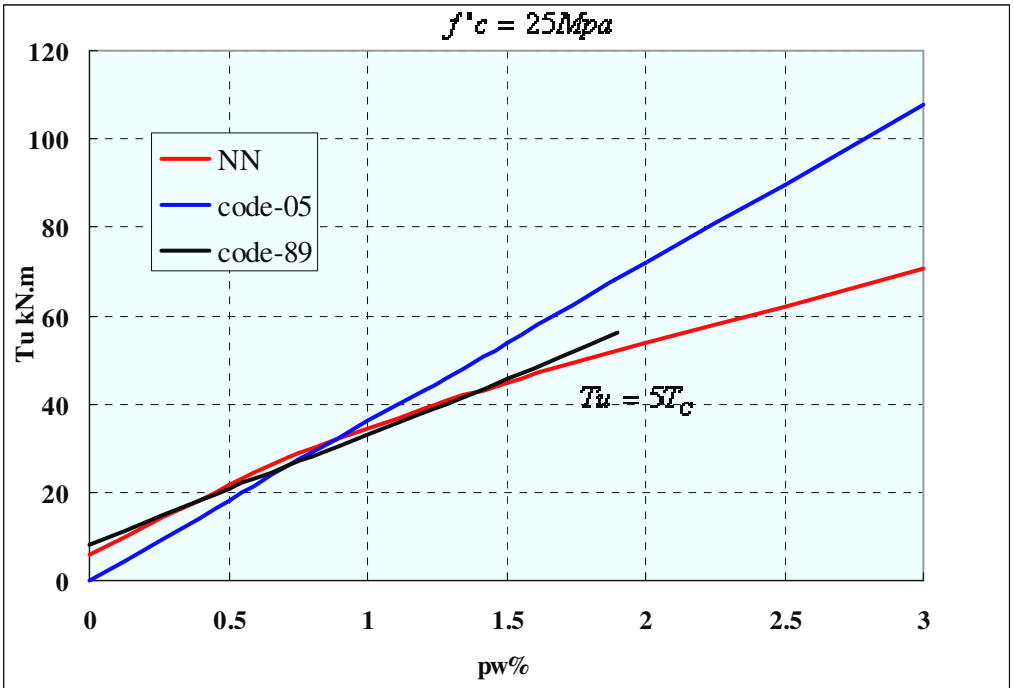

Fig.(4.15) Influence of transverse reinforcement in relation to the concrete compressive strength (f 'c =25 MPa)

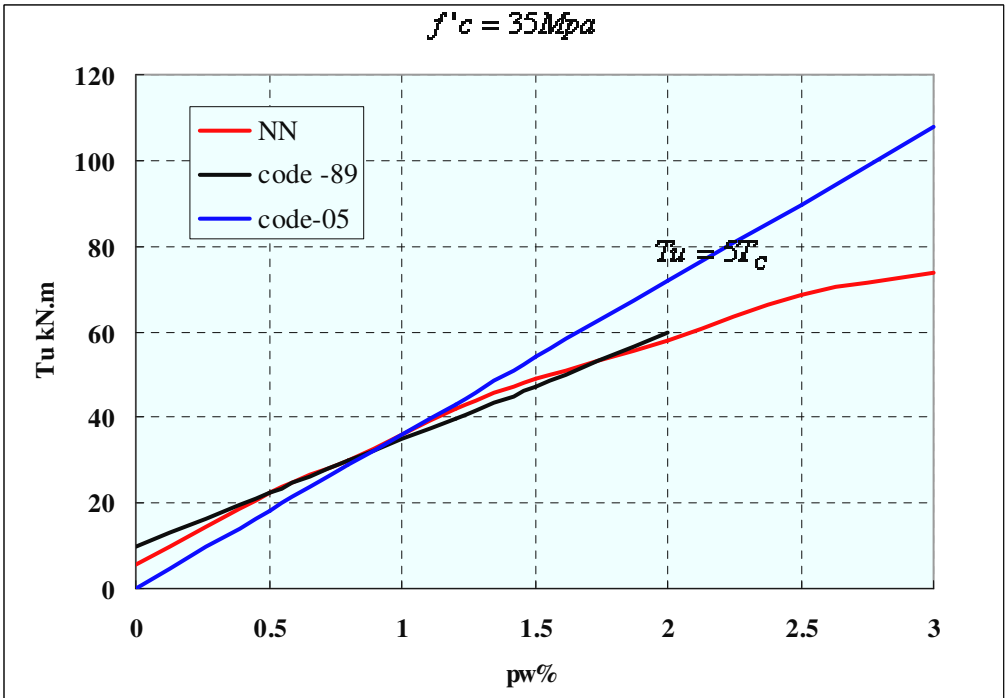

Fig.(4.16) Influence of transverse reinforcement in relation to the concrete compressive strength (f 'c =35 MPa)

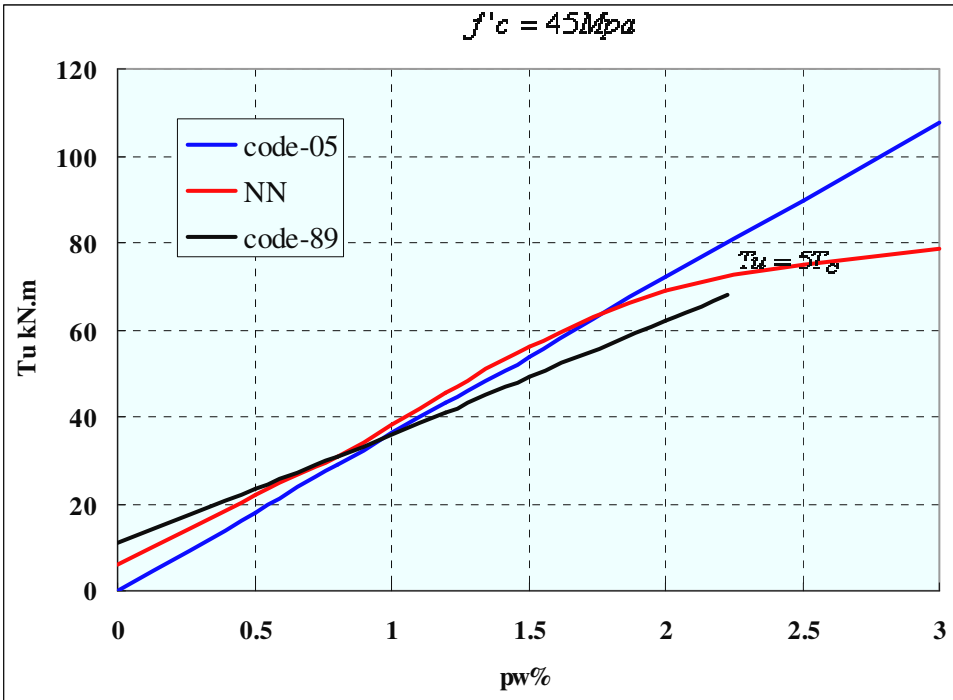

Fig.(4.17) Influence of web reinforcement in relation to the concrete compressive strength (f 'c=45 MPa)

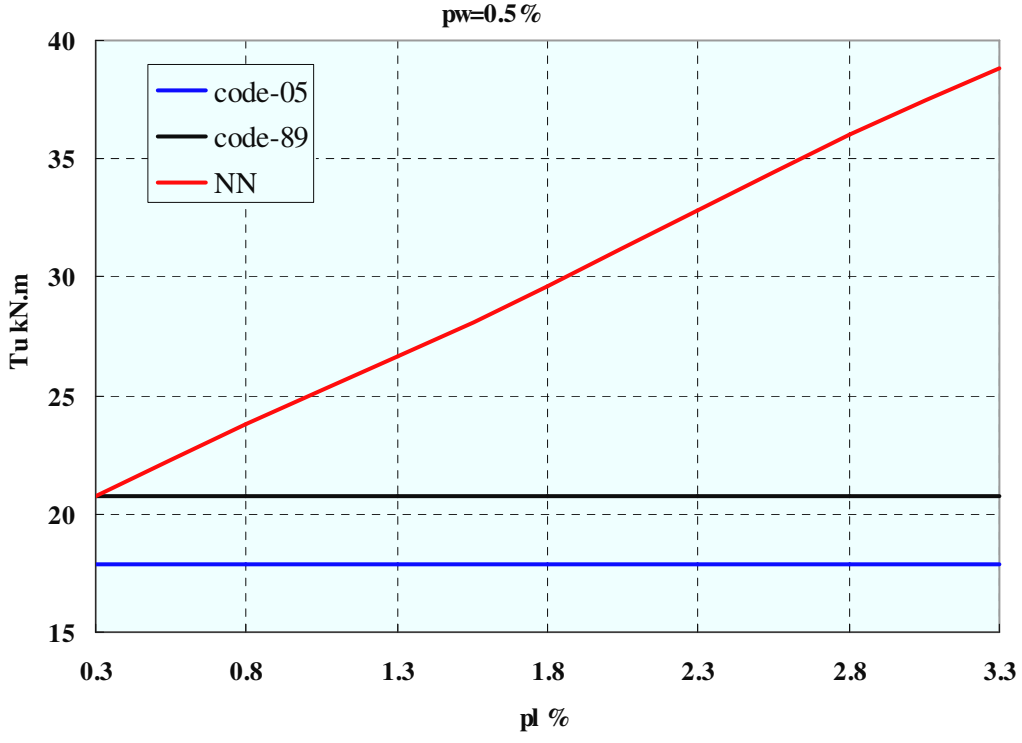

Fig.(4.18) Influence of the amount of longitudinal reinforcement in relation to the amount of transverse reinforcement (pw=0.5%)

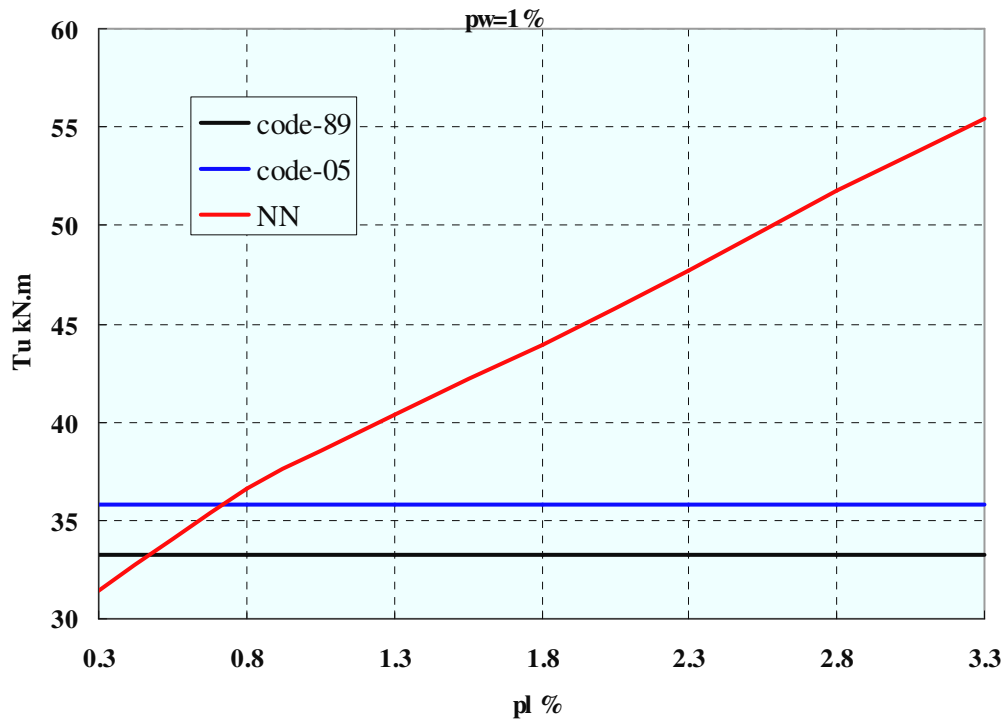

Fig.(4.19) Influence of the amount of longitudinal reinforcement in relation to the amount of transverse reinforcement (pw=1%)

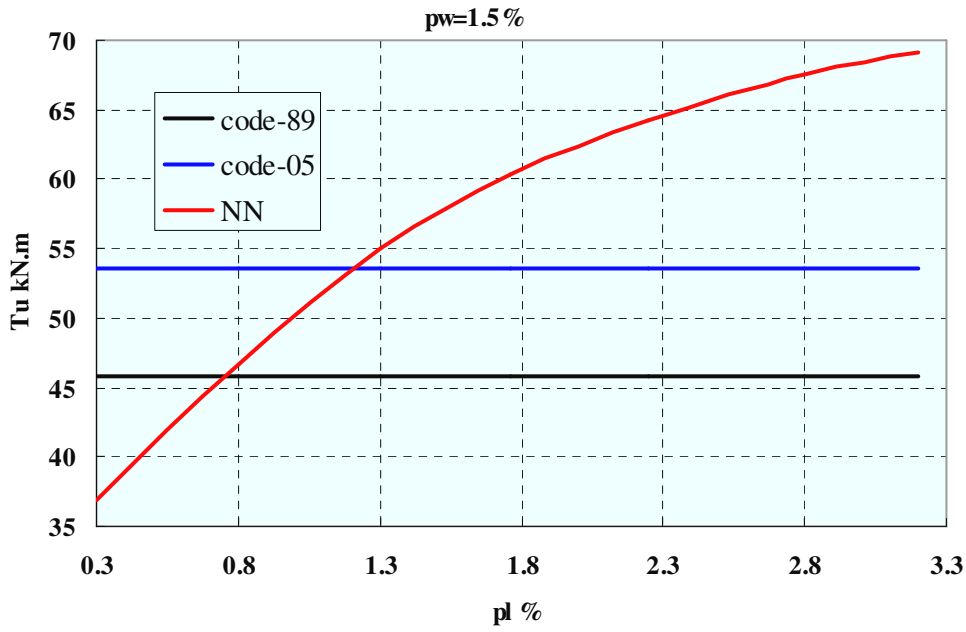

Fig.(4.20) Influence of the amount of longitudinal reinforcement in relation to the amount of transverse reinforcement (pw=1.5%)

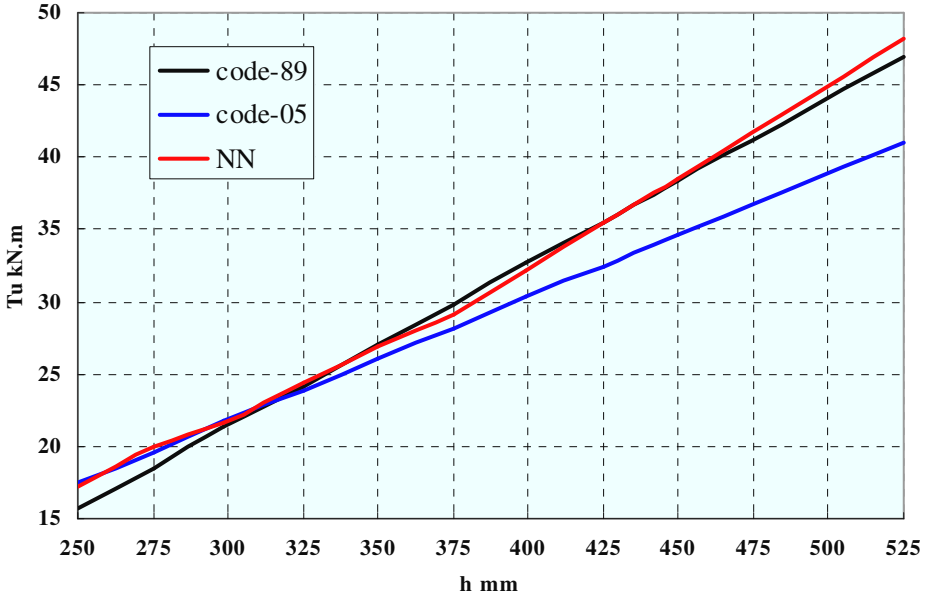

Fig.(4.21) Influence of size effect on the ultimate torsional strength

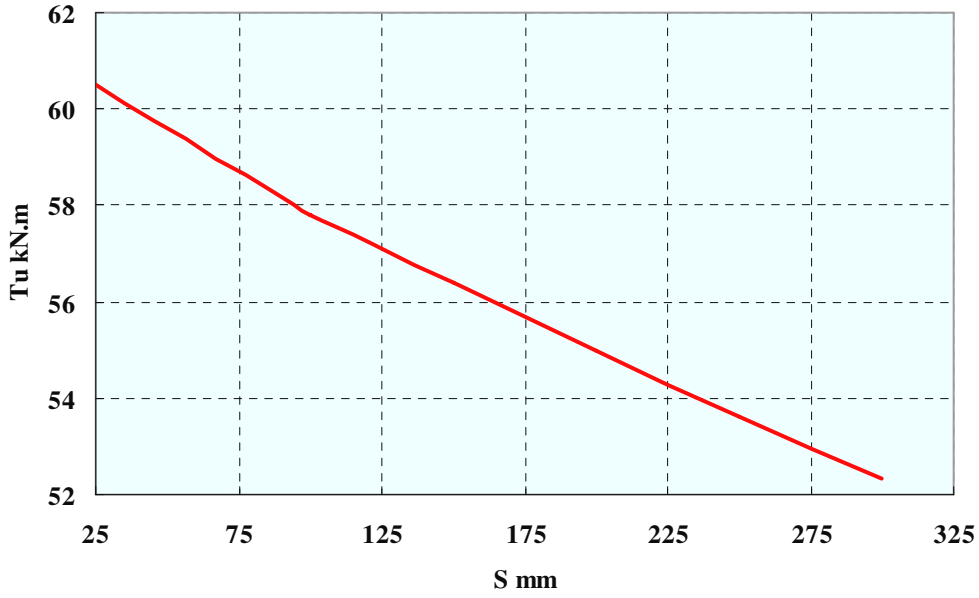

Figure (4.22) Influence of spacing of stirrups on ultimate torsional strength

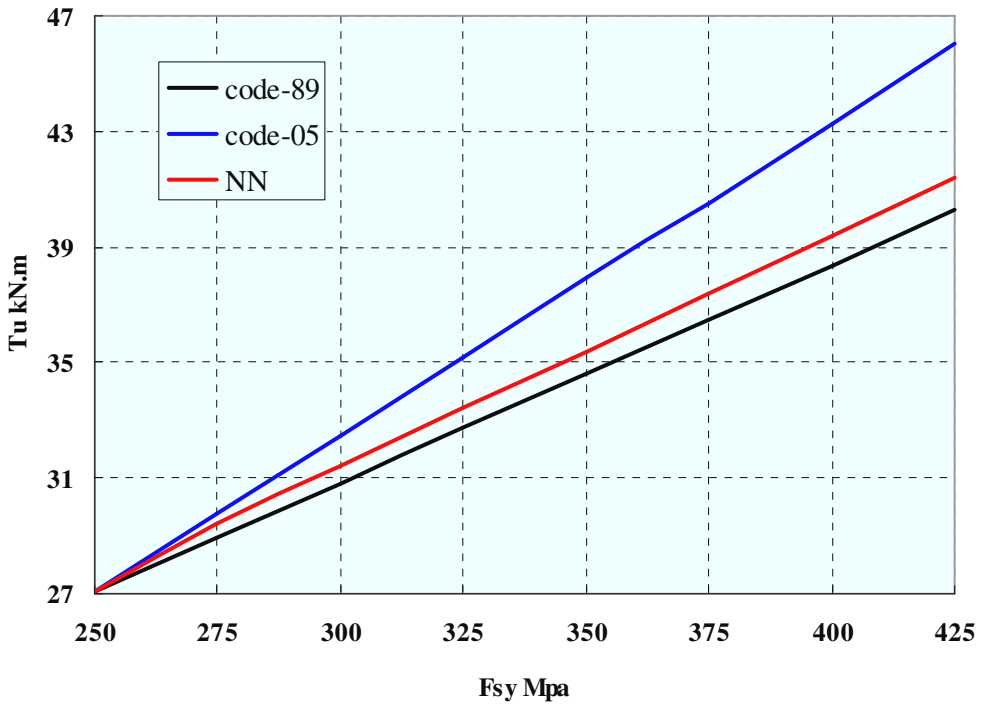

Figure (4.23) Influence of yield stress of transverse reinforcement on ultimate torsional strength

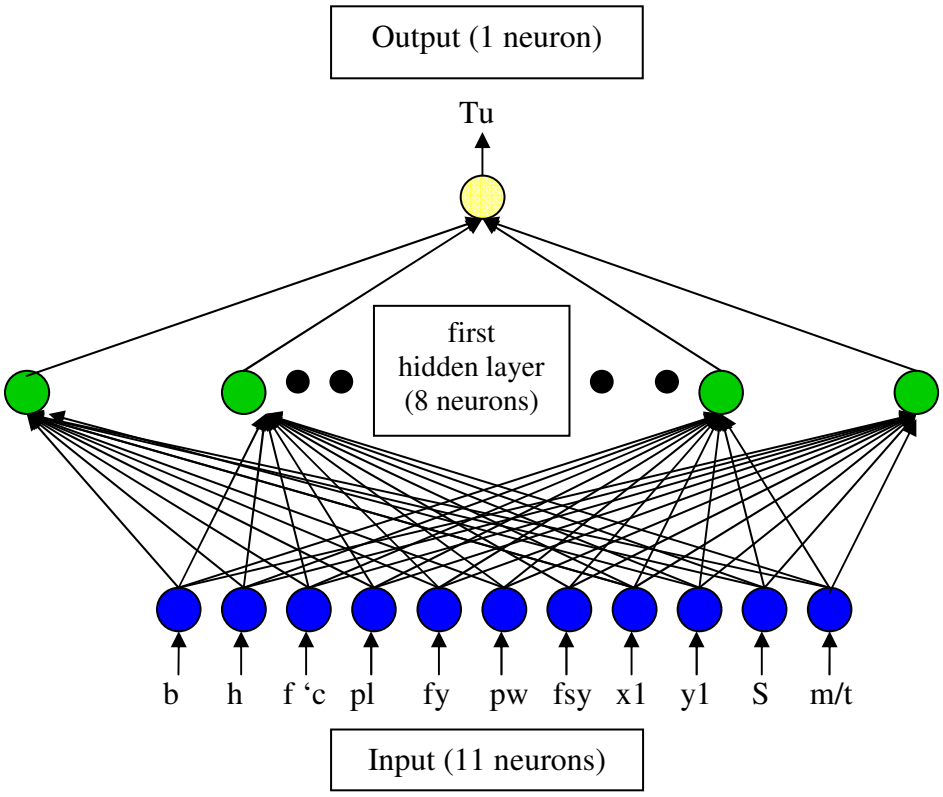

Fig. (4.24) The structure of the proposed NN model

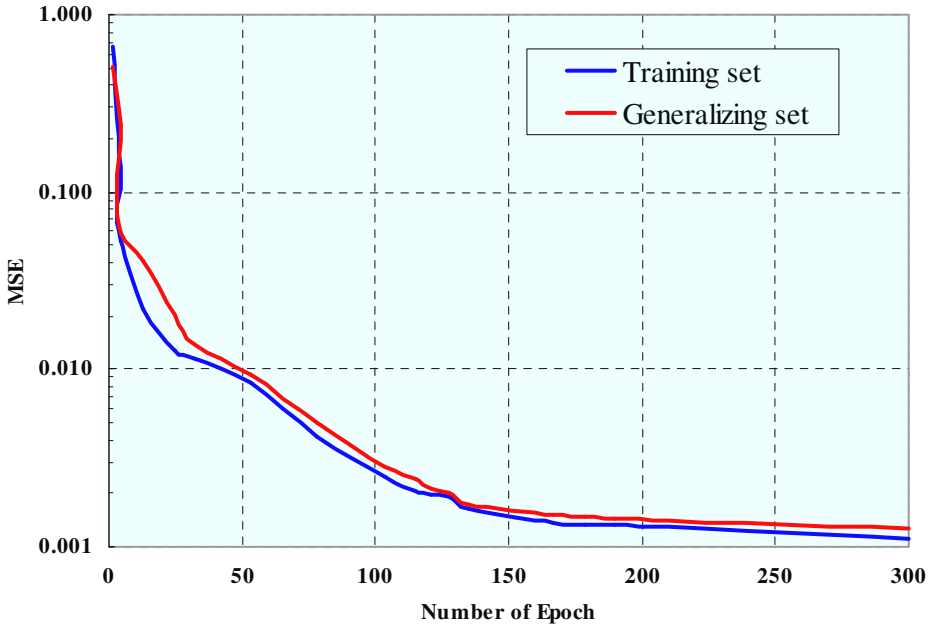

Fig.(4.25) Convergence of the NN for training and testing sets based on the RPROP algorithim

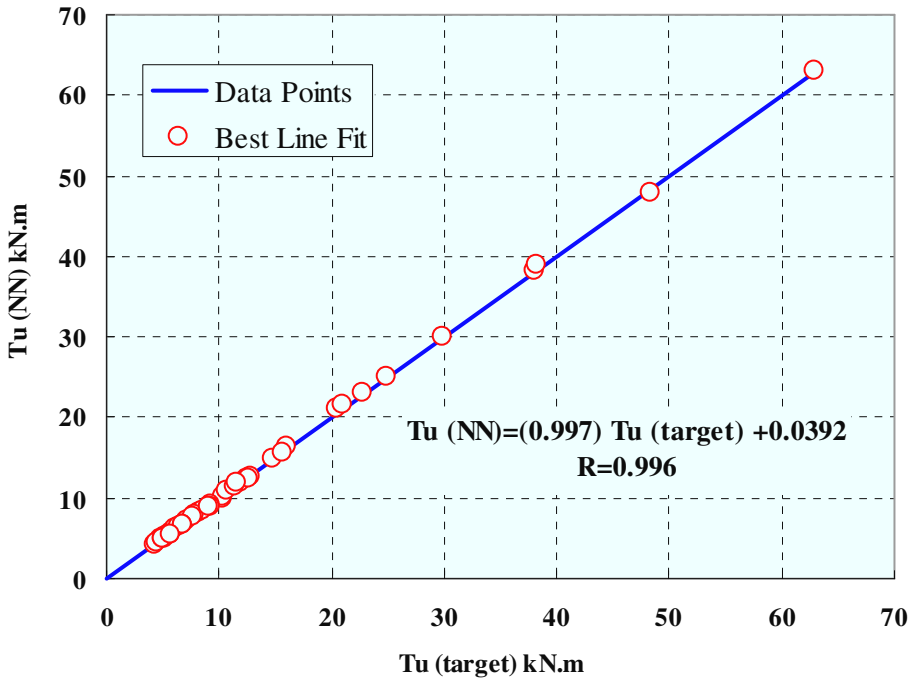

Figure (4.26) Comparsion between NN results and target results for training patterns based on RPROP algorithm

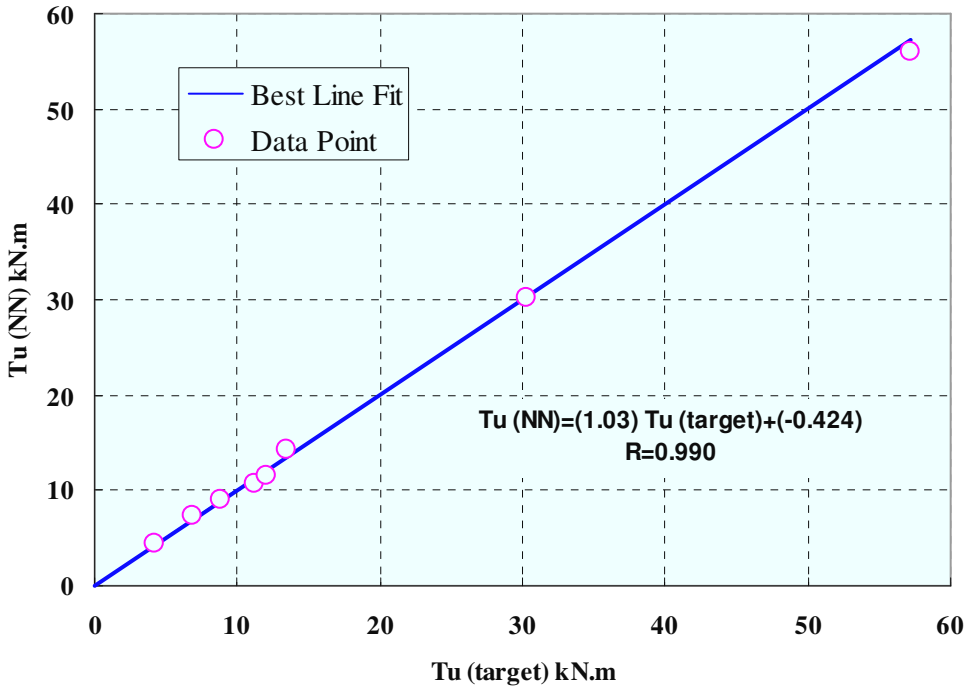

Figure (4.27) Comparsion between NN results and target results for testing patterns based on RPROP algorithm

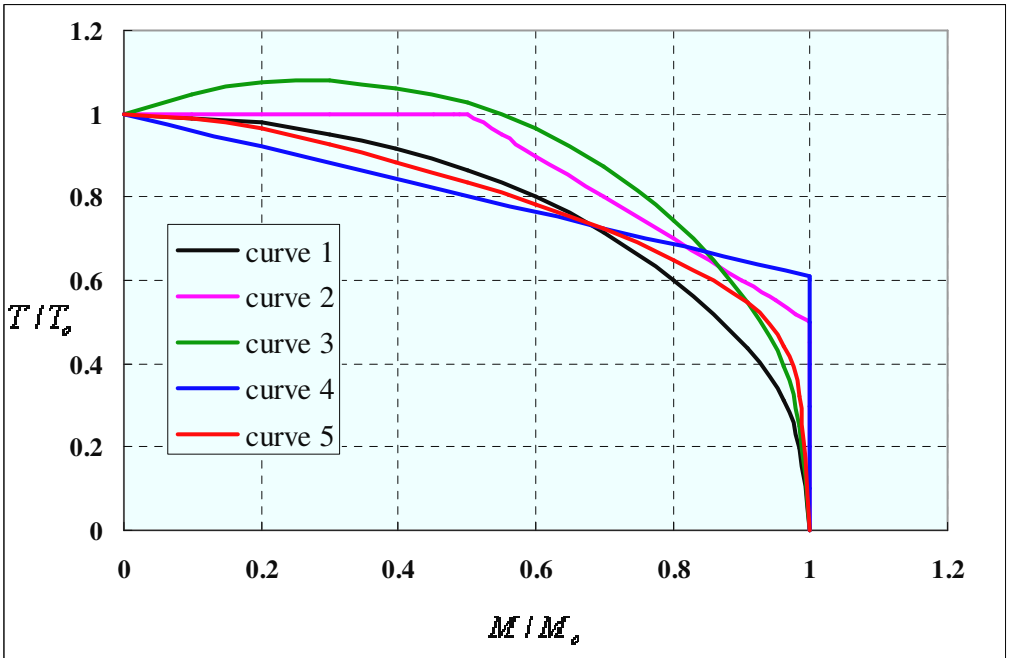

Figure (4.28) comparsion between the bending -torsion interaction curve proposed in this study and different curves proposed by other investigators

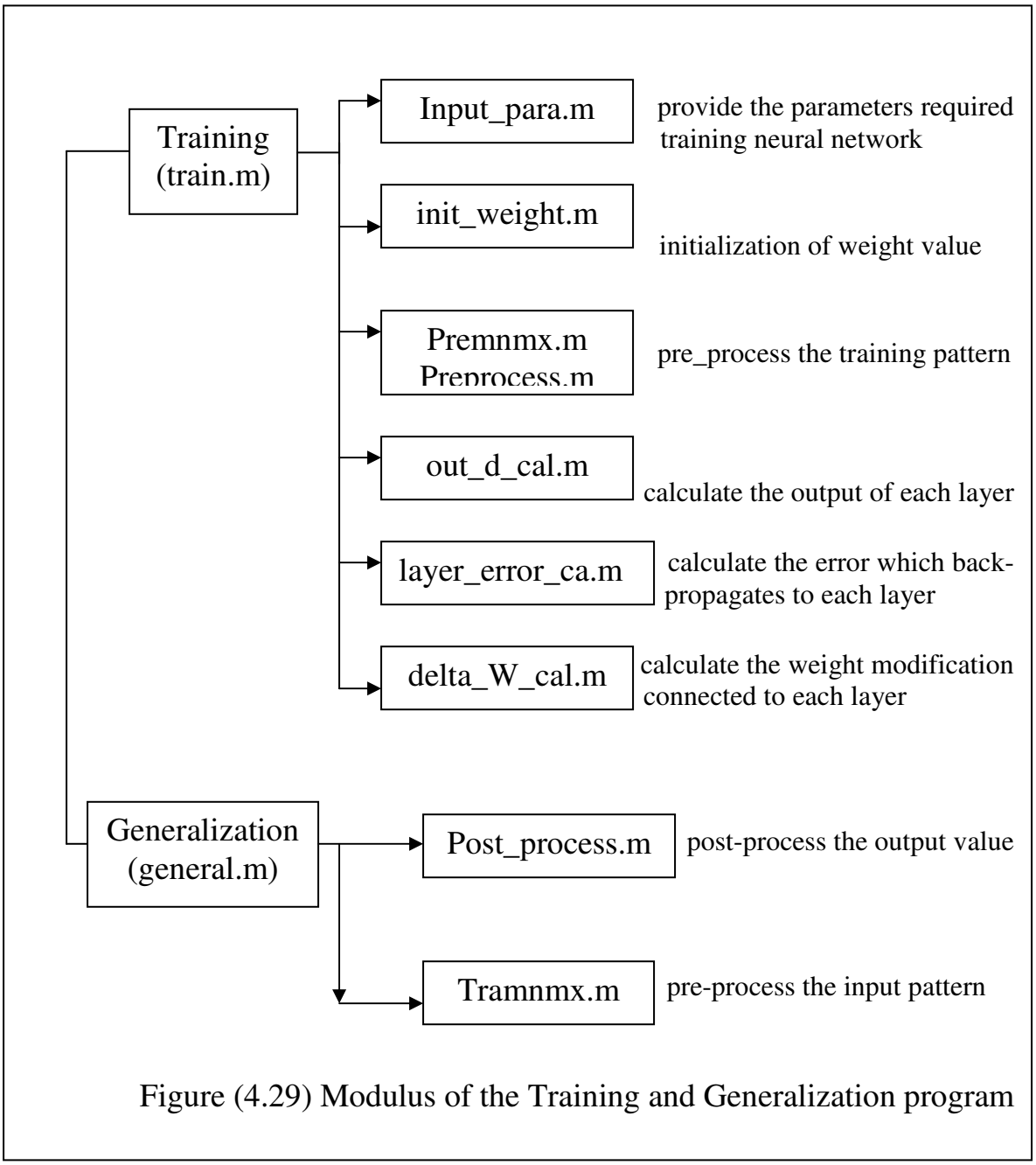

Figure (4.29) Modulus of the Training and Generalization program

Chapter five

Conclusions and Recommendations for Future Researches

5.1 Conclusions

This study investigates the feasibility of using the artificial neural network to evaluate the ultimate strength of reinforced concrete rectangular beams under pure torsion and combined torsion and bending. The neural network is particularly usefulness for evaluating systems with multitude of variables. The backpropagation neural network, which is a multi-layered feedforward neural network, has been proved to accurate in predicting the ultimate torsional strength of reinforced concrete beams.

The most important conclusions that can be drawn from the present study are the followings:

1. Neural network model has been very effective in predicting the ultimate strength of reinforced beams under pure torsion and combined torsion and bending.
2. In the process of training the neural network, the values of input patterns has a large influence on the training time (No. of epoch) of the neural network as a result of the activation function. Normalizing the input and target values of the training patterns seems to greatly reduce the training time.
3. The initial values of the weight factor and biases have greatly influenced the performance mean square error (MSE) of neural

network model. The Gaussian weight-factor distribution with range ±1 is found to give a minimum mean square error (MSE).

4. For gradient descent (GD) algorithm the convergence of the training becomes faster when the learning rate and momentum coefficient are 0.5 and 0.8 respectively.
5. The neural network trained with the resilient backpropagation (RPROP) algorithm exhibited better behaviour than that trained with the gradient descent (GD) algorithm. This was found from the reduced training time (No. of epoch) and better mapping of the neural network for the training patterns and generalization for the test patterns.
6. Influence of the amount of web reinforcement was non-linearly proportional to the ultimate torsional strength of beams under pure torsion.
7. The increasing of amount of longitudinal reinforced steel leads to increases of ultimate torsional strength.
8. The influence of concrete compressive strength predicted by neural network was in agreement with ACI-89 code.
9. Neural networks can be used as a reliable alternative to costly experimental testing as well as lengthy empirical calculations for predicting ultimate strength of concrete beams.
10. The results obtained from the neural network confirms the provision of ACI-89-Code which states that the distribution of stirrups should no be longer than four times the contribution of concrete.

5.2 Recommendations for Future Researches

The following recommendations are suggested for future works:

1. Using ANN model to predict the ultimate strength of reinforced concrete rectangular beams under combined torsion, shear and bending moment.
2. Using ANN model to predict the ultimate torsional strength of flanged beams.
3. Using ANN model to predict the ultimate torsional strength of spandrel beams.
4. Using ANN model to predict the ultimate torsional strength of fiber reinforced concrete beams.
5. Using Fuzzy-Neural network model to predict the ultimate torsional strength of reinforced concrete beams.

References

[1] Al-Radi, S.N.A, "Three Dimensional Nonlinear Analysis of Reinforced Concrete Beams Subjected to Combined Shear and Torsion Using Finite Element Method", M.Sc. Thesis, College of Engineering, University of Basrah, 2002

[2] Khalaf, Y.Y., "Strength and Behaviour of Reinforced Concrete Spandrel Beams under Repeated Loads", M.Sc. Thesis, College of Engineering, University of Basrah, 2002

[3] Hsu, T.T.C, "Torsion of Reinforced Concrete", Van Nostrand Reinhold Company, New York, 1984

[4] Smith, J.O., and Sidebottom, O.M., "Inelastic Behaviour of Load Carrying Members", John Wiley and Sons, New York, 1965

[5] Everad, N, J., and Tonner, J.L., "Theory and Problems of Reinforced Concrete Design", Schaum's Outline Series, McGraw-Hill Book Company, 1966

[6] Timoshenko, S., and Gooder, J.N., "Theory of Elasticity", McGraw-Hill, New York, 1951

[7] Nadia, A., "Plasticity", McGraw-Hill, New York, 1931

[8] Sadowsky, M.A., "An Extension to the Sand Heap Analogy in Plastic Torsion Applicable to Gross-Sections Having One or More Holes", Journal of Applied Mechanics, Vol.62, 1944, pp.166-168

[9] Hsu, T.T.C, "Torsion of Structural Concrete-Plain Concrete Rectangular Sections", Torsion of Structural Concrete, SP-18, American Concrete Institute, Detroit, 1968, pp.203-238

[10] Cowan, H.J., "Design of Beams Subjected to Torsion, Related to the New Australian Code", ACI-Structural Journal, Vol.31, NO.7, January 1960, pp.360-365.

[11] Mohamad Ali, A.A., "Strength and Behaviour of Reinforced Concrete Spandrel Beams", Ph.D Thesis, University of Edinburgh, 1983.

[12] Adi, A. A., "Strength and Behaviour of Reinforced Concrete Spandrel Beams under Repeated Loads", M.Sc. Thesis, College of Engineering, University of Basrah, 1999.

[13] McHenry, D.and Karni, J., "Strength of Concrete under Combined Tensile and Compressive Stresses" ACI-Journal, Proc.Vol.54, April 1958, pp.12-22

[14] Csikos, A., and Hegedus, I., "Torsion of Reinforced Concrete Beams", 2nd Int.Ph.D Symposium in Civil Engineering, University of Budapest, 1998

[15] Hsu, T.T.C, and Mo, Y.L., "Softening of Concrete in Torsional Members-Theory and Tests", ACI Journal, May-June1985, pp.290-303

[16] Andersen, P., "Experiments with Concrete in Torsion", Proceedings, ASCE, Vol.60, May 1934, pp. 641-652

[17] Lampert, P., and Thurlimann, B., "Torsion Tests of Reinforced Concrete Beams", Report No.6506-2, June 1968

[18] Collins, M.P., and Mitchell, D., "Shear and Torsion Design of Prestressed and Non-Prestressed Concrete Beams", Journal Prestressed Concrete Institute, Vol.25, No.5, September-October 1980, pp.32-100

[19] Hsu, T.T.C, and Mo, Y.L., "Softening of Concrete in Torsional Members-Design Recommendations", ACI Journal, July-August 1985, pp.443-452

[20] Hsu, T.T.C, "Ultimate Torque of Reinforced Rectangular Beams", Journal of Structural Division, Proceedings of ASCE, Vol.94, No.ST2, February 1968, pp.485-510

[21] Hsu, T.T.C, "Torsion of Structural Concrete-Behaviour of Reinforced Concrete Rectangular Members", Torsion of Structural Concrete, SP-18, American Concrete Institute, Detroit, 1968, pp.261-306

[22] Collins, M.P., Walsh, P.E., Archer, F.E., and Hall, A., "Ultimate Strength of Reinforced Concrete Beams Subjected to Combined Torsion and Bending", Torsion of Structural Concrete, SP-18, American Concrete Institute, Detroit, 1968, pp.379-402

[23] Hsu, T.T.C, "Torsion of Structural Concrete-A Summary on Pure Torsion", Torsion of Structural Concrete, SP-18, American Concrete Institute, Detroit, 1968, pp.165-178

[24] American Concrete Institute," Building Code Requirements for Reinforced Concrete", ACI-318-63, Detroit, 1963

[25] ACI-Committee-438, "Tentative Recommendations for the Design of Reinforced Concrete Members to Resist Torsion", ACI Structural Journal, Vol.66, No.1, January 1969

[26] American Concrete Institute, "Building Code Requirements for Reinforced Concrete", ACI-318-71, Detroit, 1971

[27] American Concrete Institute, "Building Code Requirements for Reinforced Concrete", ACI-318-89, Detroit, 1989

[28] American Concrete Institute, "Building Code Requirements for Reinforced Concrete", ACI-318-05, Detroit, 2005

[29] American Concrete Institute, "Building Code Requirements for Reinforced Concrete", ACI-318-95, Detroit, 1995

[30] Ernst, G.C., "Ultimate Torsional Properties of Rectangular Reinforced Concrete Beams", ACI Journal, Proceedings, Vol.54, No.4, October 1957, pp.341-356

[31] Gesund, H., and Boston, L.A., "Ultimate Strength in Combined Bending and Torsion of Concrete Beams Containing Only Longitudinal Reinforcement", ACI Journal, Proceedings, Vol.61, No.11, November 1964, pp.1453-1471

[32] Gesund, H., Schuette, F.J., Buchannan, G.R., and Gray, G.A, "Ultimate Strength in Combined Bending and Torsion of Concrete Beams Containing Both Longitudinal and Transverse Reinforcement", ACI Journal, Proceedings, Vol.61, No.12, December 1964, pp.1453-1471

[33] Ramakrishnan, V., and Vijayarangan, B., "Influence of Web Reinforcement of Reinforced Concrete Beams Subjected to Combined Bending and Torsion", India Concrete Journal, Vol.39, No.3, March 1965, pp.89-93

[34] Klus, J.P., "Ultimate Strength of Reinforced Concrete Beams in Combined Torsion and Shear", ACI Journal, Vol.65, No.3, March 1968, pp.210-216

[35] McMullen, A.E., and Warwaruk, J., "Strength of Reinforced Concrete Beams with Web Reinforcement in Combined Bending and Torsion", International Conference on Shear, Torsion and Bond

in Reinforced and Prestressed Concrete, P.S.G., College of Technology (Coimbatore, India), Jan. 1969

[36] Lampert, P., and Thurlimann, B., "Torsion-Bending Tests on Reinforced Concrete Beams", Report No.6506-3, June 1969

[37] McMullen, A.E., and Rangan, B.V., "Pure Torsion in Rectangular Section-A Re Examination", ACI Journal, Vol.75, October 1978, pp. 511-518

[38] Ewida, A.A., and McMullen, A.E., "Concrete Members under Combined Torsion and Shear", Journal of Structural Division, Proceedings of ASCE, Vol.108, No.ST4, April 1981, pp.911-928

[39] Abas, M.S., "Reinforced Concrete Beams Subjected to Torsion, Bending and Shear", M.Sc Thesis, College of Engineering, University of Basrah, 1985

[40] Rasmussen, L.J., and Baker, G., "Torsion in Reinforced Normal and High-Strength Concrete Beams-Part 1: Experimental Test Series", ACI Journal, Vol.92, No.1, January-February 1995, pp.56-62

[41] Rahal, K.N., and Collins, M.P., "Effect of Thickness of Concrete Cover on Shear-Torsion Interaction-An Experimental Investigation", ACI Journal, Vol.92, No.3, May-June 1995, pp.334-342

[42] Panchacharam, S., and Belarbi, A., "Torsional Behaviour of Reinforced Concrete Beams Strengthened with FRP Composites", Proc., First FIB Congress, Osaka, Japan, October 13-19, 2002, pp.1-10

[43] Chaisomphob, T., Kritsanawonghong, S., and Hansapinyo, C., "Experimental Investigation on Rectangular Reinforced Concrete

Beams Subjected to Bi-Axial Shear and Torsion", Sonklanakarin Journal Sci.Technol., Vol.25, No.1, Jan-Feb.2003, pp.41-52

[44] Abdalkarim, A.K., "The Effect of Section Aspect Ratio on Reinforced Concrete Beams in Torsion", Journal of Engineering and Technology, Vol.23, No.10, 2004, pp.537-544

[45] Chiu, H.J., Fang, I.K., Young, W.T., and Shiaw, J.K.,"Behaviour of Reinforced Concrete Beams with Minimum Torsional Reinforcement", Engineering Structures, Vol.29, Issue 9, Sep. 2007, pp.2193-2205

[46] Ameli, M., Ronagh, H.R., and Dux, P.F, "Behaviour of FRP Strengthened Reinforced Concrete Beams under Torsion", Journal of Composites for Construction, Vol.11, No.2, April 2007, pp.192-200

[47] Vanluchence, R.D., and Sun, R., "Neural Networks in Structural Engineering", Microcomp.in Civil Engineering, Vol.5, 1990, pp.207-215

[48] Hajela, P. and Berke, L., "Neurobiological Computational Models in Structural Analysis and Design", Computers and Structures, Vol. 41, No. 4, 1991, pp. 657-667

[49] Hajela, P. and Berke, L., "Neural Networks in Structural Analysis and Design: An Overview", Computing Systems in Engineering, Vol.3, Nos.1-4, 1992, pp.525-538

[50] Szewezyk, Z.P., and Hajela, P., "Damage Detection in Structures Based on Feature-Sensitive Neural Networks", Journal of Computing in Civil Engineering, Vol.8, No.2, April 1994, pp.163-177

[51] Gagarin, N., Flood, I., and Albrecht, P., "Computing Truck Attributes with Artificial Neural Networks", Journal of Computing in Civil Engineering, Vol.8, No.2, April 1994, pp.179-200

[52] Zeng, P., "Artificial Neural Network Computing in Structural Engineering", Developments in Neural Network and Evolutionary Computing for Civil and Structural Engineering, Edinburgh, UK, 1995, pp. 37-50.

[53] Mukherjee, A.D., and Anmala, J.M., "Prediction of Buckling Load of Columns Using Artificial Neural Networks", Journal of Structural Engineering, Vol.122, No.11, 1996, pp.1385-1387

[54] Tully, S.H., "A Neural Network Approach for Predicting the Structural Behaviour of Concrete Slabs", M.Sc Thesis, College of Engineering and Applied Science, University of Newfoundland, 1997

[55] Hajela, P., "Neural Networks-Applications in Modeling and Design of Structural Systems", Neural Networks in Mechanics of Structures and Materials, Udine, October 19-23, 1998.

[56] Lu, W., "Neural Network Model for Distortional Buckling Behaviour of Cold-Formed Steel Compression Members", Ph.D. Thesis, Helsinki University of Technology, 2000.

[57] Boligas, A.C., "Shear Design of Reinforced High-Strength Concrete Beams", Ph.D. Thesis, Technical University of Catalonia, Barcelona, 2002.

[58] Yildiz, E., "Lateral Pressure on Rigid Retaining Walls: A Neural Network Approach", M.Sc Thesis, Graduate School of Natural and Applied Sciences, the Middle East Technical University, 2003.

[59] Hadi, M.N.S., "Neural Networks Applications in Structures", Computers and Structures, Vol.81, 2003, pp.373-381

[60] Lima, L.R.O., Vellasco, P.C.G., Andrade, S.A.l., and Silva, J.G.S., "Neural Networks Assessment of Beam-to-Column Joints", Journal of the Braz.Soc.of Mech.Sci. and Eng., Vol.XXVII, No.3, July-September 2005, pp.314-324

[61] Hola, J., and Schabowicz, K., "Application of Artificial Neural Networks to Determine Concrete Compressive Strength Based on Non-Destructive Tests", Journal of Civil Engineering and Management, Vol.XI, No.1, 2005, pp.23-32

[62] Jeng, D.S., Bateni, S.M., and Lockett, E., "Neural Network Assessment for Scour Depth around Bridge Piers", Department of Civil Engineering, the University of Sydney, Research Report No.R855, November 2005

[63] Neural Network Toolbox User's Guide: for Use with MATLAB 2004, http://www.mathworks.com

[64] Basheer, I.A., and Hajmeer, M., "Artificial Neural Networks: Fundamentals, Computing, Design and Application", Journal of Microbiological Methods, Vol.43, 2000, pp.3-31

[65] Kinnebrock, W., "Neural Networks, Fundamentals, Applications, Examples", Technical University Rheiland-Pfals, R.Oldenbourg Publishing House Munich-Vienna, 1995.

[66] Laftah, R.M., "Buckling Behaviour of Stiffened Plate Panels Using Artificial Neural Networks", Ph.D Thesis, College of Engineering, University of Basrah, 2007.

[67] Rafiq, M.Y., Bugmann, G. and Easterbrook, D.J, "Neural Network Design for Engineering Applications", Journal of Computers and Structures, Vol.79, Issue 17, Sep. 2001, pp.1451-1552

[68] Flood, I., and Kartam, N., "Neural Networks in Civil Engineering I: Principles and Understanding", Journal of Computing in Civil Engineering, Vol.8, No.2, 1994, pp.131-148

[69] Al-Shayji, K.A., and Liu, Y.A.,"Predictive Modeling of Large-Scale Commercial Water Desalination Plants: Data-Based Neural Network and Model-Based Process Simulation", Industrial Engineering Chemical Reserches.41, 2002, pp.6460-6474

[70] Huieydi, I.T.,"Arabic Phoneme Recognition Using Hierarchical Neural Networks" M.Sc Thesis, College of Engineering, University of Basrah, 2006.

[71] Simpson, P., "Artificial Neural Systems: Foundations, Paradigms, Applications and Implementations", Pergamon Press, New York, N.Y., 1990.

[72] Baughman, D.R., and Liu, Y.A.,"An Expert Network for Predictive Modeling and Optimal Design of Extractive Bioseparations in Aqueous Two-Phase Systems", Ind.Eng.Chemical Res.33, 1994, pp.2668-2687

[73] Makay, D.J.C, "Information Theory, Interference, and Learning Algorithms", Copyright Cambridge University press, 2003, Third addition, August 2004.

[74] Jasim, A.A., "Hybrid Approaches for Arabic Phoneme Recognition", M.Sc Thesis, College of Engineering, University of Basrah, 2004.

[75] Riedmiller, M., and Braun, H., "RPROP A Fast Adaptive Learning Algorithm", Technical Report, University of Kharlsruhe, 1992.

[76] Eberhart, R.C. and Dobbins, R.W., "Neural Network PC Tools A Practical Guide", Academic Press, San Diego, CA, 1990.

[77] Carpenter, W.C. and Barthelemy, J.F., "Common Misconceptions about Neural Networks as Approximations", Journal of Computing in Civil Engineering, Vol. 8, No. 3, 1994, pp. 345-358.

[78] Youssef, M.A.R and Bishara, A.G., "Dowel Action in Concrete Beams Subjected to Torsion", Journal of Structural Division, Proceedings of ASCE, Vol.106, No.ST6, June 1980, pp.1263-1277

[79] Winter, G., Nilson, A.H., Urquhart, L.C., and O'Rourke, C.E., "Design of Concrete Structures", McGraw-Hill International Book Company, Ninth Edition, 1981.

[80] Zararis, P.D and Penelis, G.Gr., "Reinforced Concrete T-Beams in Torsion and Bending", ACI Journal, Vol.83, NO.1, January-February 1986, pp.145-155

[81] Iyengar, T.S. and Ramprakash, N.., "Combined Torsion and Flexure Tests on Reinforced Rectangular Concrete Beams", ACI Journal, Vol.71, NO.1, July 1974, pp.362-367

[82] Zia, P., "What Do We Know about Torsion in Concrete Members", Journal of the Structural Division, Proceedings of ASCE, June 1970, ST6, pp.1185-1199

Appendix A: Experimental Database for Beams under Pure Torsion

Author	ID	ANN	b, mm	h,mm	f'c,Mpa	pl%	fy Mpa	pw%	fsy Mpa	S mm	x1 mm	y1 mm	Tu kN.m
Youssef ,M.A.R And Bishara ,A.G [78]	A	T	150	250	46.9	0.734	401	No stirrups					1.3
	B	T	150	250	47.9	1.33	428						1.54
	C	T	150	250	48.3	2.066	445						1.9
	D	V	150	250	48.6	2.066	445						1.1
	G	T	150	250	46.9	2.066	445						1.53
	Aw	T	150	250	46.9	2.066	445	0.802	297	70	110	210	4.51
	BW	T	150	250	47.2	2.066	445	0.551	297	100	110	210	3.73
	CW	T	150	250	47.6	2.066	445	0.551	297	100	110	210	3.71
	Dw	T	150	250	47.6	2.066	445	0.368	297	150	110	210	3.71
	EW	T	150	250	46.2	2.066	445	0.84	288	150	110	210	4.27
	FW	V	150	250	46.5	2.066	445	0.575	288	220	110	210	3.35
Ernst, G.C [30]	3TR-0	T	152.4	304.8	27.5	0.62	370	No stirrups					4.25
	3TR-1#2	T	152.4	304.8	27.5	0.62	370	0.071	383	711	114.3	254	3.95
	3TR-3#2	T	152.4	304.8	27.5	0.62	370	0.141	383	356	114.3	254	3.9
	3TR-7#2	T	152.4	304.8	27.5	0.62	370	0.282	383	178	114.3	254	5.65
	3TR-15#2	T	152.4	304.8	27.5	0.62	370	0.494	383	89	114.3	254	6.97
	3TR-30#2	V	152.4	304.8	27.5	0.62	370	0.985	383	89	114.3	254	8.6
	4TR-0	T	152.4	304.8	27.5	1.1	283	No stirrups					3.88
	4TR-1#2	T	152.4	304.8	27.5	1.1	283	0.071	383	711	114.3	254	3.63
	4TR-3#2	T	152.4	304.8	27.5	1.1	283	0.141	383	356	114.3	254	4
	4TR-7#2	T	152.4	304.8	27.5	1.1	283	0.282	383	178	114.3	254	6.2
	4TR-15#2	T	152.4	304.8	27.5	1.1	283	0.494	383	89	114.3	254	8.36
	4TR-30#2	V	152.4	304.8	27.5	1.1	283	0.985	383	89	114.3	254	9.6

	5TR-0	T	152.4	304.8	27.5	1.7	335	No stirrups					3.82
	5TR-1#2	T	152.4	304.8	27.5	1.7	335	0.071	383	711	114.3	254	3.77
	5TR-3#2	T	152.4	304.8	27.5	1.7	335	0.141	383	356	114.3	254	4.85
	5TR-7#2	V	152.4	304.8	27.5	1.7	335	0.282	383	178	114.3	254	6.8
	5TR-15#2	T	152.4	304.8	27.5	1.7	335	0.494	383	89	114.3	254	8.64
	5TR-30#2	T	152.4	304.8	27.5	1.7	335	0.985	383	89	114.3	254	10.5
Rasmussen, L.J and Baker, G [40]	B30.1	T	180	275	41.7	3.86	640	1.345	665	90	150	245	16.62
	B30.2	T	180	275	38.2	3.86	638	1.345	669	90	150	245	15.29
	B30.3	T	180	275	36.3	3.86	605	1.345	672	90	150	245	15.25
	B50.1	T	180	275	61.8	3.86	612	1.345	665	90	150	245	19.95
	B50.2	T	180	275	57.1	3.86	614	1.345	665	90	150	245	18.46
	B50.3	T	180	275	61.7	3.86	612	1.345	665	90	150	245	19.13
	B70.1	V	180	275	77.3	3.86	617	1.345	658	90	150	245	20.06
	B70.2	T	180	275	76.9	3.86	614	1.345	656	90	150	245	20.74
	B70.3	T	180	275	76.2	3.86	617	1.345	663	90	150	245	20.96
	B110.1	V	180	275	109.8	3.86	618	1.345	655	90	150	245	24.72
	B110.2	T	180	275	105	3.86	634	1.345	660	90	150	245	23.62
	B110.3	T	180	275	105	3.86	629	1.345	655	90	150	245	24.77
McMullen, A.E and Rangan, B.V [37]	B3	T	175	353	38.6	1.23	352	1.26	360	82.5	143	321	25.3
	B4	T	175	353	38.5	1.77	352	1.52	360	60	143	321	31.8
	B1	T	178	356	39.9	0.44	360	0.58	285	82.5	146	324	12.8
	B1R	T	178	356	36.3	0.44	360	0.58	285	82.5	146	324	12.3
	B2	V	178	356	39.6	0.44	380	1.08	285	44.5	146	324	20.8
	A3	T	251	251	39.4	1.23	352	1.21	360	80	219	219	27.8
	A4	V	251	251	39.2	1.77	352	1.69	360	57	219	219	34.5
	A1	T	254	254	39.6	0.44	360	0.56	285	80	222	222	13.1
	A1R	T	254	254	36.9	0.44	360	0.56	285	80	222	222	12.5

	A2	T	254	254	38.2	0.78	380	1.08	285	42	222	222	22.6
Hsu, T.T.C [21]	N1	T	254	254	27.6	0.44	348	0.44	348	216	216	216	11.52
	N1a	T	254	254	27	0.8	341	0.802	352	117	216	216	15.55
	N2a	T	254	254	27.4	1.24	337	1.24	336	140	216	216	20.4
	N3	T	254	254	27.7	1.76	343	1.76	334	99	216	216	25.8
	N4	V	254	254	27.8	2.4	335	2.36	336	73	216	216	30.3
	K2	T	254	254	28.1	3.16	322	3.2	334	54	216	216	34.9
	K3	T	254	381	28.1	0.534	320	0.537	348	152.4	216	343	22.7
	C1	T	254	381	29	0.827	316	0.823	326	181	216	343	29.8
	C2	T	254	381	28.6	1.17	334	1.17	326	127	216	343	38.24
	C3	T	254	381	31	1.6	326	1.61	330	92	216	343	48.27
	C4	T	254	381	29.6	2.11	339	2.13	328	70	216	343	57.25
	C5	V	254	381	29.4	2.67	338	2.61	329	57	216	343	62.9
	C6	T	254	381	26.5	0.534	326	1.17	325	123	216	343	27.42
	B1	T	254	381	27.3	0.534	328	2.61	326	57	216	343	33.18
	B2	T	254	381	29.4	1.17	325	0.537	349	152.4	216	343	30.4
	B3	T	254	381	27	2.67	341	0.537	349	152.4	216	343	35
	B4	T	254	381	30.4	0.827	333	0.549	360	150	216	343	31
	B5	T	254	381	31	1.17	335	0.781	364	105	216	343	41.36
	B6	V	254	381	27.3	1.6	328	1.07	333	140	216	343	44.7
	B7	T	254	381	27	2.11	325	1.42	333	105	216	343	50.6
	B8	T	254	381	28.5	2.67	342	1.81	337	83	216	343	56.8
	B9	T	254	381	22.91	3.16	324	2.13	347	70	216	343	61.3
	B10	T	254	381	46	0.827	332	0.832	356	99	216	343	36.75
	M1	T	254	381	45.6	1.17	350	1.17	340	127	216	343	46.54
	M2	T	254	381	45.8	1.6	321	1.61	333	92	216	343	59.2
	M3	T	254	381	45.9	2.11	316	2.13	332	70	216	343	72

	M4	V	254	381	46.6	2.67	332	2.61	335	57	216	343	78.2
	M5	T	254	381	14.6	0.534	334	0.537	353	152.4	216	343	21.89
	M6	T	254	381	14.8	0.827	326	0.832	347	99	216	343	29.72
	I1	T	254	381	17.2	1.17	345	1.17	344	127	216	343	35.94
	I2	T	254	381	17	1.6	330	1.61	338	92	216	343	41.47
	I3	T	254	381	27.1	0.534	339	0.537	344	152.4	216	343	22.7
	I4	V	254	381	26.1	0.827	329	0.823	337	181	216	343	28.25
	I5	T	254	381	29	1.17	348	1.17	339	127	216	343	39.9
	I6	T	254	381	31.2	1.6	337	1.61	339	92	216	343	48.8
	J1	T	152.4	309	30	0.611	359	0.622	348	92	130	283	9.27
	J2	T	152.4	309	29.2	0.611	353	0.622	352	92	130	283	9.17
	J3	T	152.4	309	31	1.11	337	1.13	344	51	130	283	14.75
	J4	V	152.4	309	29	1.11	340	1.1	368	114	130	283	13.48
	D1	T	152.4	309	27.8	0.916	358	0.903	358	64	130	283	12.4
	D2	T	152.4	309	27.8	1.42	350	1.42	350	89	130	283	16
	D3	T	152.4	495	31.2	1.025	342	1.027	344	105	114.3	457	24.19
	D4	T	152.4	495	29.6	1.59	322	1.58	329	124	114.3	457	29
	G1	T	254	508	30.4	0.4	328	0.402	346	187	216	470	27.3
	G2	V	254	508	31.5	0.62	329	0.626	340	121	216	470	24.13
	G3	T	254	508	27.4	0.88	345	0.882	334	156	216	470	50.57
	G4	T	254	508	28.8	1.2	332	1.2	328	114	216	470	66.12
	G5	T	254	508	27.4	1.58	337	1.6	334	86	216	470	73.38
	G6	T	254	508	30.5	0.6	328	0.594	356	127	216	470	39.9
	G7	T	254	508	31.6	0.93	325	0.938	329	146	216	470	53.68
	G8	T	254	508	28.9	1.32	358	1.31	335	105	216	470	75

Appendix B: Experimental Database for Beams under Combination of Bending Moment and Torsion

Author	ID	ANN	b, mm	h,mm	f'c,Mpa	pl%	fy Mpa	pw%	fsy Mpa	S mm	x1 mm	y1 mm	m/t	Tu, kN.m
Zararis, P.D and Penelis, G.Gr [80]	A-1	T	100	210	42	1.55	540	1.024	330	75	72	180	0.04	4.8
	A-2	T	100	210	42	1.55	540	1.024	330	75	72	180	1.25	5.6
	A-3	V	100	208	40	1.57	540	1.024	330	75	72	180	4.33	4.2
Gesund, H. and Boston, L.A [31]	1	T	203	203	30.8	0.69	352	No stirrups					0	4.15
	2	T	203	203	30.8	1.25	358.5						0	4.5
	3	T	203	203	30.6	0.68	352						1	6.68
	4	T	203	203	30.6	1.565	358.5						1	5.53
	5	T	203	203	16.3	1.565	358.5						2	4.95
	6	T	203	203	16.3	1.565	358.5						3	4.15
	7	T	203	203	39.3	1.565	358.5						3	6.8
	8	T	203	203	39.3	1.565	358.5						4	5.64
	9	V	152.4	304.8	33	1.944	358.5						2	4.84
	10	T	152.4	304.8	19.7	1.39	358.5						4	4.5
Gesund, H.,Schette, F.J,Buchanan, G.R.and Gray, A. [32]	1	T	203.2	203.2	35.4	1.562	358.5	0.688	351.5	127	127	127	1	9.1
	2	T	203.2	203.2	37.3	1.562	358.5	1.72	351.5	50.8	127	127	1	11.75
	3	V	203.2	203.2	37.33	1.562	358.5	0.688	351.5	127	127	127	2	7.03
	4	T	203.2	203.2	33	1.562	358.5	1.72	351.5	50.8	127	127	2	7.72
	5	T	203.2	203.2	29.8	1.562	358.5	0.688	351.5	127	127	127	3	5.64
	6	T	203.2	203.2	28.5	1.562	358.5	1.72	351.5	50.8	127	127	3	6.45
	7	T	203.2	203.2	37.1	1.562	358.5	0.688	351.5	127	127	127	4	4.95
	8	V	203.2	203.2	40.3	1.562	358.5	1.72	351.5	50.8	127	127	4	5.07
	9	T	152.4	304.8	34.2	1.39	358.5	0.401	351.5	203.2	63.5	203.2	2	6.9
	10	T	152.4	304.8	27.4	1.39	358.5	0.401	351.5	203.2	63.5	203.2	4	5.07
	11	T	152.4	304.8	34.2	1.39	358.5	0.802	351.5	101.6	63.5	203.2	2	7.83
	12	V	152.4	304.8	27.4	1.39	358.5	0.802	351.5	101.6	63.5	203.2	4	6.11
Abas, M.S [39]	RB1	T	152	310	34.8	1.2	460.3	0.935	350.3	50	120	270	1.33	12.78

	RB2	T	152	310	31.5	1.2	460.3	0.468	350.3	100	120	270	1.33	11.28
	RB3	T	152	310	29.8	1.2	460.3	0.334	350.3	140	120	270	1.33	10.24
	RB4	T	152	310	32.25	1.2	460.3	0.468	350.3	100	120	270	2	10.26
	RB5	T	152	310	34.61	1.2	460.3	0.468	350.3	100	120	270	4	8.99
	RB11	T	152	310	29.14	1.2	460.3	0.468	350.3	100	120	270	0	10.46
Iyengar, K.T.S and Ramprakash, N.[81]	A5	V	127	203.2	33.75	2.07	404	0.899	370	71	89	165	5.42	5.44
	B5	T	127	203.2	30.4	2.38	426	1.575	370	40.6	89	165	3.4	5.48
	C5	T	127	203.2	36	3.64	454	1.832	370	35	89	165	4.81	7.55
	D5	T	127	203.2	34.3	1.51	442	1.18	370	54	89	165	1.17	5.01
	E5	T	127	203.2	35.2	0.9	420	0.899	370	80	89	165	0.88	3.66
	F	V	127	203.2	30.2	0.4	470	No stirrups					7	2.22
	G	T	127	203.2	29.3	1.106	420	0.806	370	80	89	165	1.895	3.63
	H	T	127	203.2	29	1.106	420	0.806	370	80	89	165	2.443	4.42
	I	T	127	203.2	29.5	1.464	420	1.185	370	40.6	89	165	1.633	4.5
	J	T	127	203.2	29.5	1.96	420	1.68	370	38.1	89	165	1.076	5.37
Hsu, T.T.C [21]	C1	T	254	254	27.6	0.44	348	0.44	348	216	216	216	0	11.52
	C2	T	254	254	27	0.8	341	0.802	352	117	216	216	0	15.55
	C3	T	254	254	27.4	1.24	337	1.24	336	140	216	216	0	20.4
	C4	T	254	254	27.7	1.76	343	1.76	334	99	216	216	0	25.8
	C5	V	254	254	27.8	2.4	335	2.36	336	73	216	216	0	30.3
	C6	T	254	254	28.1	3.16	322	3.2	334	54	216	216	0	34.9
	B1	T	254	381	28.1	0.534	320	0.537	348	153	216	343	0	33.7
	B2	T	254	381	29	0.827	316	0.823	326	181	216	343	0	29.8
	B3	T	254	381	28.6	1.17	334	1.17	326	127	216	343	0	38.24
	B4	T	254	381	31	1.6	326	1.61	330	92	216	343	0	48.27
	B5	V	254	381	29.6	2.11	339	2.13	328	70	216	343	0	57.25
	B6	T	254	381	29.4	2.67	338	2.16	329	57	216	343	0	62.9

V beams used for the verification process of the ANN
T beams used for the training process of the ANN

الخُلاصة

تعتبر هذه الدراسة محاولة لاستخدام تقنية الشبكات العصبية لتحديد مقاومة العتبات الخرسانية المسلحة والمستطيلة المقطع والمعرضة إلى عزوم اللي الصرفة وعزوم اللي مع عزوم الانحناء. فتمت دراسة المبادئ والمفاهيم العملية للشبكات العصبية الصناعية ومعرفة طرق تمثيل تلك الشبكات وترتيبها ونقاط قوتها. وكذلك تم استقصاء تأثير المتغيرات المختلفة للشبكة مثل عدد العقد في طبقة الإدخال والإخراج والطبقات المخفية , والمعالجة المسبقة لنماذج تدريب الشبكة, والفرض الأولي لمعاملات الأوزان, واختيار معدل التعلم ومعامل الزخم على سلوك وأداء نموذج الشبكة العصبية. وبسبب بطء التقارب عند استخدام دالة الانحدار العكسي تم استخدام دالة الرجوع العكسي لزيادة سرعة التقارب وتحسين أداء الشبكة العصبية. وبعد إنهاء تدريب الشبكة العصبية تم اختبار استقراء الشبكة بواسطة استخدام نماذج مختلفة غير موجودة في نماذج التدريب.

واستخدم نوعين من هياكل الشبكات العصبية وكما يلي:

1- الهيئة(10:25:25:1) استخدمت لإيجاد المقاومة القصوى للعتبات الخرسانية المسلحة والمستطيلة المقطع والمعرضة إلى عزوم اللي الصرفة.

2- الهيئة (11:8:1) استخدمت لإيجاد المقاومة القصوى للعتبات الخرسانية المسلحة والمستطيلة المقطع والمعرضة إلى عزوم اللي مع عزوم الانحناء.

دُربت الشبكات العصبية المستخدمة على أساس القيم المختبرية لبحوث مختلفة, وأظهرت النتائج إن استخدام المعالجة الأولية (normalizing) لنماذج التدريب تقلل زمن التدريب وكذلك استخدام توزيع كاوسين لمعاملات الأوزان للمدى ($1\pm$) يعطي اقل معدل خطأ. بالإضافة إلى ذلك وجد أن القيم الفعالة لمعدل التعلم ومعامل الزخم هو (0.5) و (0.8) على التوالي لدالة الانحدار العكسي. واستنادا إلى النتائج المستحصلة من تلك الشبكات العصبية تم دراسة تأثير العوامل المختلفة المؤثرة على المقاومة القصوى للعتبات الخرسانية المسلحة ومقارنتها مع معادلات مدونة معهد الخرسانة الأمريكي (ACI-Code).

احتساب مقاومة الالتواء القصوى للعتبات الخرسانية المسلحة باستخدام الشبكات العصبية الصناعية

رسالة مقدمة إلى

جامعة البصرة- كلية الهندسة

كجزء من متطلبات نيل درجة الماجستير

في الهندسة المدنية

من قبل

عبدالخالق عبداليمة جعفر

بكالوريوس علوم في الهندسة المدنية

2008